Superpave Mix Design and Laboratory Testing of Reacted and Activated Rubber Modified Asphalt Mixtures

by

Janak Shah

A Thesis Presented in Partial Fulfilment
Of the Requirements for the Degree
Master of Science

Approved June 2018 by the
Graduate Supervisory Committee

Kamil E. Kaloush, Chair
Michael Mamlouk
Jeffery Stempihar

ARIZONA STATE UNIVERSITY

August 2018

ABSTRACT

Crumb rubber use in asphalt mixtures using wet process technology has been in practice for years in the United States with good performance history; however, it has some drawbacks that include the need for special blending equipment, high rubber-binder temperatures, and longer waiting time at mixing plants. Pre-treated crumb rubber technologies are emerging as a new method to produce asphalt rubber mixtures in the field. A new crumb rubber modifier known as Reacted and Activated Rubber (RAR) is one such technology. RAR (industrially known as "RARX") acts like an Enhanced Elastomeric Asphalt Extender to improve the engineering properties of the binder and mixtures. It is intended to be used in a dry mixing process with the purpose of simplifying mixing at the asphalt plant. The objective of this research study was first to perform a Superpave mix design for determination of optimum asphalt content with 35% RAR by weight of binder; and secondly, analyse the performance of RAR modified mixtures prepared using the dry process against Crumb Rubber Modified (CRM) mixtures prepared using the wet process by conducting various laboratory tests. Performance Grade (PG) 64-22 binder was used to fabricate RAR and CRM mixtures and Performance Grade (PG) 70-10 was used to fabricate Control mixtures for this study. Laboratory tests included: Dynamic Modulus Test, Flow Number Test, Tensile Strength Ratio, Axial Cyclic Fatigue Test and C* Fracture Test. Observations from test results indicated that RAR mixes prepared through the dry process had excellent fatigue life, moisture resistance and cracking resistance compared to the other mixtures.

ACKNOWLEDGMENTS

I would like to express my sincere gratitude to my advisor Dr. Kamil Kaloush for giving me the opportunity to work with him, for the continuous support of my Master's study and related research, for his patience, motivation, and immense knowledge. I could not have imagined having a better advisor and mentor for my Master's study.

I am extremely thankful to Dr. Michael Mamlouk and Dr. Jeffery Stempihar for serving on my committee and for providing valuable feedback on my research work.

I am very grateful to Aswin Srinivasan and Dirk Begell for going above and beyond help throughout my research. Special thanks to Ramadan Salim for teaching me how to operate the equipment, perform mixture testing and for being available every time that I had a doubt. Thanks to Ph.D. students Jose Medina and Akshay Gundla for providing expert knowledge and long stimulating discussions which helped me answer some critical research questions.

I would like to thank Dr. Jorge Sousa from Consulpav International for providing RARX and for responding to any technical query promptly even from across the globe.

I am grateful to Mr. Robert McGennis from HollyFrontier Corporation for providing information on Crumb Rubber practices being utilized by agencies and related documents and Mr. Thomas Ludlum for constantly providing the asphalt binder needed for this study. Finally, I would like to thank the company Crumb Rubber Manufacturers, Mesa for providing the Crumb Rubber and Southwest Asphalt, El Mirage pit for providing the aggregate.

TABLE OF CONTENTS

CHAPTER Page

CHAPTER Page

CHAPTER Page

CHAPTER Page

CHAPTER Page

LIST OF FIGURES

Figure Page

Figure Page

Figure Page

LIST OF TABLES

Table Page

Table Page

LIST OF ACRONYMS

AASHTO	- American Association of State Highway Transportation Officials
AC	- Asphalt Content
AMBS	- Activated Mineral Binder Stabilizer
AMPT	- Asphalt Mixture Performance Tester
AR	- Asphalt Rubber
ASTM	- American Society for Testing and Materials
CFT	- C* Fracture Test
CR	- Crumb Rubber
CRM	- Crumb Rubber Modified
CRMB	- Crumb Rubber Modified Binder
EST	- E* Stiffness Ratio
FN	- Flow Number
GTR	- Ground Tire Rubber
HMA	- Hot Mix Asphalt
HWTT	- Hamburg Wheel Track Test
IDT	- Indirect Tension
LTTP	- Long Term Pavement Performance
LVDT	- Linear Variable Differential Transducer
NCHRP	- National Co-operative Highway Research Program
NMAS	- Nominal Maximum Aggregate Size
OBC	- Optimum Binder Content

PG	- Performance Grade
RAR	- Reacted and Activated Rubber
RPM	- Revolutions Per Minute
RTR	- Recycled Tire Rubber
SGC	- Superpave Gyratory Compactor
SHRP	- Strategic Highway Research Program
SMA	- Stone Mastic Asphalt
SSD	- Saturated Surface Dry
TSR	- Tensile Strength Ratio
VECD	- Visco-Elastic Continuum Damage
VFA	- Voids Filled with Asphalt
VG	- Viscosity Grade
VMA	- Voids in Mineral Aggregate

1. INTRODUCTION

1.1. Background

In 1990, over 1 billion of scrap tires were in stockpiles in the United States. The scrap tires in 2010 were estimated to be about 111.5 million of tires. This is about 90% reduction in 20 years. This was achieved thanks to the extended markets for scrap tires that include: the automotive industry, sports surfacing, molded products or playgrounds and animal bedding, civil engineering applications such as rubberized asphalt pavements (Rubber Manufacturers Association 2011). About 12 million scrap tires are used for crumb rubber modified asphalts (Willis, et al. 2012).

The primary purpose of using Asphalt Rubber (AR) in Hot Mix Asphalts (HMA) is that it significantly improves engineering properties over conventional paving grade asphalt (bitumen). Asphalt rubber binders can be engineered to perform in any type of climate. Asphalt rubber binder designers usually consider climate conditions and traffic data in their design to provide a suitable asphalt rubber product. At intermediate and high temperatures, asphalt rubber binder's physical properties are significantly different than those of conventional paving grade asphalts. The rubber stiffens the binder and increases elasticity (proportion of deformation that is recoverable) over these pavement operating temperature ranges; which decreases pavement temperature susceptibility and improves resistance to permanent deformation (rutting) and fatigue (Caltrans, 2003). However, despite the proven advantages of AR hot mix asphalts, there is still no breakthrough or significant development in the global practical use and implementation of this technology (Sousa et al, 2000-2009). Some reasons of this stagnation can be listed as follows:

- The tedious wet process of producing the asphalt rubber binder, involving very high temperature (over 180℃) and long blending and reaction time (45 min. up to one hour).
- The complexity and cost of the blending unit that must be installed in every asphalt mixing plant.
- The necessity to re-heat and agitate the hot asphalt rubber binder after longer rest periods.
- The high cost of the asphalt rubber paving mixes as compared to conventional HMAs (ranges between 20-100% higher).

In view of the proven advantage of AR technology, an effort was made to overcome the main disadvantages listed above. One solution that was developed is the new "Reacted and Activated Rubber" – RAR. It was designed as a rubber modifier that can be directly added to the pugmill at the end of the batching process in a mixing plant and generated superior quality rubber-modified asphalt mixes (Ishai et al. 2011).

1.2. Study Objective

The objective of this study was to perform a Superpave mix design on RAR modified asphalt mixtures and compare the performance characteristics of mixtures prepared using crumb rubber technologies namely “Reacted and Activated Rubber (RAR)”, as described above, and “Crumb Rubber (CR)” using wet process.

1.3. Scope of Work

The scope of this study included designing the first RAR Superpave mix design since all the work reported in the literature designed mixtures using the Marshall method. This study selected 35% of RAR by weight of binder for determination of optimum asphalt content. By mass, RAR consists of 56-58% crumb rubber, and the 35% was selected because it would be equivalent to the 20% typically used for the AR wet process. The RAR modified mixtures were compared with the wet process Crumb Rubber Modified (CRM) mixtures. Thus, the CRM mixtures were fabricated by modifying the binder with 20% crumb rubber which is also the crumb rubber technology used in Arizona. A PG 64-22 binder was used for both processes and was obtained from HollyFrontier Terminal located in Glendale, AZ. A PG 70-10 binder was also obtained from the same source and used to prepare a control mix to compare the mixtures performance.

The laboratory tests included: Dynamic Modulus Test (AASHTO-T342) for stiffness evaluation, Flow Number Test (AASHTO-TP79-13) for rutting evaluation, Tensile Strength Ratio (AASHTO T 283) to evaluate moisture susceptibility, C* Fracture Test to evaluate crack propagation and Axial Cyclic Fatigue Test (AASHTO TP 107-14) for cracking evaluation.

1.4. Number of Tests

Table 1. Number of Tests Conducted for each Mixture

Test	Temperature/Frequency/ Loading Rate/Strain Levels	Replicates	Total Tests
Dynamic Modulus	5 Temperatures x 6 Frequencies	3	15
Flow Number	1 Temperature x 1 Loading Rate	2	2
Tensile Strength Ratio	1 Temperature x 2 Subsets	3	6
Axial Cyclic Fatigue	1 Temperature x 3 Strain Levels	1	3
C* Fracture Test	1 Temperature x 5 Loading Rates	1	5

1.5. Report Organization

This report is divided into 9 chapters. Chapter 1 provides the background and brief description of the research work done including the study objective and scope of work. Chapter 2 provides the literature review on crumb rubber technologies, various processes used, the Superpave mix design, asphalt film thickness and the laboratory tests performed. Chapter 3 details the materials used for this research and fabrication of samples prepared using different crumb rubber technologies. Chapter 4 provides the optimum asphalt content for all mixtures obtained using the Superpave mix design. Chapter 5 documents the laboratory tests performed with their respective specimen setup. Chapters 6 and 7 present the results and analysis found from performance testing for all mixtures. Chapter 8 sheds light into an important issue related to asphalt film thickness and its consideration into the mix design. Chapter 9 presents a summary and conclusions of this research.

2. REVIEW OF LITERATURE

2.1. Materials

2.1.1. Binder

In HMA, binder functions as a waterproof, thermoplastic, viscoelastic adhesive. By weight, binder generally accounts for between 4 and 8 % of HMA and makes up about 25 to 30 % of the cost of an HMA pavement structure depending upon the type and quantity. The Superpave PG system was developed as part of the Superpave research effort to more accurately and fully characterize asphalt binders for use in HMA pavements. The PG system is based on the idea that an HMA asphalt binder's properties should be related to the conditions under which it is used. For asphalt binders, this involves expected climatic conditions as well as aging considerations. Therefore, the PG system uses a common battery of tests (as the older penetration and viscosity grading systems do) but specifies that a binder must pass these tests at specific temperatures that are dependent upon the specific climatic conditions in the area of intended use.

Superpave performance grading is reported using two numbers – the first being the average seven-day maximum pavement temperature (in °C) and the second being the minimum pavement design temperature likely to be experienced (in °C). Thus, a PG 64-16 is intended for use where the average seven-day maximum pavement temperature is 64°C and the expected minimum pavement temperature is -16°C. Notice that these numbers are pavement temperatures and not air temperatures.

2.1.2. Aggregate

"Aggregate" is a collective term for the mineral materials such as sand, gravel and crushed stone that are used with a binding medium (such as binder, lime, etc.) to form compound materials such as asphalt concrete. By volume, aggregate generally accounts for 92 to 96 % of HMA. Aggregate is also used for base and subbase courses for both flexible and rigid pavements.

Aggregate physical properties are the most readily apparent aggregate properties and they also have the most direct effect on how an aggregate performs as either a pavement material constituent or by itself as a base or subbase material.

The particle size distribution, or gradation, of an aggregate is one of the most influential aggregate characteristics in determining how it will perform as a pavement material. In HMA, gradation helps determine almost every important property including stiffness, stability, durability, permeability, workability, fatigue resistance, frictional resistance and moisture susceptibility (Roberts et al., 1996).

Maximum size: The smallest sieve through which 100 percent of the aggregate sample particles pass. Superpave defines the maximum aggregate size as "one sieve larger than the nominal maximum size" (Roberts et al., 1996).

Nominal maximum aggregate size (NMAS): The largest sieve that retains some of the aggregate particles but generally not more than 10 percent by weight. Superpave defines nominal maximum aggregate size as "one sieve size larger than the first sieve to retain more than 10 percent of the material" (Roberts et al., 1996).

2.2. Crumb Rubber

The use of crumb rubber in asphalt was first attempted by Charles McDonald, a City of Phoenix engineer. Asphalt rubber is created by the mixing of crumb rubber from waste tires and asphalt binder. This technology was first introduced in the late 1960's in treatments such as crack sealing and chip seals. Later, McDonald found that he could use tires as a waste product, at a low cost to improve the properties of asphalt binder. In his research he found that a minimum of 15% of crumb rubber was needed to achieve the desired properties and benefits. McDonald's work led to patented process, referred to as the wet mix process wherein the asphalt binder is mixed with the crumb rubber at 177 °C for about 45 minutes to let the binder digest the crumb rubber. Crumb rubber modified asphalt was first introduced in asphalt pavements in the 1980's, especially in gap and open graded mixes. The use of crumb rubber in asphalt pavement improved the mechanical properties of pavements, resistance to cracking and rutting as well as the reduction of environmental issues such as noise, energy consumption and CO_2 emissions (Way 2012).

2.2.1. Crumb Rubber Grinding Processes

In the asphalt pavement industry, scrap tires are ground into crumbs by different grinding methods, each of which produces particles with different sizes and characteristics. Some of the commonly used methods are: cracker mill process, granulator process, micromill process and the cryogenic process. A description of these methods is shown in Table 2.

Table 2. Grinding Methods for Scrap Tires (NCAT Report 12-09)

Name	Method	Size (mm)	Other Characteristics
Cracker mill	Most commonly used method. Grinding is controlled by the spacing and speeds of the drums. The rubber particles are reduced by tearing as it moves through a rotating corrugated steel drum.	5-0.5	High surface area. Irregular shapes. Usually done at ambient temperatures.
Granulator	Uses revolving steel plates to shred the tire particles.	9.5-0.5	Cubical particles. Low surface area.
Micromill	Water is mixed with crumb rubber to form a slurry which is then forced through an abrasive disk.	0.5-0.075	Reduces particle size beyond that of a granulator or cracker mill.
Cryogenic	Liquid nitrogen is used to increase the brittleness of the crumb rubber. Once frozen it can be ground to desired size.	0.6-0.05	Hammer mills and turbo mills are used to make different particle size.

2.2.2. Effect of Rubber Particle Size on Binder Properties

The surface area of rubber particles increases with decreasing particle size. Consequently, smaller particles are likely to interact with the base binder more effectively than larger particles, leading to potentially shorter reaction times at lower blending temperatures and to improved stability (i.e., the period before separation of the rubber particles from the asphalt begins). Larger particle surface areas also facilitate absorption of the light oils in the base binder, which promotes digestion of the rubber (Huang et al. 2008). Unfortunately, there was little standardization of the sizes of rubber particles assessed (75 µm up to 2.36 mm [#200 up to #8 sieve]) with no clear distinction of the boundary between

what was considered to be fine and coarse. However, the studies generally concluded that digestion times, phase angle, and fatigue cracking resistance decreased with decreasing particle size, while stability, viscosity, stiffness, and rutting resistance all increased with decreasing particle size. Low-temperature creep stiffness did not appear to be significantly influenced by rubber particle size. Binder contents in mixes also tended to decrease with decreasing rubber particle size used in the binder given that gaps in the aggregate gradation can be smaller (Xiao et al., 2009).

The particles size disruption of crumb rubber influenced the physical properties of asphalt-rubber blend. In general, small difference in the particles size has no significant effects on blend properties. However, the crumb rubber size can certainly make a big difference. A study reported that the particle size effects of CRM on high temperature properties of rubberized bitumen binders was an influential factor on viscoelastic properties. Also, coarser rubber produced a modified binder with high shear modules and an increased content of the crumb rubber decreased the creep stiffness which in tandem displayed better thermal cracking resistance (Wang et al., 2012).

In summary, the primary mechanism of the interaction is swelling of the rubber particles caused by the absorption of light fractions into these particles and stiffening of the residual binder phase. The rubber particles are constricted in their movement into the binder matrix to move about due to the swelling process which limits the free space between the rubber particles. Compared to the coarser particles, the finer particles swell easily thus developing higher binder modification. The swelling capacity of rubber particle

is linked to the penetration grade of the binder, crude source, and the nature of the crumb rubber modifier.

2.2.3. Crumb Rubber Modified Binder (CRMB)

Modification of asphalt binder with crumb rubber as an additive showed an increase in the softening point with the increase in rubber content as studied by (Albayati et al. 2011; Khadivar and Kavussi, 2013; Mansob et al. 2014). Tamimi et al. (2014) pointed out that at a particular temperature it was found that viscosity increased with the increase in CR content. Both ductility and penetration value of the modified asphalt binder decreased with increasing CR content, while elastic recovery was least for 5% and maximum for 15% CRMB. CRMB mixtures also had better modulus as compared to unmodified asphalt mixtures (Wahhab et al. 1991; Vasiljevic-Shikaleska et al. 2010). Further, Navarro et al. (2005) observed that addition of CR to asphalt binder decreased the elastic and viscous moduli at low temperatures and, therefore, caused an increase in binder flexibility. On the contrary, at high temperatures, a significant increase in both moduli and a notable drop in the loss tangent values were observed, resulting in a more elastic binder.

2.3. Reacted and Activated Rubber

RAR is composed of soft asphalt (bitumen), finely ground scrap tire rubber and fillers reacted at optimal proportions and temperatures as reported in (Ishai et al., 2011). Generally, RAR consists of about 62 to 65% crumb rubber, 20 to 25% soft asphalt, and 15 to 20% filler. During the production of the RAR material, the asphalt used will be softer to enable an improvement in the viscosity, and ensure the workability of the binders even at higher rubber contents.

The rubber particles used in the composition of RAR are of the maximum size of 600 μm. The fillers used in the RAR conglomerate are microscale additives to reduce moisture sensitivity of the asphalt mixes. When the elastomeric part of rubber in the RAR blends uniformly with the liquid asphalt binder, the charged molecules of the filler form an interconnected network with the rubber particles, thereby, forming a cohesive blend of asphalt, rubber, and the stabilizer. RAR is also coated with a special layer of fillers that is dispersed into the mixture, which latches onto the aggregate improving the moisture sensitivity response (Sousa et al., 2012; Sousa et al., 2013). Figure 1 shows a schematic representation of the mechanism of RAR in a mixture.

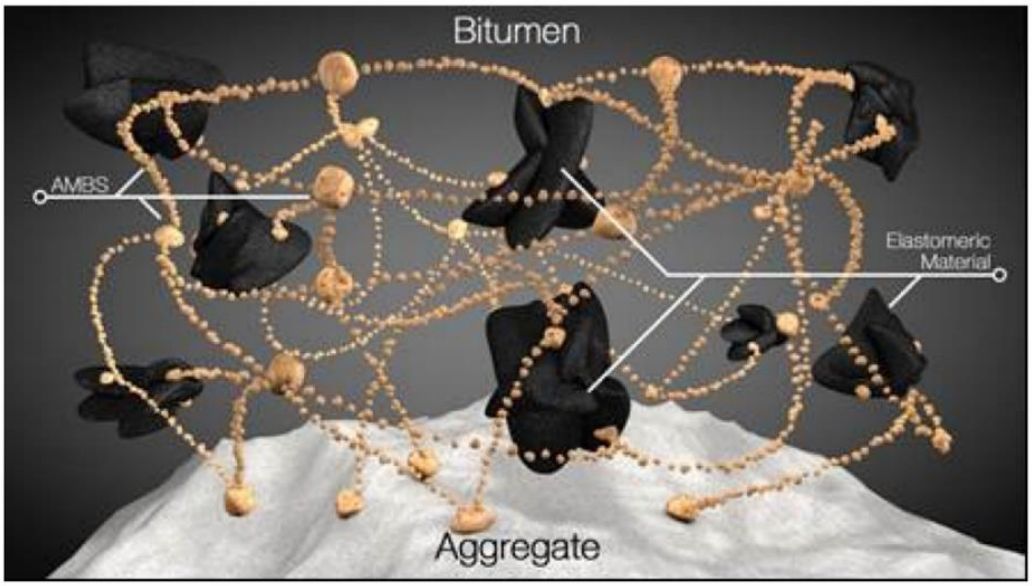

Figure 1. Model and Mechanism of RAR in a Mixture (Source: Sousa et al., 2012)

Sousa (2016) described how RAR is produced from raw constituent materials. The implementation of RAR in several types of asphalt mixtures is discussed, and demonstrative examples of test results are provided. Tests on mixtures in wheel tracking and fatigue demonstrate how the binder performance tests translate into mixture

performance. In all cases evaluated, the RAR mixtures outperformed non- modified and even conventional rubber modified equivalent materials.

Ishai et al. (2013) summarized further successful research effort in the laboratory and in the field, where actual road tests were performed and monitored in Israel, using RAR HMA mixes under hot climatic conditions. The RAR HMA mixes (Dense and Superpave "S" graded) were produced using Marshall method in conventional batch asphalt plants with the use of the regular SMA fiber-feeder for feeding the RAR directly to the pugmill without any additional heating or setting. The road tests included a residential street and highly trafficked industrial road in the city of Tel Aviv, and an access road to a very busy aggregate quarry. The performance and results after more than two years have strengthened the advantages of RAR Asphalt Rubber mixes achieved in the first phase of the research. This also led to other paving jobs, and new modified specifications for asphalt rubber in Israel.

Presti (2013) reported the results of a literature review upon the existing technologies and specifications related to the production, handling and storage of RTR-MBs. Considering that RTR-MBs technologies are still struggling to be fully adopted worldwide, Presti's work aimed to be an up-to-date reference to clarify benefits and issues associated to this family of technologies and to provide suggestions for their wide-spread use.

Sousa et al. (2016) conducted a research study for binder characterization of the Reacted and Activated Rubber (RAR) modified asphalts with varying dosages, and compared these materials with two virgin binders and one commercially available rubber

modified binders. RAR modification raised the upper Performance Grade temperatures to a higher grade than the base binder making these binders well suited to reduce rutting. Non-recoverable creep compliance decreased, and recovery increased with increasing RAR contents. RAR modified asphalts were highly resilient in nature since they had substantially lower strains than the virgin and C60 binders attributed to the presence of RAR additive that provided enduring viscoelastic characteristic. Overall, it was recommended that at least 15% RAR be used as minimal dosage in designing an asphalt mixture to obtain an effective material with an improved performance than a mixture produced using commercially available asphalts, including the rubber-modified ones.

Sampat (2016) in his study aimed at characterization of seven dense graded asphalt mixtures using VG-30 and VG-40 (Indian specifications) base virgin binders along with commercially available CRMB60 for comparison purposes. In total, thirteen conventional and RAR modified asphalt binders, and seven conventional dense graded and RAR dense graded asphalt mixtures were evaluated and analyzed. Asphalt binders' evaluation encompassed fundamental and advanced rheological characterization while the asphalt mixtures were characterized to understand the viscoelastic properties, fatigue cracking resistance, and moisture sensitivity.

2.4. Mixing Processes

The mixing of asphalt and rubber presents the user with two choices: RAR dry mixing and wet mixing. In the wet process (Figure 2), the fine crumb rubber is mixed with asphalt at high temperatures. This bitumen becomes partially modified by the rubber particles after a controlled time of digestion. In the RAR dry process (Figure 3), the RAR

particles are used as filler and blended with the warmed aggregates, before the addition of the hot bitumen binder to make the asphalt–rubber mixture (Herna'ndez-Olivares, 2006).

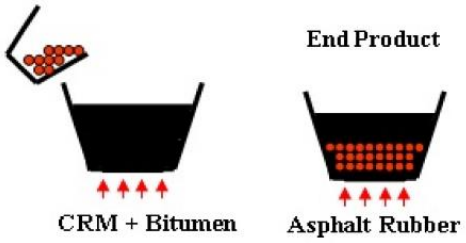

Figure 2. Wet Process Method (Hassan et. al 2014)

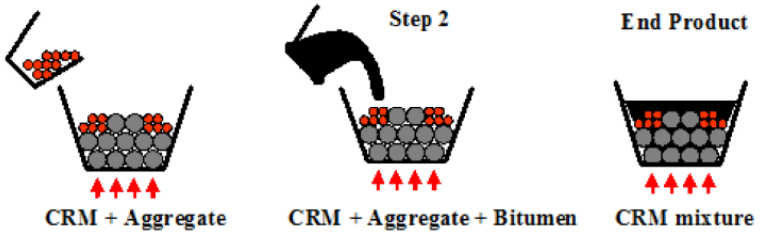

Figure 3. Dry Process Method (Hassan et. al 2014)

2.4.1. Wet Process

The process in which the crumb rubber is added to the asphalt binder to act as a modifier is called the wet process. This process has been used since the 1960's in crack sealing, chip seals and other surface treatment; and in the late 1980's in hot mix asphalt pavements (Way 2012). Overall, results from pavements around the United States have shown that the wet process for rubberized asphalt pavement outperforms both conventional pavement mixes and the old dry process (not the RAR technology). The modified process will depend on the blending temperature, the time for digestion, the mixing mechanism, the size and texture of the crumb rubber and the content of aromatics in the asphalt binder (Federal Highway Administration 1998). The binder modification occurs due to physical and chemical interaction between the asphalt and the crumb rubber. The crumb rubber

particles swell because of the absorption of lighter fractions contained in the asphalt binder (Xiao, Amirkhanian and Shen 2009). A subset of the wet process that receives interest from time to time is the terminal blend technique. A terminal blend refers to asphalt rubber binder that has been blended at a supply terminal and reacted long enough to maintain a constant viscosity. The amount and size of crumb rubber is smaller to keep the viscosity modest when the modified binder is head and pumped at asphalt plant.

Wet process rubberized asphalt involves mixing of recycled tire crumb rubber into an asphalt binder at high temperature (176 ºC and higher), followed by a period of cooking and digestion (hours or days) and continued agitation to keep the crumb rubber suspended in the binder (Hicks, 2002). Unlike polymers, the recycled tire rubber does not become a near-integral part of the binder. The crumb rubber used in the wet process has a higher density than the binder, allowing the rubber and binder to separate if not maintained in a turbulent environment. During heating, the crumb rubber will both soften and swell because of surface absorption of lighter binder components in the surface pores of the rubber (Artamendi and Khalid, 2006; Shen et al., 2012, 2015). The swelling process is caused by a selective removal of asphalt lighter ends from the binder while adding swollen crumb rubber to the mix matrix. This increases the viscosity of the binder, stiffens the mix and increases resistance to permanent deformation (rutting). The presence of softened rubber grains in the mix also makes the asphalt more flexible, thus increasing resistance to various forms of cracking (Peralta et al., 2012). In addition, dissolving rubber in asphalt binder increases its viscosity, allowing higher binder content to be used in the mix. Theoretically, this leads to asphalt mixes with improved fatigue resistance and durability

(Huang et al., 2007). Extended reaction time decreases the binder viscosity slightly because of digestion of the rubber in the asphalt binder.

According to Mturi et al. (2012), the digestion or reaction process for crumb rubber asphalt binder can be divided into 4 stages. During the first stage the rubberized asphalt will show an increase in viscosity as the rubber particles increase in dimensions. At this stage the lighter fraction of the binder will diffuse into the rubber networks composed of poly-isoprene and poly-butadiene linked by sulfur-sulfur bridges. As lighter fractions are diffused in the rubber particles the sulfur-sulfur bonds within the rubber particles will thermally dissociate. Stage two, is when the blend has reached a maximum viscosity point after thermal dissociation. Stage three is the period in after the binder has reached it maximum viscosity and starts to decrease due to the loss of the Sulphur linkages. The thermal dissociation will continue making the viscosity decrease. Finally, stage 4 is when the rubberized binder has reached constant viscosity (Mturi, O'Connell and Mogonedi 2012).

2.4.2. Old Dry Process

The old dry mix process, on the other hand is not very popular. The primary reason is the deficiency in having the crumb rubber reacts and swell when the binder is added, inconsistency of the test results, and the lack of a standardized mixing process. Nevertheless, the dry process could have potential, and can consume larger quantities of crumb rubber, if it can improve the mechanical performance of pavement structures and reduction in road noise levels (Moreno et al., 2010).

In the old dry process, the crumb rubber is added to the aggregates at a proportion of approximately 1-3% by weight of the aggregate in the mix or 0.9% to 2.7% by weight of the mix before the asphalt binder is added. Dry process crumb rubber-modified asphalt began to take root in the U.S. asphalt market in the early 2000s. Testing and commercialization of the "dry mix" process – the introduction of engineered crumb rubber at the producer's site during the production of hot and warm-mix asphalt - was one of those efforts. In the dry process, crumb rubber is added to the hot aggregates similar to reclaimed asphalt pavement (RAP) at the plant and then mixed with binder. Typically, larger rubber size particles between 0.85 to 6.4 mm are used to substitute for fine aggregates, at a 1-3% replacement rate (Huang, 2007). Dry process rubber introduction included use of engineered crumb rubber designed to reduce mix stickiness, improve workability and ease the introduction of rubber into the asphalt production process. One of the most successful reported dry process efforts uses a metered, loss in weight pneumatic feeding system to inject fine, crumb rubber into the mill during asphalt production. Rubber particles distribution within a gap graded rubberized asphalt rubber composite performed as well as wet mix and polymer-modified asphalt (Takallou et al., 1988). Depending on the performance criteria for the modified asphalt, these processes typically reported cost 15 to 50% less than wet process rubber and polymer-modified asphalt.

(Sibal et al., 2007) tested to replace a portion of the aggregates with crumb rubber particles and alter the gradation by an insignificant amount. The mixing process involved heating the aggregates to 150-160 ºC and addition of asphalt and further agitation till homogeneity is achieved. The researchers observed excellent results and recorded better

fatigue and rutting resistance as compared to conventional mixes. In a similar approach Hernandez tweaked the gradation to include a higher amount if rubber in the asphalt mixtures (Hernandez-Olivares et al., 2009). By adding the rubber, using a mixing process with no digestion time, they found that the Marshall stability of samples decreased; this was attributed to the elastic behavior of rubber particles with asphalt. To prevent this, the researchers recommended a digestion time of at least 2 hours in an oven maintained at high temperatures.

In a recent study, Hassan et al. (2014) indicated that critical design factors for designing dry processed CRM mixes are aggregate gradation, rubber gradation, binder content, and air voids content. The following general guidelines for dry process CRM mixes were suggested:

• Gap-graded or coarse densely-graded aggregates are preferred.

• Same binder grade or higher penetration binder must be used compared to HMA.

• Higher binder content should be used compared to HMA (1-2%).

• Combination of coarse and fine rubber is desirable.

• Low design air voids content is critical (approximately 3%).

• A higher mixing temperature compared to HMA must be used.

• Rubber must be added to hot aggregate prior to adding the binder.

• 1 to 2 hours curing time is needed after mixing.

2.5. HMA Mix Design

The Marshall mix design method, despite its shortcomings, is still probably the most widely used asphalt mix design method in the world. It is simple, compact and inexpensive. Marshall test for stability and flow and it facilitates rapid testing with minimal effort. However, the compaction method by impact does not simulate conditions that occurs in a real pavement compaction. In addition, the stability parameter does not adequately measure the shear strength of the HMA.

The Hveem mix design procedure was developed in the 1950s, and the California Department of Transportation (Caltrans) has used it. Over the years, refinements and adjustments have been made to the basic Hveem procedure for determining optimum binder content, which is based on the stability determined with a Hveem stabilometer and measurement of laboratory compacted air-void content. Other changes to the basic Hveem method extended its capabilities to polymer-modified mixes, and a modified version was developed so it could be used for gap-graded rubberized mixes. A retained tensile strength test CT 371 (which is similar to AASHTO T 283) is currently used to assess moisture sensitivity, another specified part of mix design. However, few other U.S. states currently use the Hveem procedure and therefore the equipment used in the tests has become increasingly difficult to acquire and maintain—specifically the kneading compactor and the Hveem stabilometer.

The Superpave (SUperior PERforming Asphalt PAVEments) mix design procedure was developed as part of the first Strategic Highway Research Program (SHRP) in the early 1990s to “give highway engineers and contractors the tools they need to design asphalt

pavements that will perform better under extremes of temperature and heavy traffic loads." Superpave (as a whole) was created to make the best use of asphalt paving technology and to present a system that would optimize asphalt mixture resistance to permanent deformation, fatigue cracking and low temperature cracking. The key parts of the process are the Performance Graded (PG) system for specifying the properties of the asphalt binder and the volumetric and densification characteristics determined by the Superpave Gyratory Compactor (SGC). The system was developed and calibrated for a wide range of applications.

The Superpave mix design system integrates material selection and mix design into procedures. The SGC can provide information about the compactability of the particular mixture by capturing data during compaction. Marshall mix design primarily address the determination of asphalt binder content, while Superpave addresses all element of mix design. The Marshall design/construction method requires in most cases compaction 95% or greater of the maximum lab value. Superpave specifications generally require 94% compaction with an allowable variance of +/-2% of maximum theoretic value. The contractors still can compact at higher levels in the field, but it is virtually impossible to achieve a density greater than 100%. If an HMA material was to be over compacted, this also result in a significantly reduced life. Volumetric properties must be met during production to ensure the projected long-term life of the pavement.

The Superpave procedure developed during SHRP included a binder specification (for conventional and polymer-modified binders, but not for rubberized asphalt binder), a volumetric mix design method, and a set of performance-related tests to be performed on

the mix resulting from the volumetric design. The performance related testing included flexural fatigue and frequency sweep tests (both of which became AASHTO T 321), repeated simple shear tests (AASHTO T 320), a low-temperature cracking test, short-term and long-term aging procedures, and a moisture sensitivity test that was later replaced by AASHTO T 283. Between the end of SHRP and the year 2005, most U.S. state highway agencies had adopted either all or part of the Superpave volumetric mix design procedure, nearly always with refinements to suit local conditions, practices, and requirements.

The current Superpave system consists of three interrelated elements: an asphalt binder specification, and a volumetric mix design and analysis system that is based on gyratory compaction. Performance-related mix analysis tests and a performance prediction system that includes environmental and performance models. This last element has been implemented inconsistently on the national scale, with different states using a variety of tests and performance-prediction methods. Several states have chosen not to use any performance-related testing other than a moisture sensitivity test (AASHTO T 283); however, interest has grown in a switch from that test to the Hamburg Wheel Track Test (HWTT) for assessing both moisture sensitivity and rutting. Additionally, many states are using both AASHTO T 324 and T 283 or their own versions of those tests.

Between 1992 and 2005, many major changes were made to the Superpave volumetric mix design procedure, most significantly the elimination of the "restricted zone" in aggregate gradations. Another important change was the simplification of the N_{design} tables. The original implementation of Superpave volumetric design generally recommended use of Superpave Coarse gradations (that is, those passing below the

restricted zone) for locations with increased risk of rutting. However, results from the WesTrack project (1995 to 1999) and experience in several states showed potential risks for rutting, compaction, and permeability with Superpave Coarse gradations, and as a result their use has decreased in some states. When the original Superpave method was developed, one determination with special significance for California was that nearly all the Hveem aggregate gradations that Caltrans had been using successfully were able to pass through the original Superpave specification's restricted zone.

2.6. Asphalt Film Thickness

Literature review has indicated that the rationale behind the minimum VMA requirement for conventional asphalt mixes was to incorporate a minimum desirable asphalt content into the mix to ensure its durability. Studies have shown that asphalt mix durability is directly related to asphalt film thickness. Therefore, the minimum VMA should be based on the minimum desirable asphalt film thickness rather than a minimum asphalt content because the latter will be different for mixes with different gradations. Mixes with a coarse gradation (and, therefore, low surface area) have difficulty meeting the minimum VMA requirement based on minimum asphalt content despite thick asphalt films.

Kandhal et.al (1998) in their review of literature stated that thicker asphalt binder films produced mixes which were flexible and durable, while thin films produced mixes which were brittle, tended to crack and ravel excessively, retarded pavement performance, and reduced its useful service life. Based on the data they analyzed, average film thicknesses ranging from 6 to 8 microns were found to have provided the most desirable

pavement mixtures. They calculated average film thickness by dividing volume of asphalt by surface area of aggregate. Surface area of aggregate depends on the gradation of aggregate being used in the mixture and surface area factor for each sieve, where surface area calculated by multiplying percent passing of aggregate for a certain sieve by surface area factor of that sieve. The Asphalt Institute proposed surface area factors to be used in calculating surface area of aggregate. They also concluded that the film thickness decreases as the surface area of the aggregate is increased.

Radovskiy (2003) analyzed the Asphalt Institute surface area factors in detail. He found that the currently used surface area factors had been calculated assuming minimum particle diameter around 0.030 mm, which underestimated the surface area of the aggregate. His analysis demonstrated that the term "film thickness" had not been properly defined, and proposed a new definition of film thickness. He developed a fundamentally sound model for film thickness calculation by applying a recent result from statistical geometry of particulated composites. The results of calculations were logical and agreed with some important data reported in previous publications.

2.7. Asphalt Mixtures Characterization Tests

2.7.1. Dynamic Modulus Test

The Dynamic Modulus (E*) laboratory test is one of the major input material properties for flexible pavement design. It has been recommended as a Simple Performance Test (SPT) under the National Cooperative Highway Research Program (NCHRP) Project.

For linear viscoelastic materials such as asphalt mixtures, the stress-to-strain relationship under a continuous sinusoidal loading is defined by its complex dynamic modulus (E*). This is a complex number that relates stress to strain for linear viscoelastic materials subjected to continuously applied sinusoidal loading in the frequency domain. The complex modulus is defined as the ratio of the amplitude of the sinusoidal stress (at any given time, t, and angular load frequency, ω), $\sigma = \sigma_0 \sin(\omega t)$ and the amplitude of the sinusoidal strain $\varepsilon = \varepsilon_0 \sin(\omega t - \phi)$, at the same time and frequency, that results in a steady state response (Figure 4):

$$E^* = \frac{\sigma}{\varepsilon} = \frac{\sigma_0 e^{i\omega t}}{\varepsilon_0 e^{i(\omega t - \phi)}} = \frac{\sigma_0 \sin(\omega t)}{\varepsilon_0 \sin(\omega t - \phi)}$$

Where, σ_0 = peak (maximum) stress

ε_0 = peak (maximum) strain

φ = phase angle, degrees

ω = angular velocity

t = time, seconds

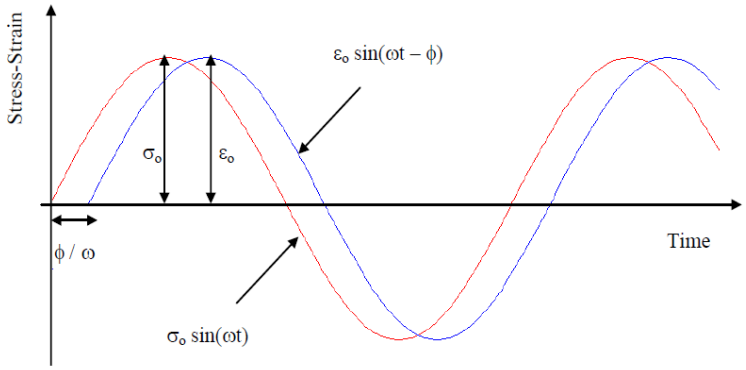

Figure 4 Stress-Strain Cycle, Dynamic Modulus Test

Mathematically, the dynamic modulus is defined as the absolute value of the complex modulus, or:

$$|E^*| = \frac{\sigma_0}{\varepsilon_0}$$

By current practice, dynamic modulus testing of asphalt materials is conducted on unconfined and confined cylindrical specimens having a height to diameter ratio equal to 1.5 and uses a uniaxially applied sinusoidal load (3). Under such conditions, the sinusoidal stress at any given time t, is given as:

$$\sigma_t = \sigma_0 \sin(\omega t)$$

Where:

ω = angular frequency in radian per second.

t = time (sec).

The subsequent dynamic strain at any given time is given by: $\varepsilon_t = \varepsilon_0 \sin(\omega t - \phi)$

The phase angle is simply the angle at which the ε_0 lags σ_0, and is an indicator of the viscous (or elastic) properties of the material being evaluated. Mathematically this is expressed as:

$$\phi = (t_i / t_p) \times (360)$$

Where:

t_i = time lag between a cycle of stress and strain (sec).

t_p = time for a stress cycle (sec).

For a pure elastic material, $\phi = 0°$, it is observed that the complex modulus (E*) is equal to the absolute value, or dynamic modulus. For pure viscous materials, $\phi = 90°$. The E* has a real and imaginary part that defines the elastic and viscous behavior of the linear viscoelastic material:

$E^* = E' + iE''$ and.

$E' = (\sigma_0 / \varepsilon_0) \cos \phi$

$E'' = (\sigma_0 / \varepsilon_0) \sin \phi$

Where:

σ_0 = peak dynamic stress amplitude (kPa).

ε_0 = peak recoverable strain (mm/mm).

ϕ = phase lag or angle (degrees).

The E' value is generally referred to as the storage (elastic) modulus component of the complex modulus, while E" is referred to as the loss (viscous) modulus. The loss tangent ($\tan \phi$) is the ratio of the energy lost to the energy stored in a cyclic deformation and is equal to: $\tan \phi = E'' / E'$

The modulus of the asphalt mixture at all temperatures and time rate of load is determined from a master curve constructed at a reference temperature (generally taken as 21.1 °C). Master curves are constructed using the principle of time-temperature superposition. The data at various temperatures are shifted with respect to time until the curves merge into single smooth function. The master curve of the modulus, as a function

of time, formed in this manner describes the time dependency of the material. The amount of shifting at each temperature required to form the master curve describes the temperature dependency of the material. In general, the master modulus curve can be mathematically modeled by a sigmoidal function described as:

$$\text{Log } |E^*| = \delta + \frac{\alpha}{1+e^{\beta+\gamma(\log t_r)}}$$

Where,

t_r = reduced time of loading at reference temperature

δ = minimum value of E*

$\delta+\alpha$ = maximum value of E*

β, γ = parameters describing the shape of the sigmoidal function

The shift factor can be shown in the following form:

$$a(T) = \frac{t}{t_r}$$

Where,

a(T) = shift factor as a function of temperature

t = time of loading at desired temperature

t_r = time of loading at reference temperature

T = temperature

While classical viscoelastic fundamentals suggest a linear relationship between log a(T) and T (in degrees Fahrenheit/Celsius); years of testing by various researchers have shown that for precision, a second order polynomial relationship between the logarithm of the shift factor i.e. log $a(T_i)$ and the temperature in degrees Fahrenheit (T_i) should be used.

The relationship can be expressed as follows:

$$\text{Log } a(T_i) = aT_i^2 + bT_i + c$$

Where,

$a(T_i)$ = shift factor as a function of temperature T_i

T = temperature of interest, °C

a, b and c = coefficients of the second order polynomial

It should be recognized that if the value of "a" approaches zero; the shift factor equation collapses to the classic linear form.

2.7.2. Repeated Load Flow Number Test

An approach to determine the permanent deformation characteristics of paving materials is to employ a repeated dynamic load test for several thousand repetitions and record he cumulative permanent deformation as a function of the number of cycles (repetitions) over the test period. Figure 5 illustrates the typical relationship between the total cumulative plastic strain and number of load cycles.

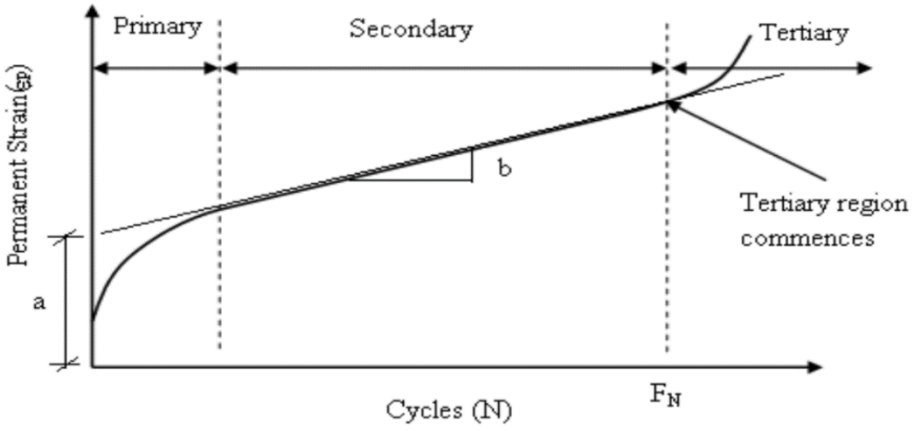

Figure 5. Relationship Between Cumulative Plastic Strain and No. of Load Cycles

The cumulative permanent strain curve is generally defined by three zones: primary, secondary, and tertiary. In the primary zone, permanent deformations accumulate rapidly. The incremental permanent deformations decrease reaching a constant value in the secondary zone. Finally, the incremental permanent deformations again increase and permanent deformations accumulate rapidly in the tertiary zone. The starting point, or cycle number, at which tertiary flow occurs, is referred to as the "Flow Number".

2.7.3. Tensile Strength Ratio

Moisture susceptibility is a significant pavement distress that needs to be addressed by any new development in the asphalt industry. One of the chief problems of CRM mixes is their gradual loss of cohesion, which makes them very vulnerable towards moisture resulting in detaching of aggregates and lower durability (Moreno et al., 2010). The usual practice of testing for moisture susceptibility is through comparison of Tensile Strength Ratios, which includes taking the ratio of Indirect tensile strengths, before and after

conditioning immersed in water at high pavement temperature and follows the AASHTO T-283 testing protocol.

2.7.4. C* Fracture Test

Fracture mechanics provides the underlying principles which govern the initiation and propagation of cracks in materials. Sharp internal or surface notches which exist in various materials intensify local stress distribution. If the energy stored at the vicinity of the notch is equal to the energy required for the formation of new surfaces, then crack growth can take place. Material at the vicinity of the crack relaxes, the strain energy is consumed as surface energy, and the crack grows by an infinitesimal amount. If the rate of release of strain energy is equal to the fracture toughness, then the crack growth takes place under steady state conditions and the failure in unavoidable. The concept of fracture mechanics was first applied to asphalt concrete by Majidzadeh (1970). Abdulshafi (1992) had applied the energy (C*-Line Integral) approach to predicting the pavement fatigue life using the crack initiation, crack propagation, and failure. He concluded that two different tests are required to evaluate first the fatigue life to crack initiation (conventional fatigue testing) and second, the crack propagation phase using notched specimen testing under repeated loading. Abdulshafi and Majidzadeh used notched disk specimens to apply J-integral concept to the fracture and fatigue of asphalt pavements. Various situations such as the effect of load magnitude on fatigue cracking, the length of rest period, load sequence, support conditions, and temperature were included in the testing protocol. Stempihar's (2013) dissertation work provided further development and refinement of the C* Fracture

Test (CFT); Stempihar and Kaloush provided a summary of this work describing specimen geometry, test temperature variation, and a refined data analysis procedure.

The relation between the J-integral and the C* parameters is a method for measuring it experimentally. J is an energy rate and C* is an energy rate or power integral. An energy rate interpretation of J has been discussed by Landes and Begle (1976). J can be interpreted as the energy difference between the two identically loaded bodies having incrementally differing crack lengths.

$$J = -\frac{dU}{da}$$

Where,

U = Potential Energy

a = Crack Length

C* can be calculated in a similar manner using a power rate interpretation. Using this approach C* is the power difference between two identically loaded buddies having incrementally differing crack lengths.

$$C^* = -\frac{\partial U^*}{\partial a}$$

Where, U^* is the power or energy rate defined for a load p and displacement u by

$$U^* = \int_0^u p\,du$$

2.7.5. Axial Cyclic Fatigue Test

Few conventional flexural beam fatigue tests (AASHTO TP 8) were conducted before equipment malfunctions forced the laboratory to pursue alternate methodologies. Several research tasks within NCHRP Project 9-19 developed advanced, fully mechanistic models for asphalt concrete, giving a comprehensive description of permanent deformation and cracking. A large portion of the NCHRP 9-19 advanced models' framework was based on viscoelastic continuum damage (VECD) theories that describe the way small microcracks develop, coalesce and grow into macrocracks (NCHRP Report 547). Research has shown contemporary VECD for asphalt offers several advantages. The primary advantage is the utilization of a single damage characteristic curve, which can be calibrated using less effort in the laboratory than classical beam fatigue tests (Lee and Kim et al., 1998). VECD test specimens can be fabricated in the Superpave gyratory compactor. Once the damage characteristic curve is found, it can theoretically be used to describe the damage and cracking response at any temperature and under any generalized inputs whether stress-control or strain-control, cyclic or monotonic, or random.

Rigorously complete VECD has been used to develop methodologies for multiple cycle fatigue tests with the advantages previously describe, but with more practicality from less mathematical and computational overhead and decreased laboratory characterization burden (Christensen and Bonaquist, et al. 2005, 2008) Another significant advantage of this approach is the characteristics of the specimen geometry, stresses, strains, and temperatures make it able to be integrated into AMPT equipment already being implemented in the broader community for dynamic modulus and flow number performance tests (Hou and Underwood et al., 2010).

3. MATERIALS USED

3.1. Binder

For this study, a PG 64-22 binder was used to prepare RAR modified mixtures and CRM mixtures. Since rubber modifications usually bump up the grade of binder, a PG 70-10 binder which is a stiffer binder was used to create unmodified Control mixtures. All the binder was provided by HollyFrontier Refinery Terminal in Glendale, Arizona.

3.2. Aggregate

For this study, the aggregates were obtained from Southwest Asphalt El Mirage Pit and the materials used for composite gradation consisted of Blended sand, Crusher Fines, 3/8-inch aggregate and 3/4-inch aggregate. Appendix A Figure 52 shows the properties of aggregates obtained from Southwest Asphalt El Mirage Pit.

Figure 6. Aggregate Stockpiles in Southwest Asphalt El Mirage Pit

3.2.1. Aggregate Gradation for RAR Mix

A Gap Gradation NMAS of 12.5mm (1/2-inch) was used to prepare RAR mixtures. Gap Graded refers to a gradation that contains only a small percentage of aggregate particles in the mid-size range. The curve is flat in the mid-size range. This facilitates the addition of RAR particles and creates a better bond with the aggregate and the binder. The aggregate stockpiles obtained from the pit were heated in an oven at 110°C overnight to remove all the moisture from it before sieving them into different sizes. (AASHTO T 2). Appendix A Figure 53 shows the Gradation specification used for RAR mix. The Specification Bands are taken based on type of gradation and NMAS described under Superpave specifications from AASHTO MP 2. Figure 7 shows the gap gradation for RAR modified mix with Superpave control limits.

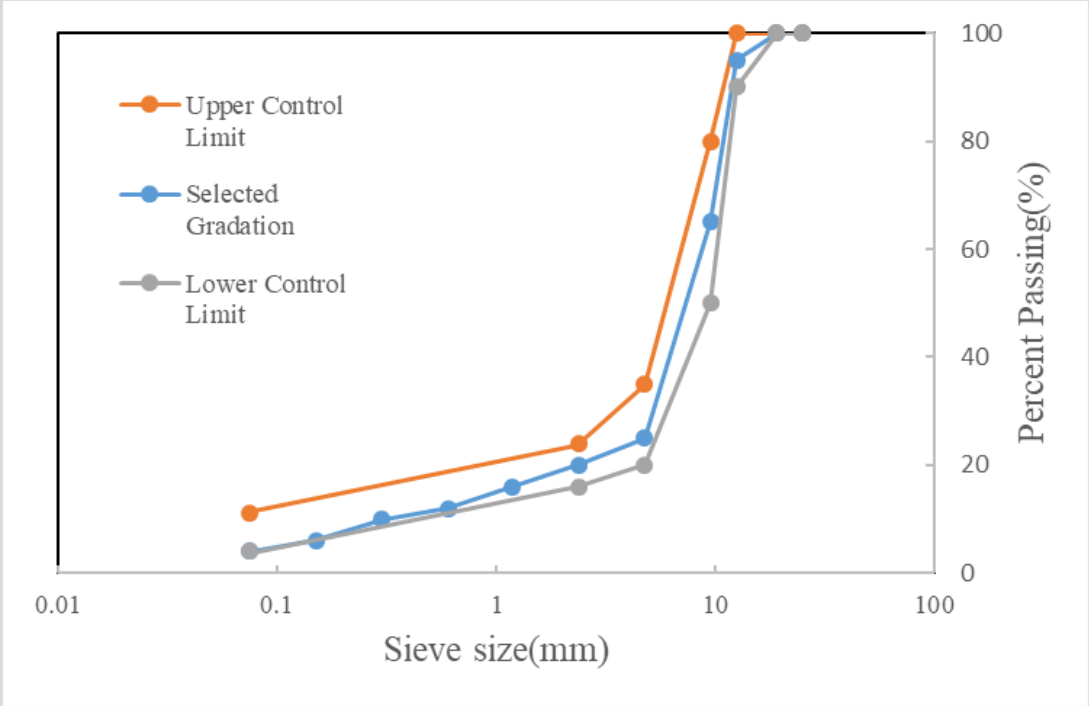

Figure 7. RAR Mix Gap Gradation with Specification Bands

3.2.2. Aggregate Gradation for CRM Mix

A Gap Gradation with NMAS of 12.5mm (1/2-inch) was used to prepare CRM mixtures. Appendix A Figure 54 shows the Gradation specification used for CRM mix. Figure 8 shows the gap gradation for CRM modified mix with Superpave control limits.

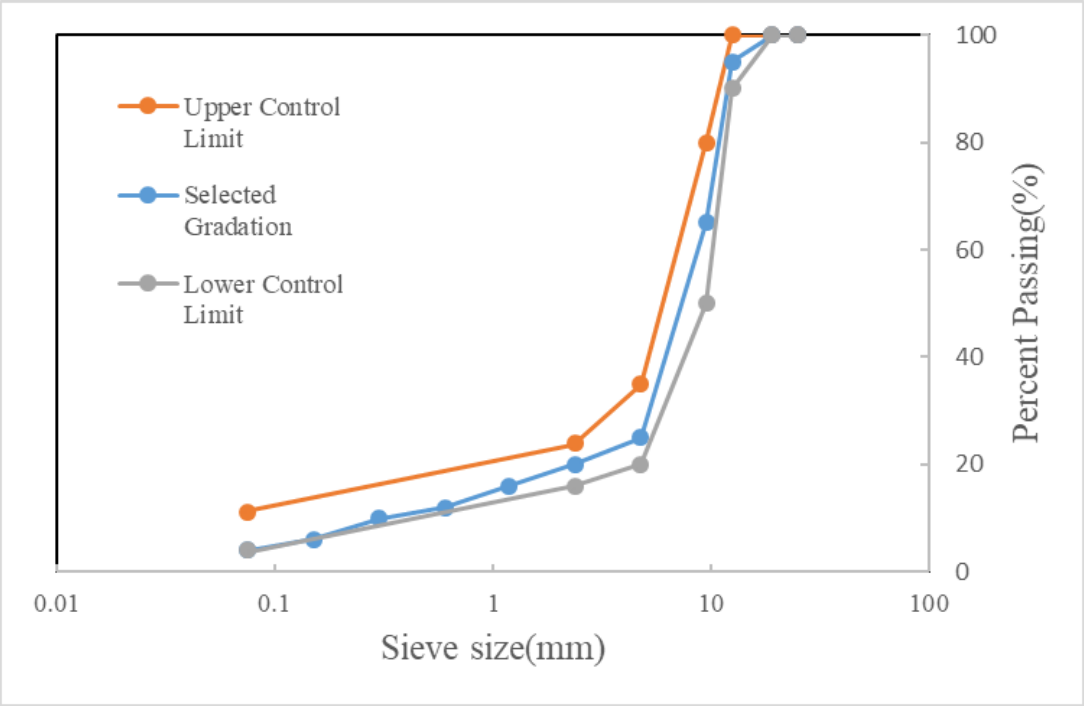

Figure 8. CRM Mix Gap Gradation with Specification Bands

3.2.3 Aggregate Gradation for Control Mix

A Dense Gradation with NMAS of 19mm (3/4-inch) was used to prepare Control mixtures. The gradation of the aggregate was selected following City of Phoenix specifications limits. Appendix Figure 55 shows the Gradation specification used for Control mix. Figure 9 shows the dense gradation for Control mix with Superpave control limits.

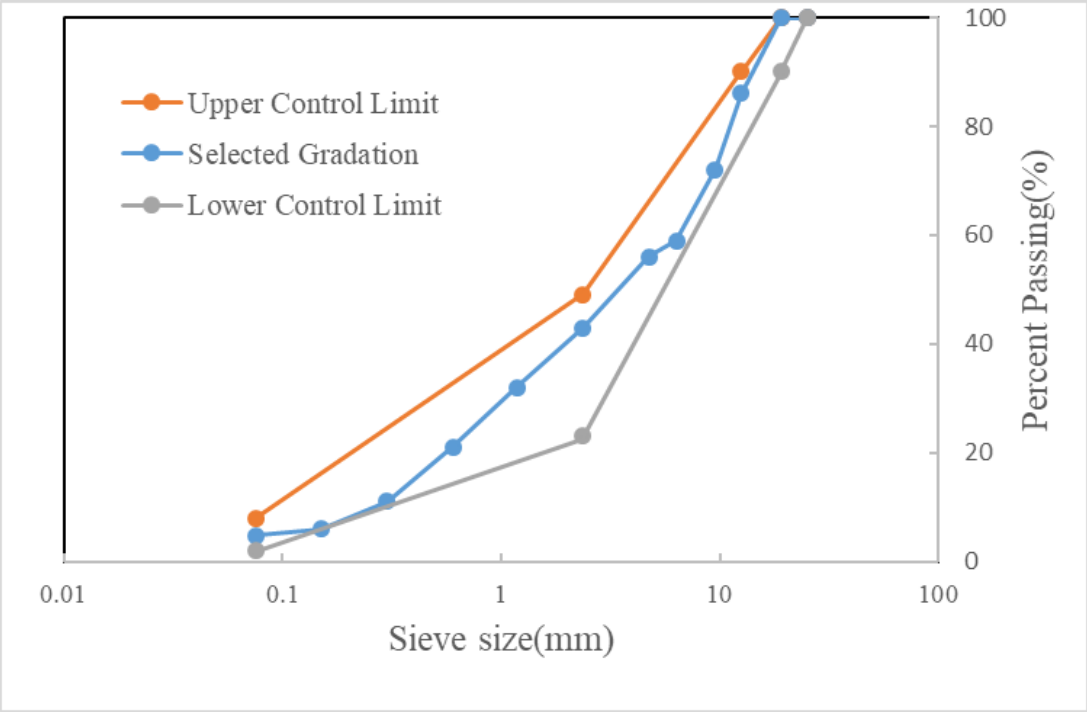

Figure 9. Control Mix Dense Gradation with Specification Bands

3.3 Reacted and Activated Rubber (RAR)

RAR is composed of soft asphalt cement (bitumen), fine crumb tire rubber (usually #30 mesh) and an Activated Mineral Binder Stabilizer (AMBS) at optimized proportions as shown in Figure 10 below. RAR (commercially known as "RARX") was generously provided by Consulpav, Portugal.

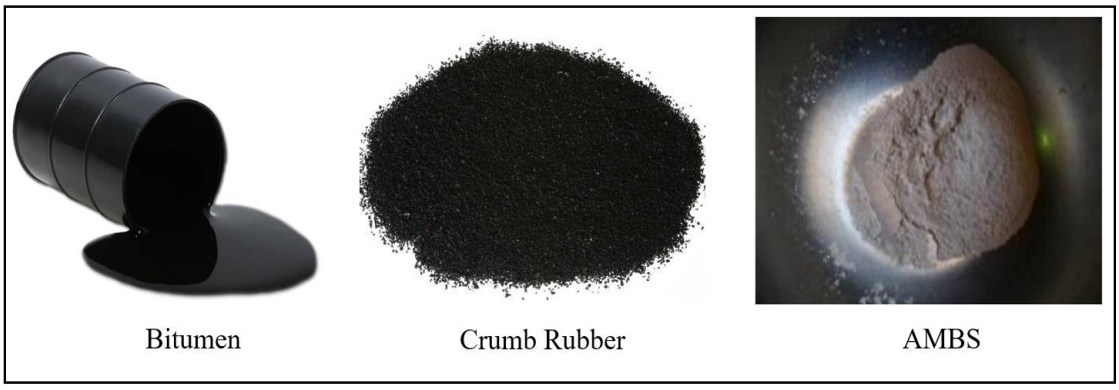

Figure 10. Composition of RARX (Source: Consulpav 2013)

By mass, a typical RAR is made of 56% crumb rubber, 20% bitumen, 20% AMBS and 4% hydrated lime. The composition by volume of RAR, assuming typical specific gravity values from crumb rubber, hydrated lime, bitumen and fine silica (AMBS) are as follow: 65% of crumb rubber, 23% soft bitumen, 10% AMBS and 2% hydrated lime. A brief description of the ingredient is as follows:

The binder can be straight run neat soft bitumen. Binder graded as Pen 100-200 to Pen 35/50, or AC 20, or PG 52 to PG 70, are used. The use of the softer bitumen enables to produce HMA's at common mixing and laying temperatures without losing the proper workability, despite the addition of the crumb rubber.

The Crumb Rubber is usually consisting of scrap tires that are processed and finely ground by any proven industrial method. The scrap tires consist of combination of automobile tires and truck tires, and should be free of steel, fabric or fibers before grinding. To produce RAR, the crumb rubber particles should be finer than 1.0 mm. A #30-mesh maximum particle size is preferred. Cryogenic or ambient ground crumb rubber can be used.

The AMBS is a new micro-scale binder stabilizer that was developed to prevent excessive drainage of the bitumen in SMA mixes during mix haulage, storage and laying. This stabilizer is an activated micro-ground raw silica mineral (40 μm and finer), which is a waste by-product of phosphate industries mining. The activation, achieved by nano monomolecular particle coating was aimed at obtaining thixotropic and shear-thickening properties for the bitumen, since the mastic in the mix should possess high viscosity at rest (haulage, storage and after laying) - for reducing draindown, and low viscosity in motion

(mixing and laying) - for maintaining the proper workability (Ishai et al., 2011). The activator of the silica mineral particles of the AMBS is composed of organic molecules that are partly electrostatically surface charged (ammonium head) and contains organic hydrophobic chains. When the activator particles are present in a liquid medium (bitumen), they can be attracted and connected to other particles with opposite charge. When the fine RAR particles (elastomeric material) are blended in the liquid medium with the activated silica particles, then charged molecules of the AMBS particles are connected to the rubber particles in charged places of the inorganic materials. In this way, where all the above materials are blended together with the hot liquid bitumen, an inner network of the elastomeric material and the AMBS particles is formed in the bitumen. Figure 12 shows the size distribution for the RAR.

Figure 11. Reacted and Activated Rubber (RAR)

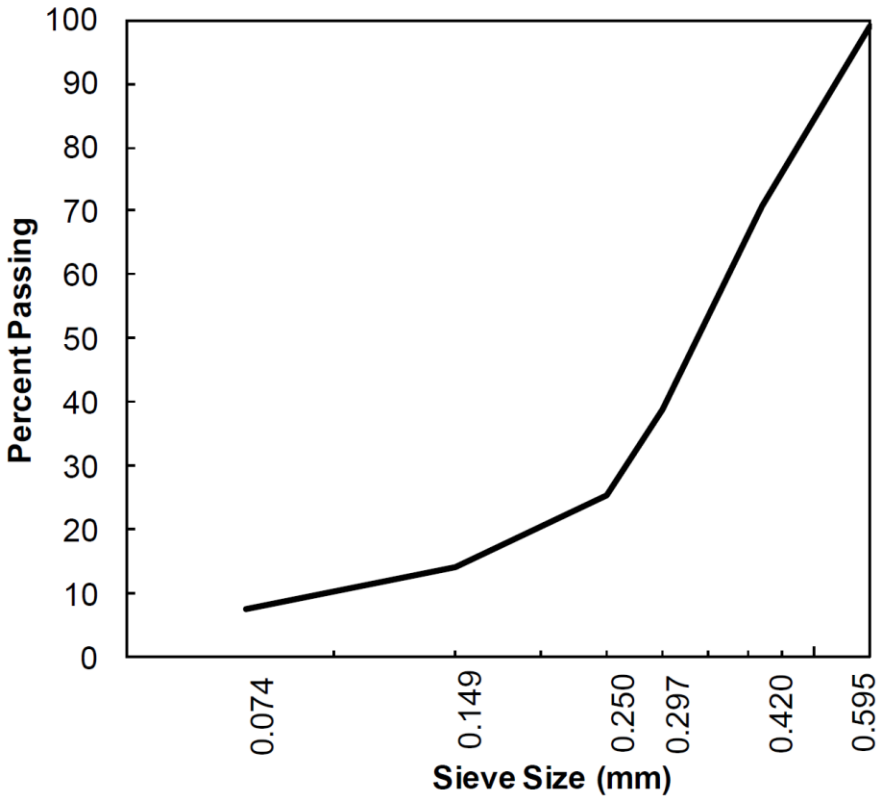

Figure 12. Size Distribution for RAR

3.3.1. RAR Mixture Composition

For this study, 35% RAR (by weight of binder) was added to the aggregate prior to mixing with the neat binder. The optimized percentage of 35% RAR was suggested by Consulpav (Portugal) based on ongoing projects at the time. Figure 13 represents a phase diagram example of a 1000g RAR mixture with 10% total binder content and 35% RAR for better understanding of the mixture composition.

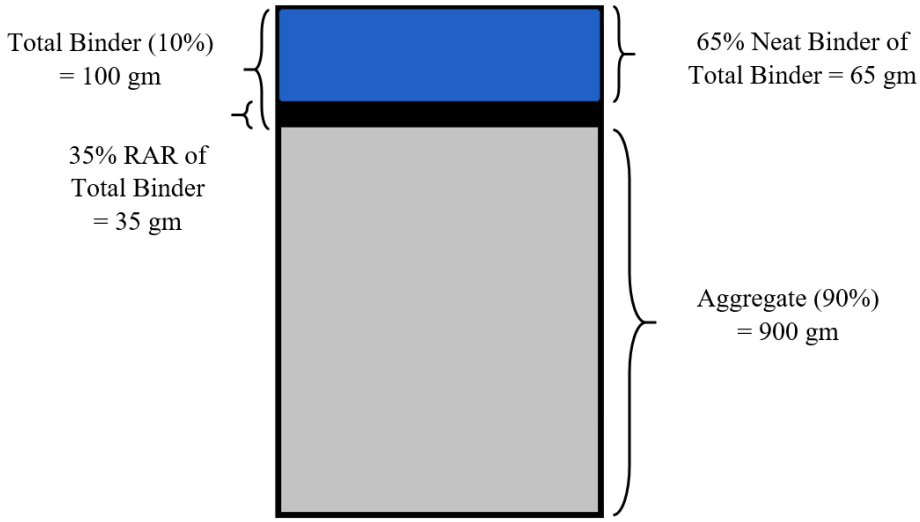

Figure 13. RAR Mixture Composition

3.3.2. RAR Mixture Preparation

The aggregates were heated to 190 °C for 6 hours then hand mixed with RAR kept at ambient temperature for 30 seconds to ensure a homogenous mix just before mixing with the binder. The PG 64-22 binder was heated at 175°C for 2 hours. To compensate for the fact that RAR is added at regular ambient temperature, it is recommended that the heating of the binder is 5°C above the normal temperature used for this kind of mixtures but not exceeding 195°C. After the temperature of aggregates reached 175°C after addition of RAR, the binder was added to the mix. This mix was then subjected to short-term aging of 4 hours at a temperature of 135°C. Before compaction, the mix was placed into moulds and heated for 1.5 hours at 165°C before compaction. During this time, RAR coatings activate the binder and aggregate surfaces. The samples were released from moulds after 30 mins.

3.4. Crumb Rubber

The crumb rubber for this study was provided by Crumb Rubber Manufacturers, Mesa. A #30 mesh maximum particle size is preferred. Cryogenic or ambient ground crumb rubber can be used. The particle gradation was similar to RAR.

Figure 14. Crumb Rubber (CR)

3.4.1. Crumb Rubber Modified Binder (CRMB) Preparation

CRMB was prepared by adding 20% CRM (by weight of total binder) to PG 64-22 Binder. The binder was heated at 177°C for 1 hour to liquefy it before setting it up in the mixing apparatus. As part of the wet process, CRMB was prepared using a High Shear Mixer set at 7000 RPM and a temperature of 177℃ for 45 mins to let the crumb rubber swell. Figure 15 shows the High Shear Mixer used for mixing crumb rubber with the binder.

Figure 15. Ross High Shear Mixer

Figure 16 shows the CRMB after mixing. The effect of mixing Crumb Rubber can be easily seen from the gritty texture of the CRMB.

Figure 16. Crumb Rubber Modifier Binder (CRMB)

3.4.2. Mixture Composition

For this study, 20% (by weight of binder) of crumb rubber was added to binder prior to mixing with the aggregate. To make true comparison between RAR mixtures and CRM mixtures, 20% CR (by weight of binder) was selected since RAR consists of 56-58% crumb rubber by weight. Thus, for 35% RAR, the CR amount equals to 20% which is also what is conventionally used in the US.

Figure 17 represents a phase diagram example of a 1000g CR mixture with 10% binder content and 20% CR for better understanding of the mixture composition.

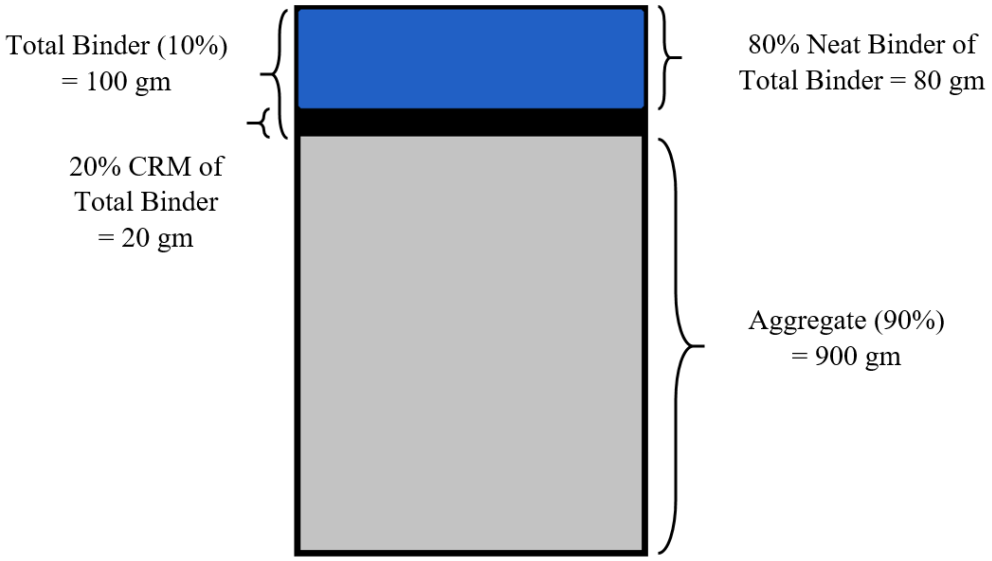

Figure 17. CRM Mixture Composition

3.4.3. Mixture Preparation

The Aggregates were heated to 175 °C overnight. The CRMB was heated at 175°C for 2 hours before mixing. This mix was then subjected to short-term aging of 4 hours at a temperature of 135°C. Then the mix was placed into moulds and heated for 1.5 hours at 165°C before compaction. The sample was released from mould after 30 mins.

3.5. Hydrated Lime

Type N Hydrated Lime was used as a filler added to the aggregates in preparation of Control mixtures obtained from Lhoist North America (LNA), USA.

4. SUPERPAVE MIX DESIGN

As noted earlier, the Superpave mix design was developed by SHRP to replace the older Hveem and Marshall design methods. Superpave primarily addresses two pavement distresses: permanent deformation (rutting), which results from inadequate shear strength in the asphalt mix, and low temperature cracking, which occurs when an asphalt layer shrinks and the tensile stress exceeds the tensile strength. The Superpave system consists of three interrelated elements:

1) An Asphalt binder specification.

2) A Volumetric mix design and analysis system based on gyratory compaction.

3) Performance-related mix analysis tests and a performance prediction system that includes environmental and performance models.

The Superpave mix design method considers density and volumetric analysis, but unlike the Hveem method Superpave also considers regional climate and traffic volume in the aggregate and binder selection processes. Superpave uses the SHRP gyratory compactor for production of cylindrical test specimens. Its compaction load is applied on the sample's top while the sample is inclined at 1.25 degrees. This orientation is aimed at mimicking the compaction achieved in the field using a rolling wheel compactor.

Typical Superpave mix design consists of the following general steps:

(1) PG Binder Selection

A binder grade is first selected by geographic area, pavement temperature, or air temperature. For example, Caltrans published a map designating PG binder grades for different climate regions in California, with boundaries on each route in the state defined by post mile. If traffic volume is heavy, an adjustment is made to a higher binder grade.

(2) Aggregate Selection

An acceptable aggregate structure has to first meet the consensus properties including coarse aggregate angularity, flat and elongated particle percentage, fine aggregate angularity, and clay content. A trial compaction is then performed to estimate volumetric properties and dust proportion to check against the criteria. An estimate of binder content is also calculated for specimen preparation.

(3) Specimen Preparation and Compaction

A minimum of two specimens are prepared at each of these four binder contents (by total weight of mixture [TWM]): estimated binder content, estimated binder content ±0.5%, and estimated binder content +1.0%. These specimens are compacted to N_{max}.

(4) Data Analysis

Compaction densities at different levels of gyration are back calculated from the measured bulk specific gravity. Volumetric properties (%VMA and %VFA) and dust proportion are calculated at N_{design} and plotted versus the four binder contents tested.

(5) Optimal Binder Content Selection

The binder content at 4 percent air-void content is selected as the OBC. Volumetric properties, dust proportion, and compaction density at $N_{initial}$ and $N_{maximum}$ are determined and then verified regarding whether they are met at the OBC.

4.1. RAR Mix

4.1.1. Sample Preparation

Three Asphalt Binder content 8.5%, 9.0% and 9.5% were selected with 35% RAR for optimum asphalt binder percent selection using Superpave Mix Design. Two samples of 150 mm (6-inch) diameter cylinder approximately 115 mm (4.5 inches) in height and 4700 g in weight were compacted for each asphalt binder content. Servopac Gyratory Compactor was used for compaction. A flat and circular load was applied with a diameter of 149.5 mm and a compaction pressure of 600 kPa (87 psi). For traffic level 3 to < 10 million Design ESALs, $N_{initial} = 8$, $N_{design} = 100$, $N_{maximum} = 160$.

The mixture preparation procedure followed was same as described in section 3.3.2. except the short-term aging which was done at compaction temperature for 2 hours. For each binder content, one mix batch was prepared to determine the maximum specific gravity (AASHTO T 209). Two mix batches were prepared for gyratory compaction (AASHTO T 312).

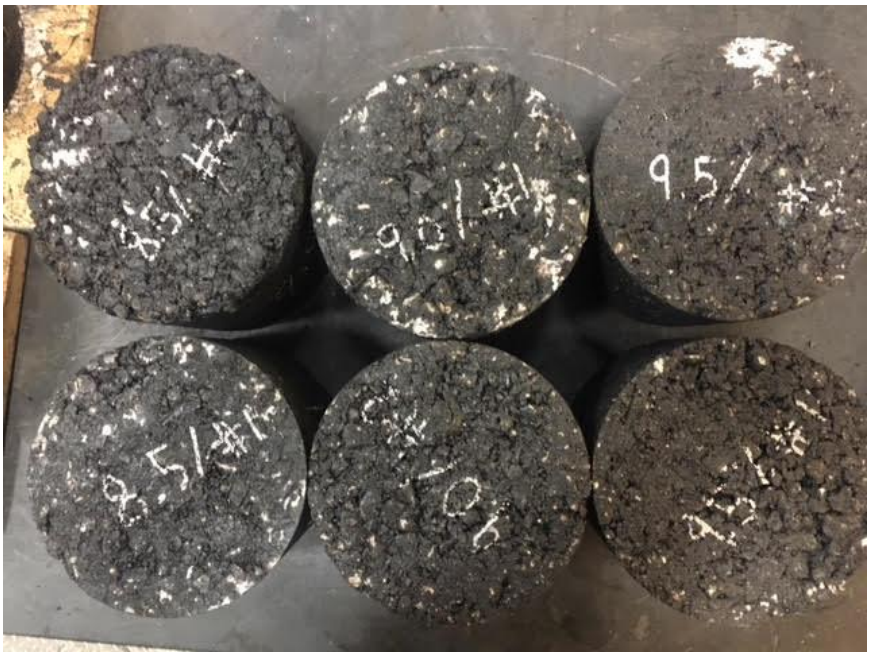

Figure 18. Compacted Superpave Mix Design Samples for RAR Mixtures

4.2. Crumb Rubber Mix

4.2.1 Sample Preparation

Three Asphalt Binder content 7.0%, 7.5% and 8.0% were selected with 20% CRM for optimum asphalt binder percent selection using Superpave mix design. Two samples of 150 mm (6-inch) diameter cylinder approximately 115 mm (4.5 inches) in height and 4700g in weight were compacted for each asphalt binder content. Servopac Gyratory Compactor was used for compaction. A flat and circular load was applied with a diameter of 149.5 mm and a compaction pressure of 600 kPa (87 psi). For traffic level 3 to < 10 million Design ESALs, $N_{initial}$ = 8, N_{design} = 100, $N_{maximum}$ = 160.

The mixture preparation procedure followed was same as described in section 3.4.3. except the short-term aging which was done at compaction temperature for 2 hours.

For each binder content, one mix batch was prepared to determine the maximum specific gravity (AASHTO T 209). Two mix batches were prepared for gyratory compaction (AASHTO T 312).

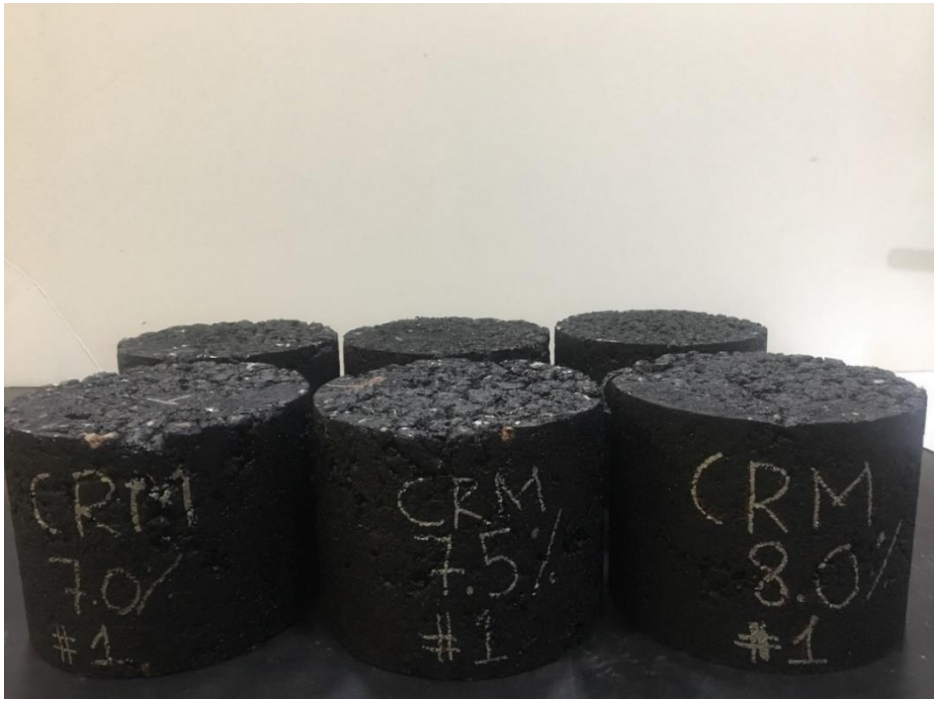

Figure 19. Compacted Superpave Mix Design Samples for CRM Mixtures

4.3. Control Mix

4.3.1. Sample Preparation

Three Asphalt Binder content 4.5%, 5.0% and 5.5% were selected for Control mixtures for optimum asphalt binder percent selection using Superpave Mix Design. Two samples of 150 mm (6-inch) diameter cylinder approximately 115 mm (4.5 inches) in height and 4700g in weight were compacted for each asphalt binder content. Servopac Gyratory Compactor was used for compaction. A flat and circular load was applied with a diameter of 149.5 mm and a compaction pressure of 600 kPa (87 psi). For traffic level 3 to < 10 million Design ESALs, $N_{initial}$ = 8, N_{design} = 100, $N_{maximum}$ = 160.

The Aggregates were heated to 163 °C for overnight. The PG 70-10 binder was heated at 160°C for 2 hours before mixing with the aggregates. This mix was then short-term aging of two hours at a compaction temperature of 150°C. For each binder content, one mix batch was prepared to determine the maximum specific gravity (AASHTO T 209). Two mix batches were prepared for gyratory compaction (AASHTO T 312).

Figure 20 Compacted Superpave Mix Design Samples for Control Mixtures

4.4. Optimum Binder Content Volumetric Properties

Superpave mix design was performed using the asphalt binder contents stated above for each mix. Optimum binder content of 9.25% was achieved for RAR mix. Optimum binder content of 7.60% was achieved for CRM mix. Optimum binder content of 5.10% was achieved for Control mix. Summary of volumetric properties for optimum binder content of each mix is summarized in Table 3 below.

Table 3. OBC Volumetric Properties

Property	**RAR Mix 9.25%**	**CRM Mix 7.6%**	**Control Mix 5.1%**	**Criteria**
% Air Voids	4.0 %	4.0%	4.0 %	4.0 %
% VMA	22.1 %	18.3%	14.6 %	14 % Min
% VFA	81.7 %	78.0%	73.0 %	65 – 75%
Dust Proportion	0.7	0.6	1.0	0.6 – 1.2
% G_{mm} @ $N_{initial}$	86.4 %	87.6 %	88.7 %	89 % Max
% G_{mm} @ N_{max}	97.3 %	97.2 %	97.0 %	98 % Max

VFA represents the portion of the voids in the mineral aggregate that contain binder. This represents the volume of the effective asphalt content. The criteria for VFA is a function of traffic level and the current specifications doesn't take into consideration mixtures modified with crumb rubber. VFA is a somewhat redundant term since it is a function of air voids and VMA (Roberts et al., 1996). VFA is inversely related to air voids; as the air voids decreases, the VFA increases.

The Gap Graded RAR mix and Gap Graded CRM mix were compacted to 4% air voids and both the mixes had high volume of effective binder which resulted in high VFA values to ensure the density of the mixture. If not, the interlock of aggregates would not have been good enough.

5. LABORATORY TESTS PERFORMED

5.1. Dynamic Modulus Test

5.1.1. Summary of Test Method

The AASHTO T 342 was followed for E* testing. For each mix, three replicates were used. For each specimen, E* tests were conducted at -10, 4.4, 21.1, 37.8 and 54.4 °C and 25, 10, 5, 1, 0.5 and 0.1 Hz loading frequencies. A 60 second rest period was used between each frequency to allow some specimen recovery before applying the new loading at a lower frequency.

5.1.2. Test Specimen Preparation

The axial deformations of the specimens were measured through three spring-loaded Linear Variable Differential Transducers (LVDTs) placed vertically on diametrically opposite sides of the specimen. Parallel brass studs were used to secure the LVDTs in place. Two pairs of studs were glued at 120° to each pair on cylindrical surfaces of a specimen; each stud in a pair, being 100-mm apart and located at approximately the same distance from the top and bottom of the specimen. To eliminate any top or bottom surface friction, pairs of rubber membranes, slightly coated with vacuum grease between the membranes, were placed on top and bottom of each specimen during testing. Figure 21 shows the schematic presentation of the instrumentation. An instrumented sample used for the |E*| test is presented in Figure 22.

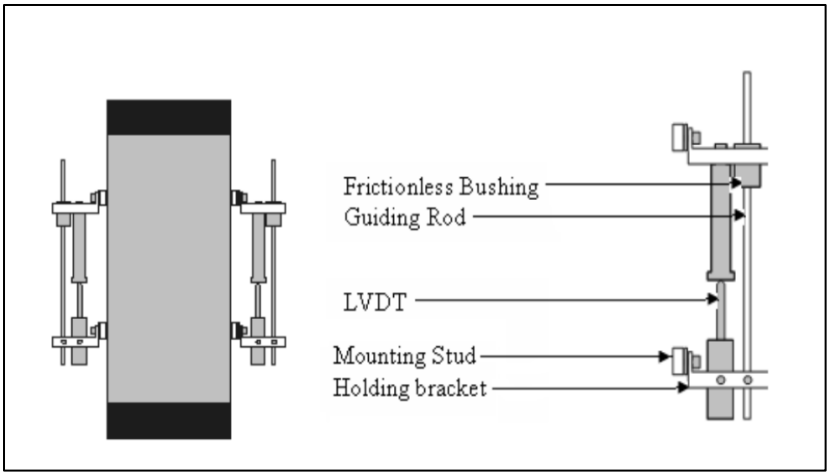

Figure 21. Schematic Presentation of |E*| Sample Instrumentation

Figure 22. Instrumented Dynamic Modulus |E*| Test Sample

5.2. Repeated Load/ Flow Number Test

5.2.1. Summary of Test Method

Repeated load tests were conducted using two replicate test specimens for both reference gap graded and asphalt rubber gap graded mixtures. All tests were carried out on cylindrical specimens, 100 mm in diameter and 150 mm in height. Figure 23 shows a photograph of an actual specimen set-up for unconfined test.

Thin and fully lubricated membranes at the test specimen ends were used to warrant frictionless surface conditions. All tests were conducted within an environmentally controlled chamber throughout the testing sequence (i.e., temperature was held constant within the chamber to ±0.5 °C throughout the entire test). The tests were conducted unconfined at 50 °C and at a stress level of 400 kPa (58 psi).

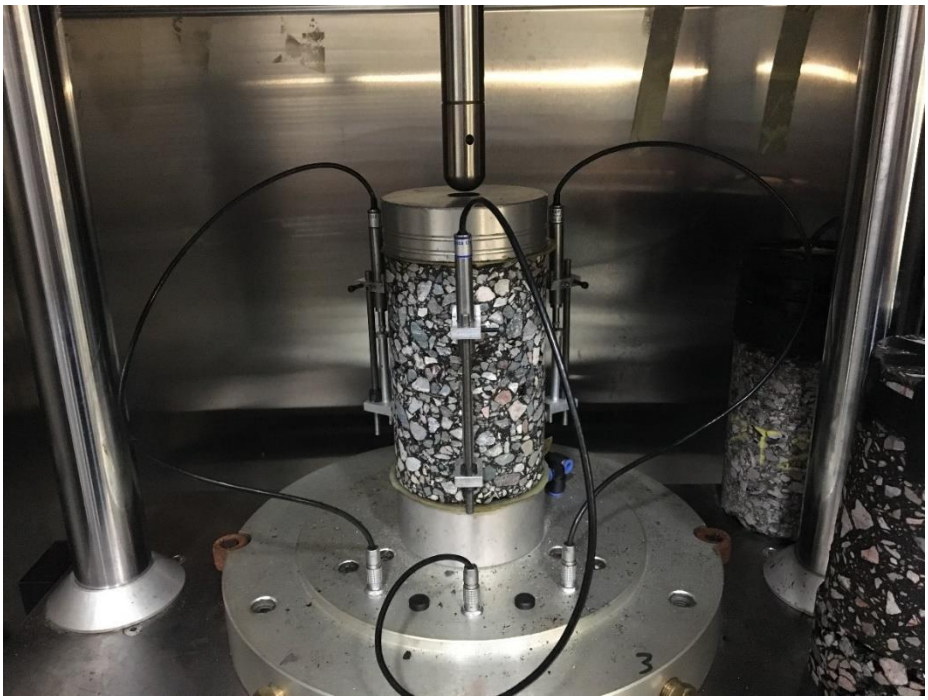

Figure 23. Instrumented and Set-up Specimen for Flow Number Test

5.3. Tensile Strength Ratio

5.3.1. Conditioning of samples

i. One of the subsets were conditioned to test indirect tensile strength.

ii. The specimens were subjected to vacuum saturation with a minimum of 25mm water level above the specimens.

iii. Vacuum of 13 to 67 kPa (10 to 26 in. Hg partial pressure) absolute pressure was applied for 5 to 10 min. Then Vacuum was removed, and sample left submerged for 5-10 min.

iv. The surface saturated dry mass (B' gm) of the vacuum saturated was recorded and percentage saturation (S') was calculated by knowing the dry weight (A gm.) of the specimen.

$$S' = 100 * \frac{(B' - A)}{Va}$$

where Volume of air voids $Va = Pa * \frac{E}{100}\ cm^3$

E is the volume of specimen in cm^3 and P_a is the percentage air voids in specimen.

v. The degree of saturation between 70 to 80 percent were targeted. Once the sample is in this saturation range, the procedure continued

vi. The specimens were wrapped tightly with plastic film and were placed into the plastic bag with 10 ml of water in it and were sealed and cooled at -18°C for a minimum of 16 hours.

vii. Later the samples were placed in the water bath maintained at 60 °C with at least 25 mm water above the specimen surface for 24 +/- 1 hours and removed.

5.3.2. Summary of Test Method

This test involves comparing the indirect tensile strengths of moisture conditioned and unconditioned asphalt samples. The conditioning of the asphalt samples is achieved by keeping the asphalt samples submerged under water in an environment control chamber maintained at 60 °C for a period of 24 hours. After the temperature conditioning, the samples are brought to the room temperature by conditioning at 25°C for 2 hours. The unconditioned samples are kept in room temperature during the conditioning period of the samples and the temperature is normalized by submerging in a water bath for 2 hours maintained at 25 °C. Both the conditioned and unconditioned samples are tested for indirect tensile strengths by loading cylindrical samples along their diameters. The calculations for TSR are given below:

$$\sigma = \frac{2S}{\pi * t * d}$$

Where σ is the strength of cylindrical asphalt sample, MPa

S is the maximum indirect tensile load sustained by the specimen, N

t is the thickness of cylindrical asphalt sample, mm

d is the diameter of cylindrical asphalt sample, mm

The strength of the samples was determined for both the conditioned and unconditioned asphalt samples. TSR is given by:

$$\text{TSR} = \frac{\sigma_C}{\sigma_{UC}}$$

Where σ_C is the conditioned tensile strength of the asphalt mixture specimen

and σ_{UC} is the unconditioned tensile strength of the asphalt mixture specimen

Figure 24. Dry and Wet Conditioning Subsets for TSR

5.4. C* Fracture Test

5.4.1. Specimen Preparation

The specimens were produced by cutting two 50 mm thick specimens from the center of a 150mm diameter by 180 mm tall gyratory compacted sample. A right-angle notch (25 mm deep) was carefully cut into the specimen using a water-cooled diamond blade and a jig to hold the specimen. The specimen was rotated 45° in each direction from the vertical centerline to facilitate cutting the notch edges vertically. Next, a diamond coated scroll saw blade was used to introduce a 3 mm deep by 1.6 mm wide initial crack into the specimen. Finally, the specimen face was painted white using acrylic paint and 10

mm incremental lines were marked on the specimen face to monitor crack progression during the test. Testing was conducted using a servo-hydraulic, Universal Testing Machine with 100kN load capacity and environmental control chamber. Crack propagation rate was captured using a high definition digital video camera and crack length versus time measurements were extracted visually from video playback.

5.4.2. Method for C* Determination

- For multiple specimens tested at different displacement rates, the data are collected as load and crack length versus time for a constant displacement rate.
- The load value is adjusted taking into consideration the sample thickness. This is done by dividing the load value by the sample thickness; then the load and crack length versus time are plotted for each displacement rate.
- The load and the displacement rates are plotted for each crack length. The energy rate input U* is measured as the area under the curve in step above. The areas under the curve were calculated by end area method. After that, the U* values were obtained and plotted versus crack length for each displacement rate. The slope of these curves is C* value for each displacement rate.
- The crack growth rates were calculated for each displacement rate as the total crack length divided by the time. These values also were corrected according to the sample thickness. The crack growth rate versus the displacement rate values were plotted for all the mixtures.

- The C* versus the crack growth rate are plotted for the mixes to compare the performance of each mix through the slope of this relationship where the higher the slope the higher the resistance of the mix to crack propagation.

Table 4. Displacement Rates used for all mixtures

Displacement Rate, Δ* (mm/min)	Displacement Rate, Δ* (mm/sec)
0.38	0.0063
0.51	0.0085
0.64	0.0107
0.76	0.0127
0.89	0.0148

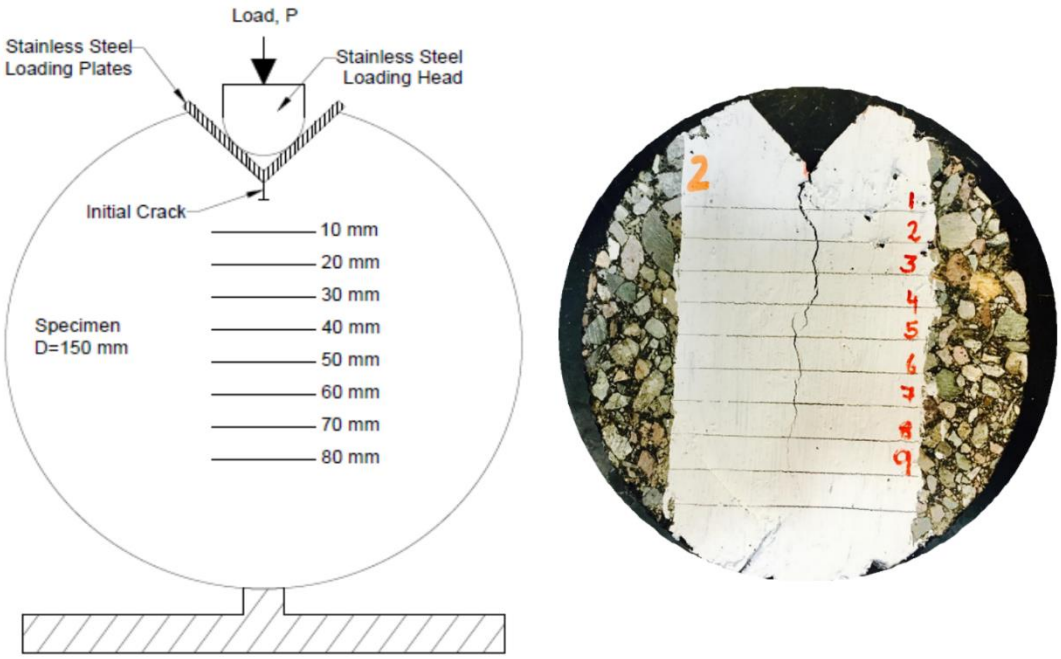

Figure 25. Schematic and Actual C* Sample Using RAR

Figure 26. 3D Printed Template Used for C* Fracture Test Sample Markings

5.5. Axial Cyclic Fatigue Test

Ideally, only one temperature and one strain level condition are required to obtain the damage characteristic curve (C-S curve), which relates material integrity to microstructural damage. The C-S curve has been shown to be a unique material property of asphalt concrete that is independent of temperature and strain conditions. A fingerprint dynamic modulus (|E*|) test is performed before initiation of the fatigue testing; this not only checks the variation of the replicates but also obtains the machine compliance. The Axial Cyclic Fatigue Test is controlled by actuator displacement, which is determined from the target on-specimen peak to peak strain level (entered by the user) and the machine compliance factors. As noted in AASHTO TP 107, the strain level calculated for the actuator displacement will not necessarily be the same as what the specimen experiences

because the machine compliance factors are likely to be notably large and specific to the testing equipment and specimen.

The current AASHTO TP 107 protocol recommends an initial on-specimen peak-to-peak strain level of 300 με, with adjustments for the second and third specimens depending on the number of cycles to failure of the first specimen. Although the 300-με strain could be appropriate for some asphalt mixtures, it may not work for others. Trial and error is usually needed to identify the actuator displacement amplitude that results in failure at either 1,000 cycles or 10,000 cycles, corresponding to high strain and low strain, respectively.

The loading process can be divided into three stages to better explain the relationship between the microdamage and the macroscopic behavior of the test specimen during the test. In the first stage (from start to about 100 cycles in this example), |E*| decreased at a very steep rate, whereas the phase angle increased dramatically; this behavior signifies that an appreciable amount of damage accumulated in the specimen early in the loading history. After that, the |E*| decreased, and the phase angle increased at a relatively flat rate, indicating the damage induced by fatigue was developing and building in magnitude. In the last stage, the |E*| underwent a rapid drop and, conversely, the phase angle increased to a maximum value and then dropped dramatically, indicating the specimen had failed and a macrocrack had formed (Resse et. al, 1997).

5.5.1. Specimen Preparation

The mixtures were characterized using axial, DT-compression push-pull fatigue characterization tests on laboratory-produced specimens fabricated in the gyratory

compactor at 4.0 percent ±0.5 percent air void content. The test temperature was 64 °F (18 °C) but the cylindrical test specimens were a standard 5.8-inch (150-mm) height and a smaller 3-inch (75-mm) diameter (Kutay et al., 2009). This gave a narrower aspect ratio because the specimens were bonded at the ends to metal platens to avoid end effects caused by the complex stress states near the fixed ends. LVDTs were mounted on the specimen over the center portion, where the axial stress is essentially one dimension, simple uniaxial. Subsequent research found this specimen geometry was not necessary and standard AMPT size specimens are acceptable. The equipment used to conduct the test was a universal load frame because AMPT equipment was not readily available at the time of these tests. Fixtures and grips are required to connect the test specimen to the load frame that effectively eliminates eccentricity to avoid a torque or stress moment in the test specimen thereby providing uniaxial stress conditions in the center portion.

Figure 27. Mounted Axial Cyclic Fatigue Sample

6. RESULTS AND ANALYSIS

6.1. Dynamic Modulus Test

The E* values of all mixes were compared for 6 frequencies and 5 temperatures along with the Control mix. The Master Curve below in Figure 28 shows that RAR modified mixes have lower moduli at lower temperatures, which is desirable for better resistance to thermal cracking; whereas CRM mix had higher moduli value at higher temperatures indicating best potential resistance to permanent deformation. The RAR mixture had higher moduli at higher temperatures than the control mix; but lower moduli at high temperatures compared to the CRM mix

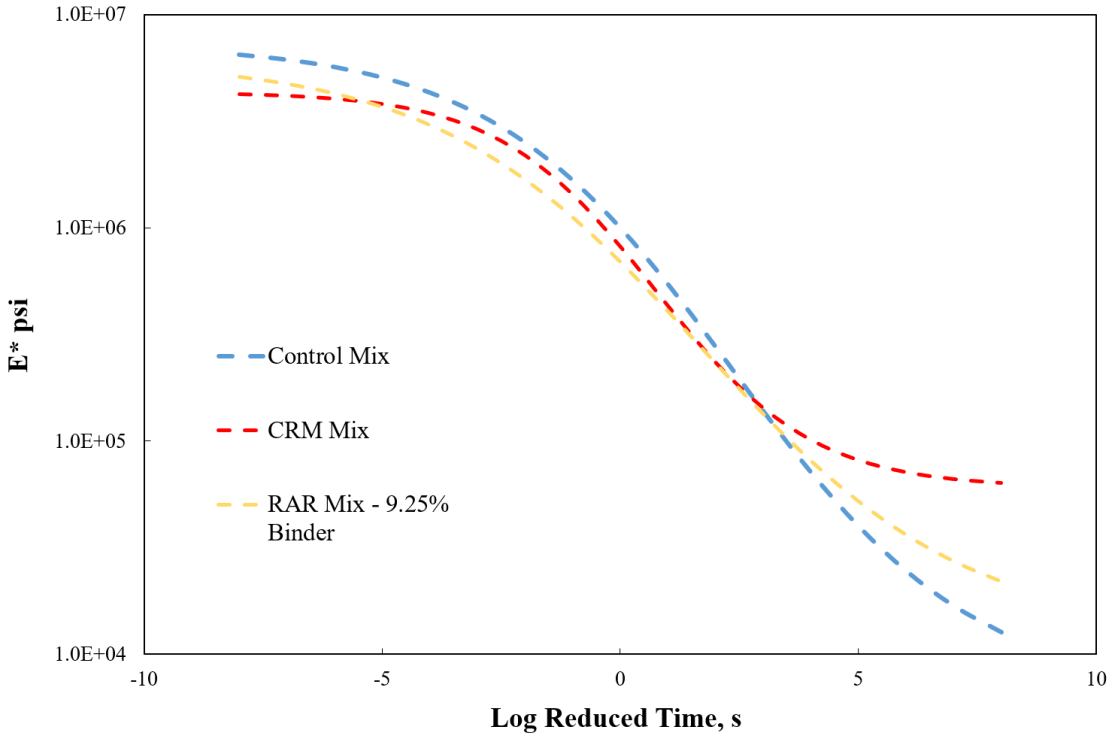

Figure 28. Master Curve - Average E* Values of All Mixtures

6.1.1. Comparison of Results by Frequency and Temperature

The modulus values obtained from the dynamic modulus tests can be better compared for each mix at the specific combinations of frequencies and temperatures. The modulus values were plotted against frequency for each temperature. The plots for each temperature are shown in the figures below.

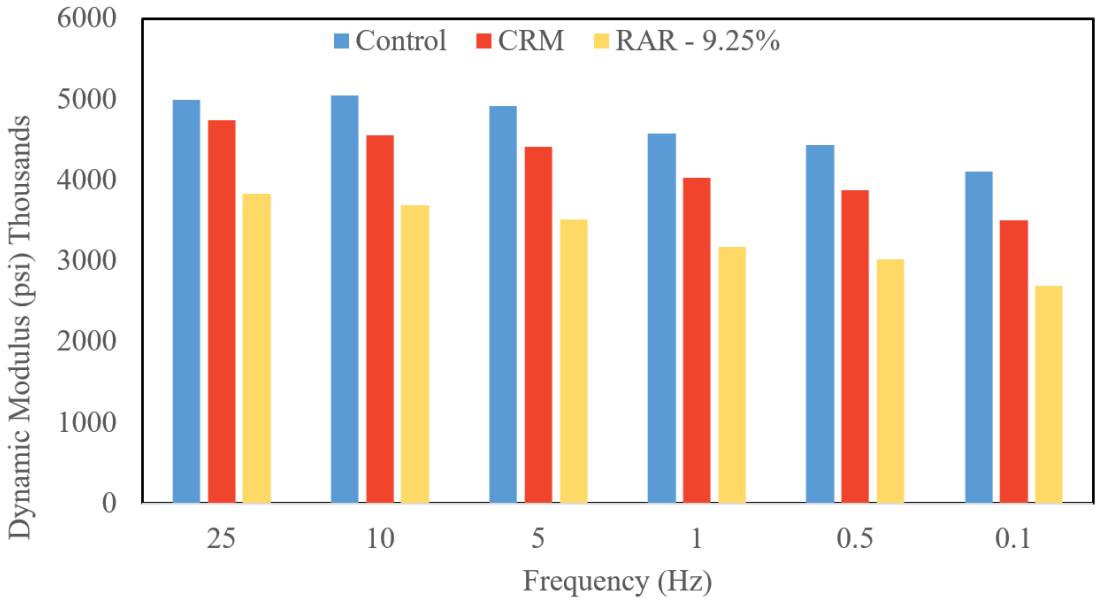

Figure 29. Modulus Comparison of All Mixtures at All Frequencies for -10°C

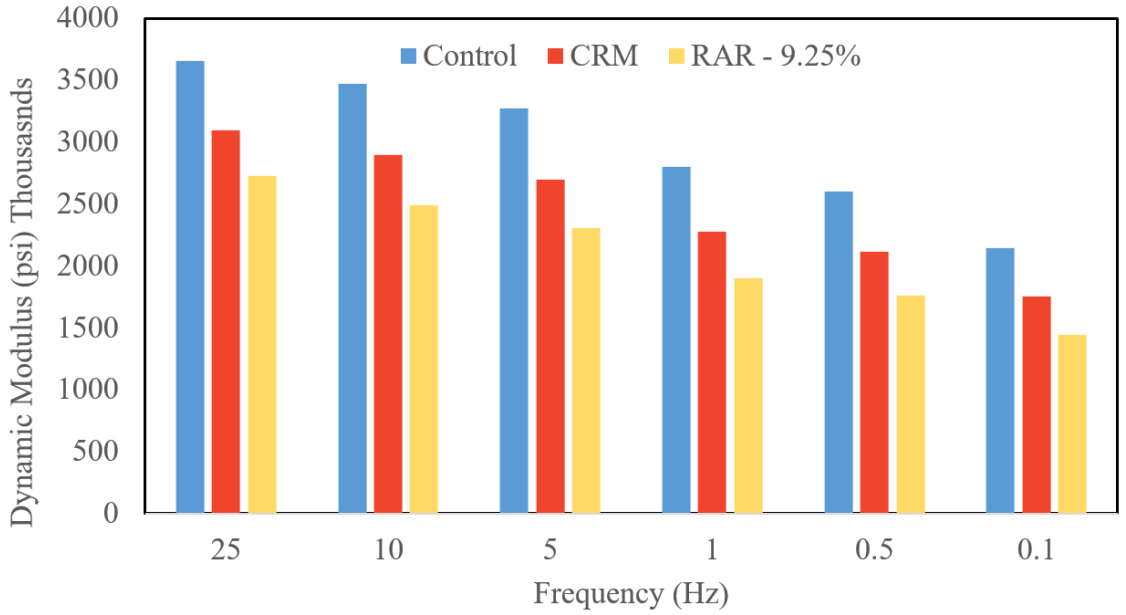

Figure 30. Modulus Comparison of All Mixtures at All Frequencies for 4.4°C

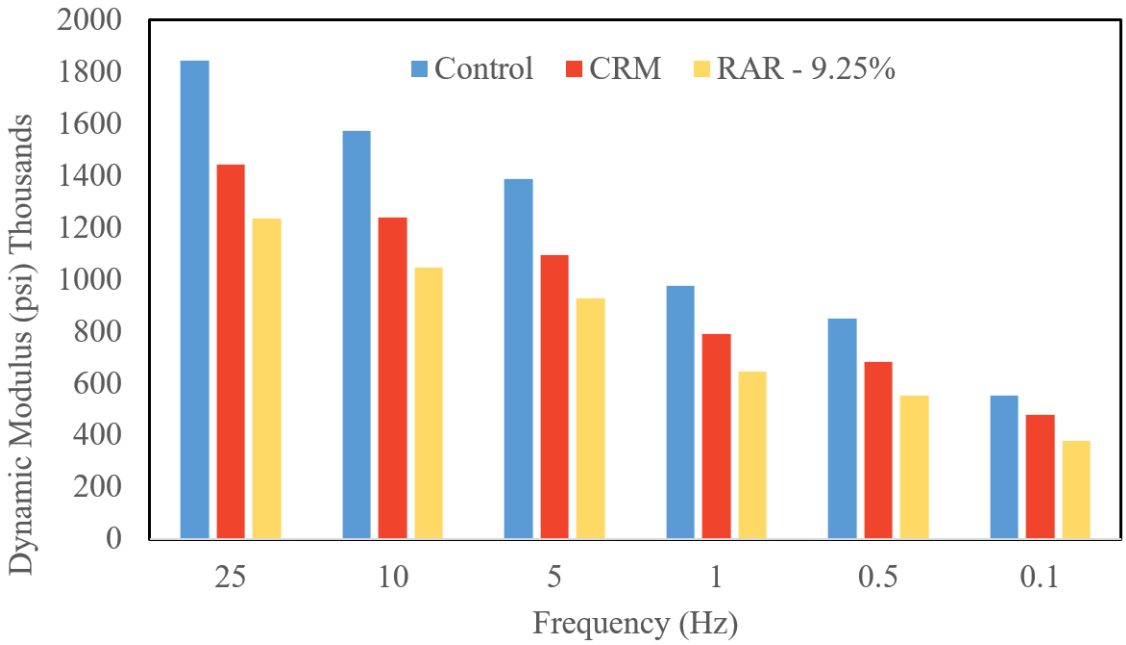

Figure 31. Modulus Comparison of All Mixtures at All Frequencies for 21.1°C

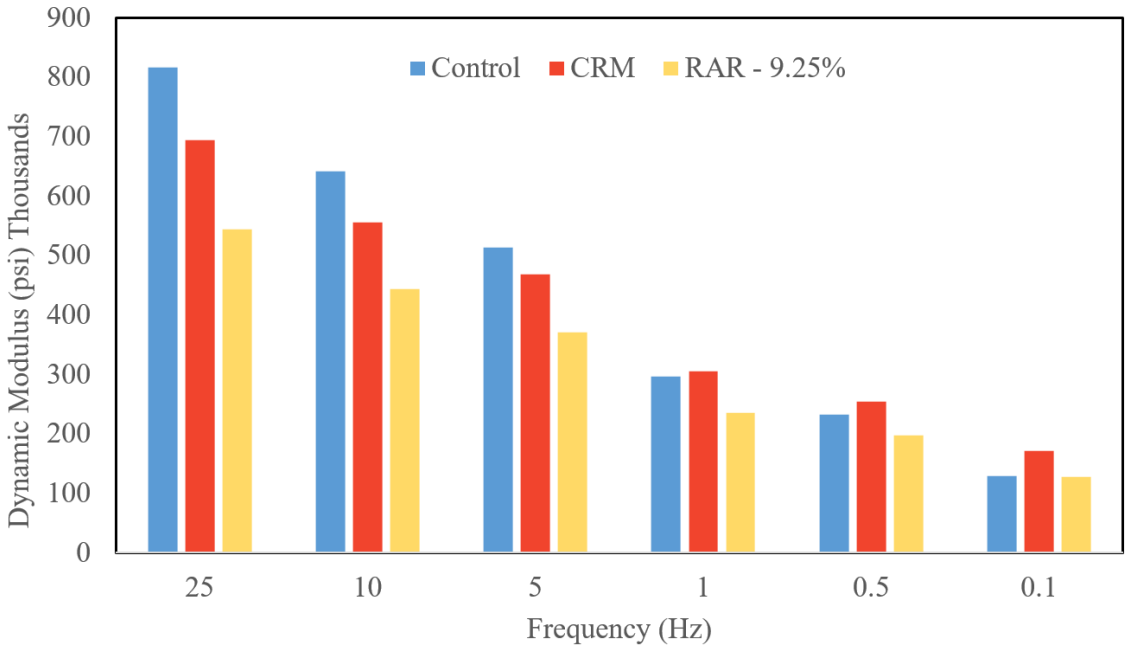

Figure 32. Modulus Comparison of All Mixtures at All Frequencies for 37.8°C

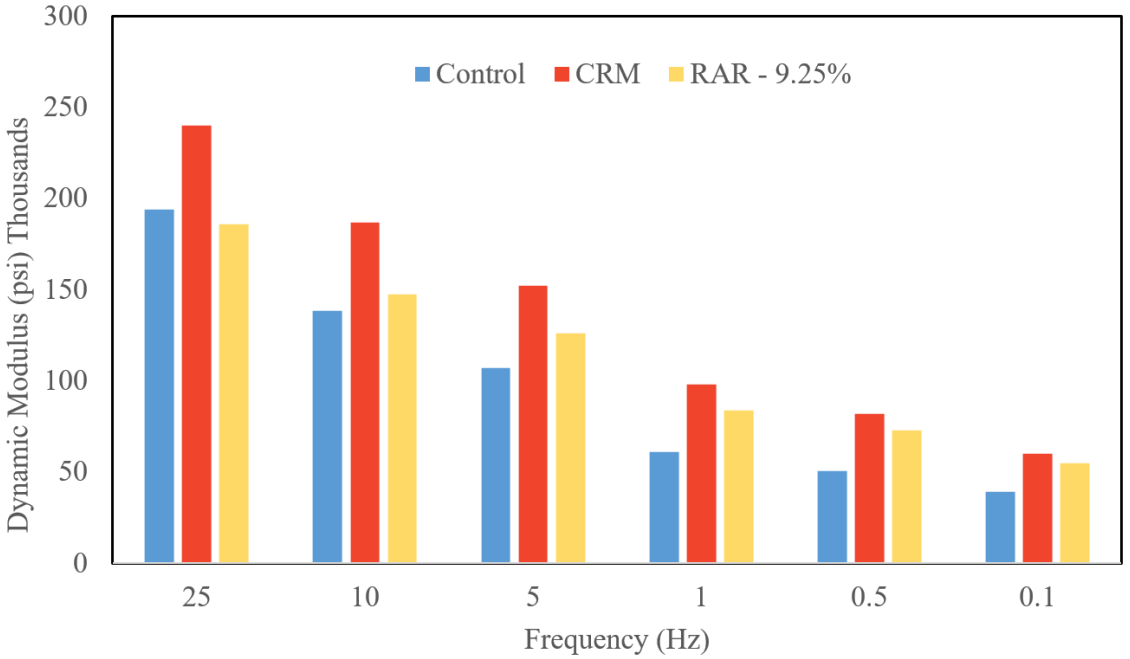

Figure 33. Modulus Comparison of All Mixtures at All Frequencies for 54.4°C

6.2. Flow Number Test

Samples for all the mixes were tested at a deviator loading stress of 400KPa and a temperature of 50°C. The results for the Flow Number test are summarized in this section. Table 5 shows the results with average FN values used for comparison of all the mixtures. It also includes the Resilient modulus values as well as axial permanent strain at failure for each mix. Note that the control is a dense graded mix; whereas the CRM and RAR are gap graded mixtures. Confined tests are better suited for gap graded mixtures, but they were not used in this study to compare the results independent of the stress state. Despite this fact, both the CRM and RAR produced higher FN values than the control mixture. Appendix C Figure 68 to Figure 71 show plots for accumulated strain versus the number of cycles of all replicates for all the mixes.

Table 5. Summary of Flow Number Test Results

Mix	Flow Number Rep.1	Flow Number Rep.2	Average Flow Number	Resilient Modulus (psi) at FN Rep.1	Resilient Modulus (psi) at FN Rep.2	Axial Permanent strain at failure εp (%) Rep.1	Axial Permanent strain at failure εp (%) Rep.2
CRM	6879	5823	6351	111490	162496	1.19	1.27
RAR (9.25% Binder)	2639	2343	2491	108874	102098	1.76	1.84
Control	1311	959	1135	107331	118489	1.56	1.20

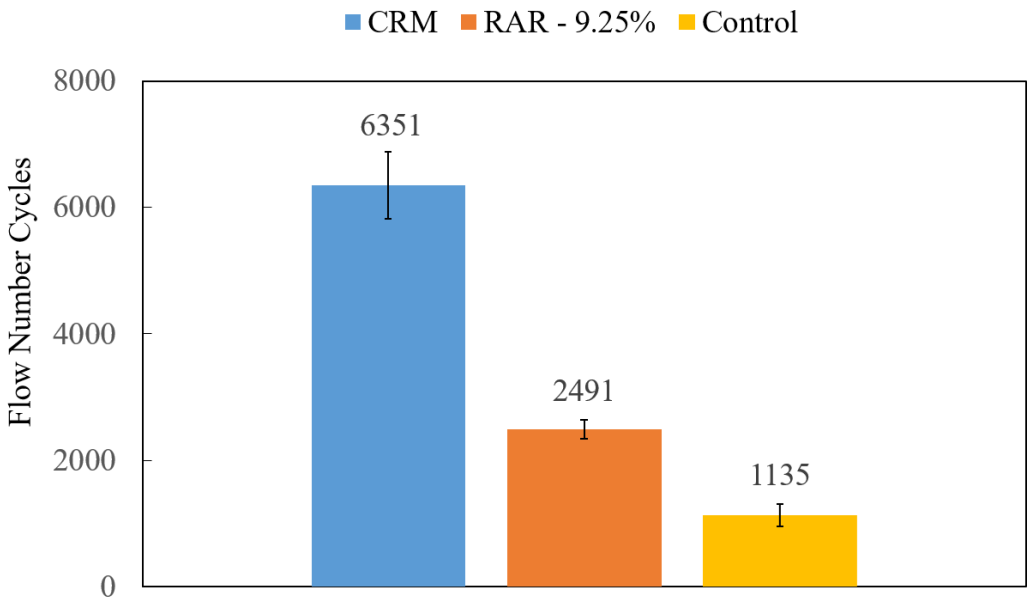

Figure 34. Flow Number Result for All Mixes

Figure 35. Deformed Samples After Flow Number Test

The results show that the CRM mixture had higher average FN compared to the RAR and Control mixtures. However, visual observation of the RAR modified samples showed much less deformation compared to other mixes after the test was completed (Figure 35). The CRM and Control samples had bulges at the center along with cracks developed at both top and bottom of the samples. The RAR samples had a small bulge at the top with no visible signs of crack. Therefore, even though the RAR mix samples achieved flow early, they exhibited good resistance to deformation as well.

6.3. Tensile Strength Ratio

Tensile strength ratio was performed to determine the moisture resistance of mix. The test was conducted by following AASHTO T 283. The load was applied on the test samples at a rate of 50 mm/min. The results for the Control and CRM mixes are tabulated in Table 6 and Table 7 respectively. The tables give information about the average air voids of the subset, tensile strength of each specimen and tensile strength ratio of mix. Due to reasons mentioned later, the RAR mix as designed so far was not included in this testing sequence. The RAR mix was re-designed at higher binder content, and the TSR test results are included later in Section 7.3.

Table 6. Tensile Strength Ratio Results for Control Mix

Control Mix	**Conditioned**			**Dry (Unconditioned)**		
Average Air Voids	6.326 %			6.350 %		
Tensile strength (kPa)	1219.7	1245.8	1274.4	1561.1	1516.0	1518.8
Average tensile strength (kPa)	1246.6			1532		
Tensile Strength Ratio (%)	81					

Table 7. Tensile Strength Ratio Results for CRM Mix

CRM Mix	Conditioned			Dry (Unconditioned)		
Average Air Voids	6.608 %			6.610 %		
Tensile strength (kPa)	682.7	740.7	752.6	815.4	872.4	1010.3
Average tensile strength (kPa)	725.3			899.4		
Tensile Strength Ratio (%)	81					

A minimum tensile strength ratio (TSR) of 0.70 (70%) to 0.80 (80%) is often specified. Actually, even a lower TSR value (65%) is considered acceptable for gap graded rubber mixtures (Nadkarni et al, 2009). In either case, all the mixes had a TSR value above 80% indicating good resistance to mositure damage.

6.3.1. E* Stiffness Ratio (ESR)

ESR and TSR are well correlated (Nadkarni et al, 2009). The ESR test was used instead of TSR to calculate the moisture resistance of the RAR mixtures. Dynamic Modulus E* laboratory test can be used as an alternative property to evaluate moisture damage as in the indirect tensile strength test, AASHTO T 283. To obtain a modulus (E*) Stiffness Ration (ESR), laboratory samples are conditioned in accordance with AASHTO T 283, but the E* Dynamic modulus test is performed on the same samples before and after conditioning. The test after moisture conditioning is performed at 70°F (21.1°C) and the 6 loading frequencies. The ratio of E* before and after moisture conditioning are compared to find the effect of moisture susceptibility on the asphalt mixtures. The ESR values for the 9.25% RAR mix are shown in Table 8.

Table 8. ESR values for RAR Samples

Temp °(F)	Hz	Average E* of 3 samples (wet) ksi	Average E* of 3 samples (Dry) ksi	E* retained % (ESR)
70	25	826.1	1058.1	78
	10	706.9	873.8	81
	5	612.6	758.5	81
	1	417.1	513.7	81
	0.5	350.7	435.6	80
	0.1	227.7	288.6	79

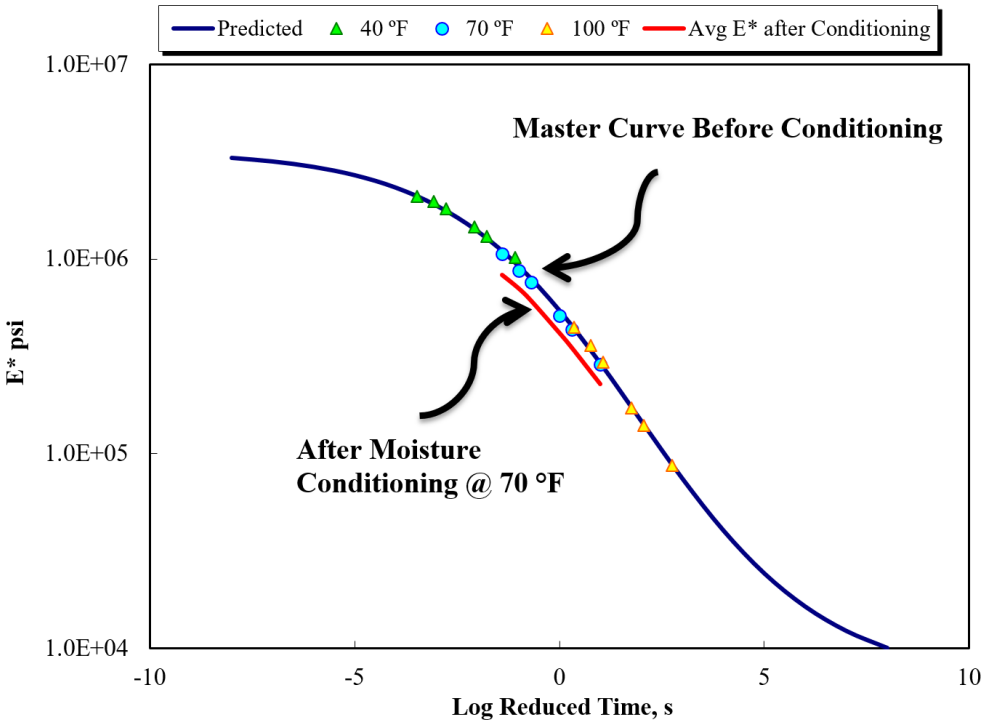

Figure 36. Master Curve - E* Values for Wet and Dry Specimens

The ESR test results also indicated good resistance to moisture susceptibility and the E* retained was approximately 80%, which has been reported as good resistance indicator of the RAR asphalt mixture to stripping and moisture damage. Again, it is also worth mentioning that, in general, lower ESR (or TSR) are expected for Gap graded asphalt

mixes because of the gradation structure present. (Nadkarni et al, 2009) reported that ESR values greater than 65% could be considered as passing value for Gap graded mixes.

6.4. C* Fracture Test

The Crack Growth Rate versus the C* are plotted for the three mixtures in Figure 37. To compare the performance of each mix, the higher the slope the lower the resistance of the mix to crack propagation. In other words, for a given crack growth rate, the power release rate parameter (C*) to fracture the sample is the lowest for the Control mix, followed by the 9.25% RAR mix and CRM mix respectively. Almost similar slope values for both RAR mix and CRM mix were observed indicating better resistance to cracking than the Control mix.

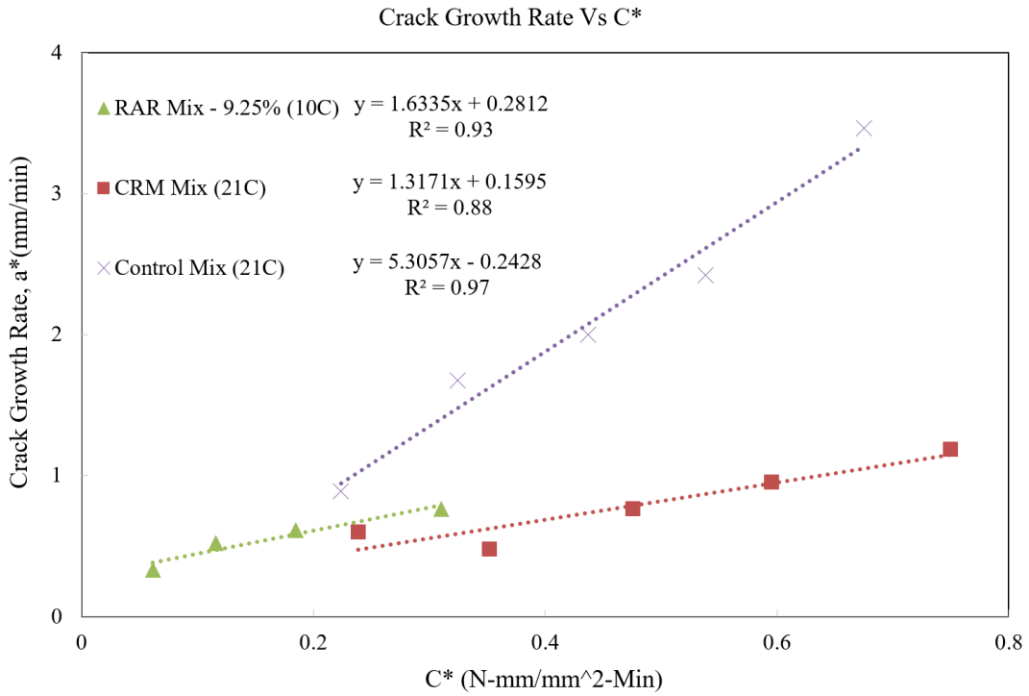

Figure 37. Crack Growth Rate Vs C* Comparison

6.5. Axial Cyclic Fatigue Test

Figure 38 shows the Material Integrity (C) versus the Damage (S) curves for all the mixes and Figure 39 shows the Strain level(100th cycle) versus Nf at 300 µs.

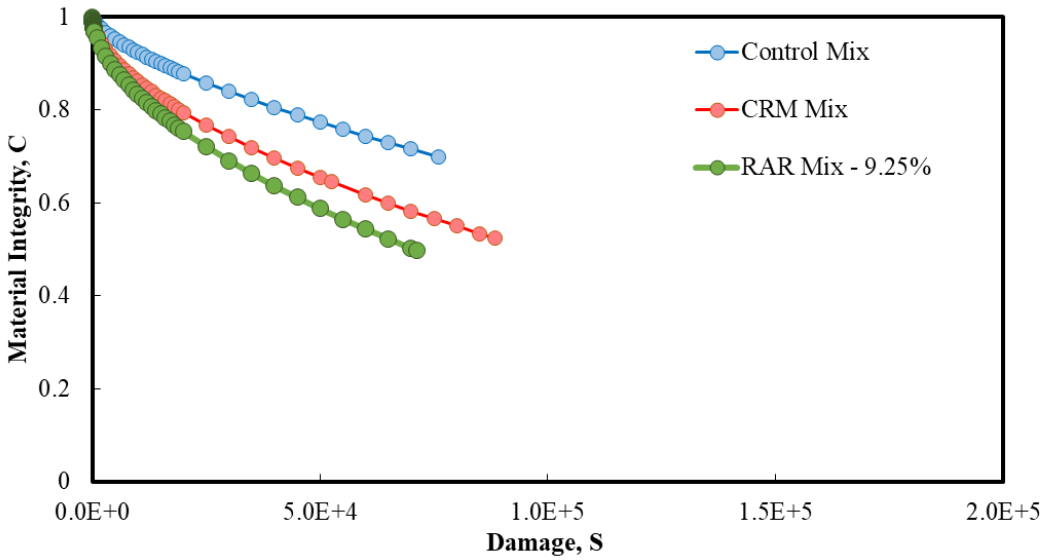

Figure 38. C vs S Curves for All Mixes

The construction of C-S curves in this report followed the most updated procedure developed by Underwood et al. (2010) to calculate S. The damage accumulation serves as a sort of "damage counting". As the asphalt mixtures present different stiffness and damage curves, higher values of material integrity for a given value of damage accumulation do not mean more resistant materials. Material integrity at failure was also higher for Control mix and CRM mix than for RAR mix. This means that the material in Control mix and CRM mix failed for less evolved damaged conditions (with less damage tolerance) compared to RAR mix.

Based on values of Nf at 300 µs, 9.25% RAR mix showed a similar trend in faigue life to CRM mix.

Both the 9.25% RAR mix and CRM mix showed an improvement of two times in fatigue life compared to Control mix.

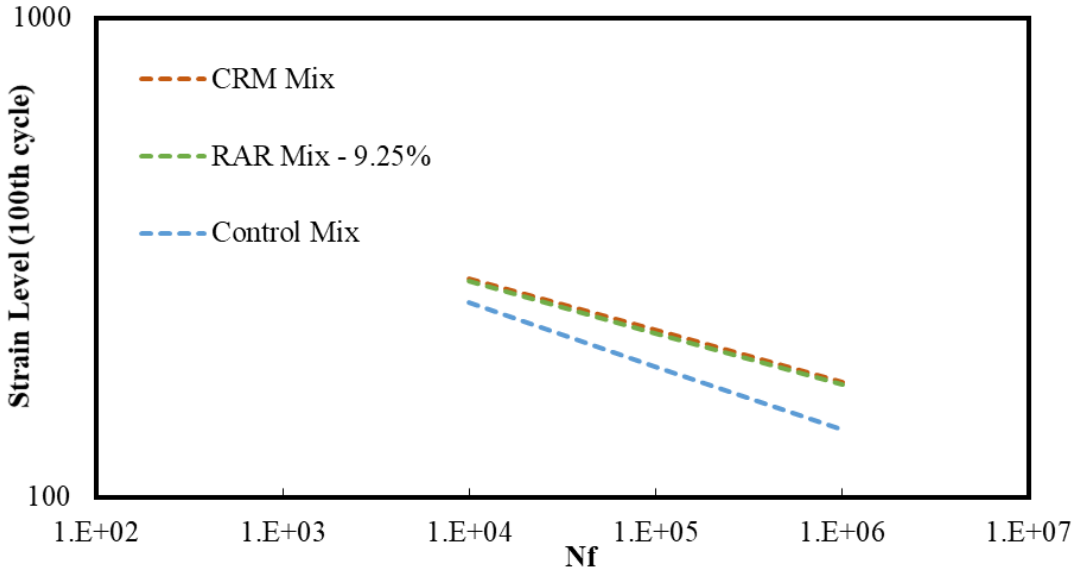

Figure 39. Nf vs Stain Level (100th cycle)

After performing the Axial cyclic fatigue test on RAR samples with the determined optimum 9.25% total binder, it was observed that the samples looked too dry and deficent of binder (aggregates not fully coated). On further investigating the issue along with the supplier of RAR and some literature review, the following points were concluded as key factors in producing a RAR mix deficient of binder which ultimately led to early failure in the Axial cyclic fatigue test.

- The mix design gradation was closely replicated to the gradation provided by the supplier of RAR based on an actual project. However, it was later found out that the coarse aggregates used by the project's supplier had almost no absorption whereas the

coarse aggregates used for this study had high absorption that contributed to the observed dryness or deficiency in binder content.

- The RAR particles absorb 5 to 10% binder to an interconnected network with the rubber particles, thereby, forming a cohesive blend of asphalt, rubber, and the stabilizer. This was not considered during the mix design process as well.
- The RAR mix was subjected to a short-term aging of 4 hours at 135°C followed by 1.5 hours of heating at 165°C after placing the mix into moulds before compaction. During this aging process and bringing up the mix temperature from 135°C to 165°C, the high absorption of coarse aggregates along with the absorption of binder by RAR particles resulted in a product deficient of binder.

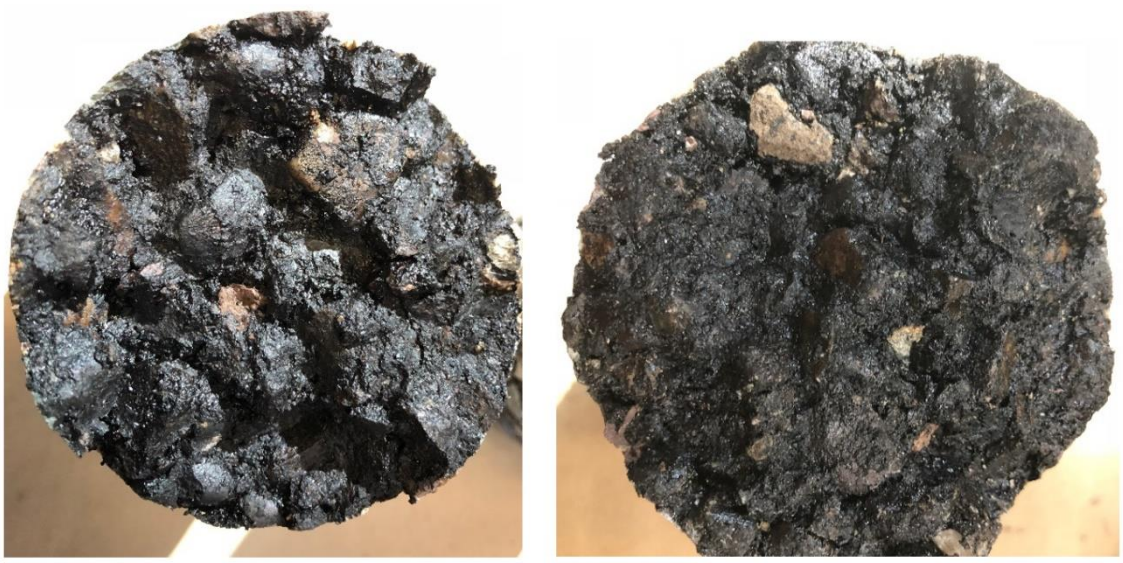

Figure 40. Axial Cyclic Fatigue RAR Samples After Testing

To account for the loss of binder based on the points stated above, a new RAR mix was created to primararily improve the performance in Axial cyclic fatigue test. This deficiency was rectified by computing the absorbed binder amount taking into consideration the high absorption of the aggregate as well as the absorption from RAR and adding it to the existing optimum asphalt content of 9.25%. This amount was caclucated as 0.7% and the asphalt content was rounded off to 10% for the RAR mix.

This new RAR mix with 10% binder content was prepared without the short-term aging of 4 hours, but was heated for 1 hour at 165°C after transferring the mix into moulds before compaction. The laboratory test results of this RAR mix along with all other mixes are presented in the next section.

7. RESULTS AND ANALYSIS WITH MODIFIED RAR MIX

7.1. Dynamic Modulus Test

The E* values of all mixes were compared for 6 frequencies and 5 temperatures along with the new modified RAR mix. The master curve below in Figure 41 shows that RAR modified mixes have lower moduli at lower temperatures which is desirable for better resistance to thermal cracking whereas CRM mix had higher moduli value at higher temperatures indicating resistance to permanent deformation. In general, the new RAR mix exhibited lower moduli across all temperatures-frequencies combinations. This was attributed to the preparation method followed by not including the 4 hours short-term oven aging.

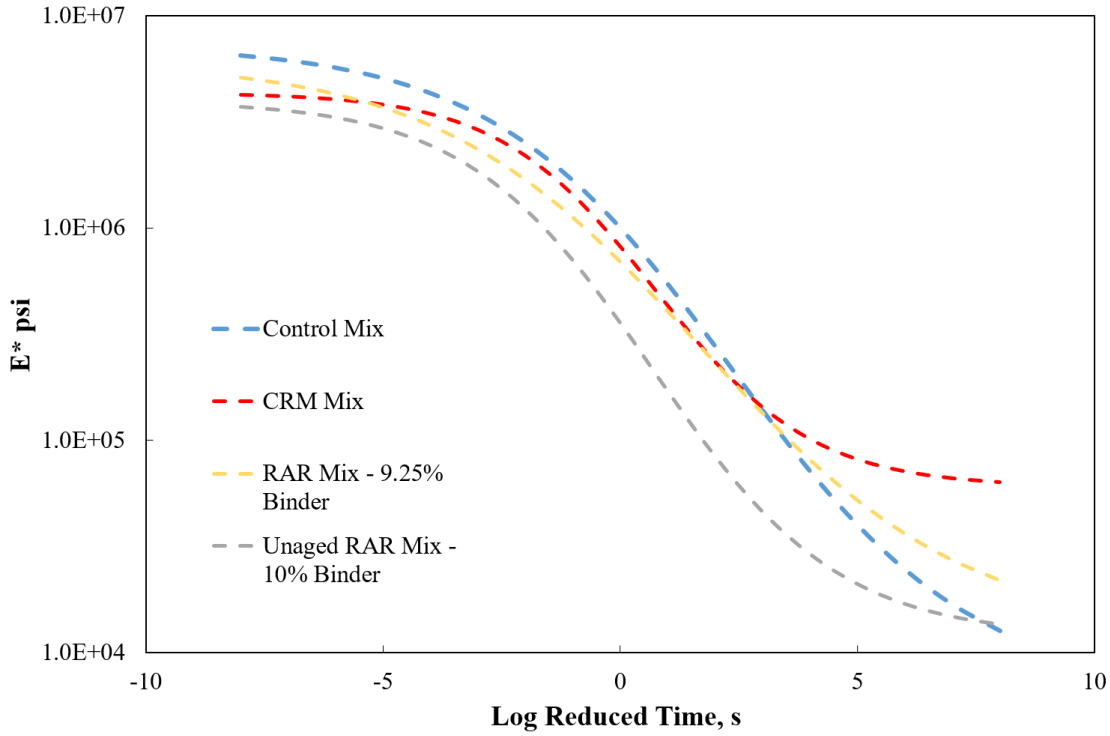

Figure 41. Master Curve - Average E* Values of All Mixtures

7.1.1. Comparison of Results by Frequency and Temperature

Similar to Section 0 analysis, the moduli values obtained from the dynamic modulus test were compared at each temperature and various frequencies combinations. The plots for each temperature are shown in Figure 42 through Figure 46. The results were similar to what stated earlier, the Unaged RAR mix exhibited lower moduli across all temperatures-frequencies combinations.

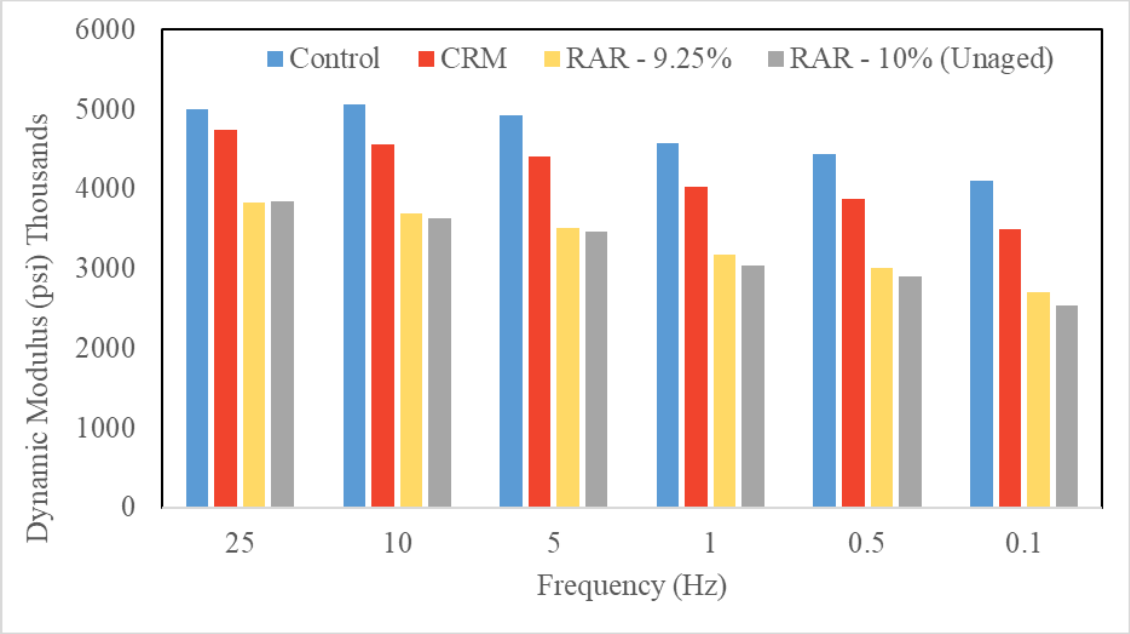

Figure 42. Modulus Comparison of All Mixtures at All Frequencies for -10°C

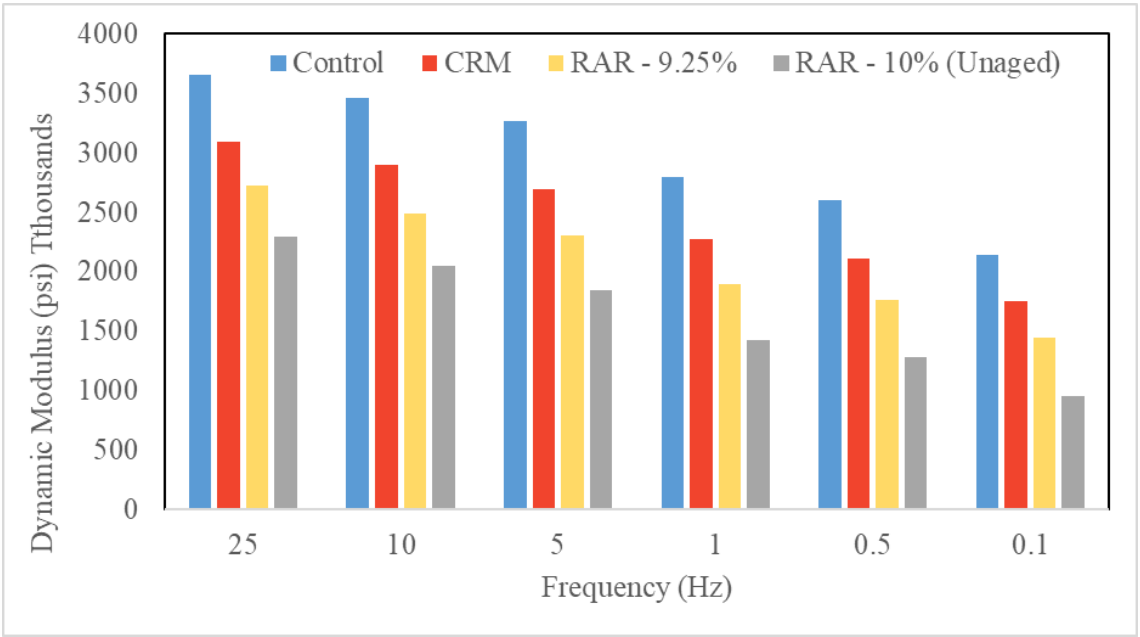

Figure 43. Modulus Comparison of All Mixtures at All Frequencies for 4.4°C

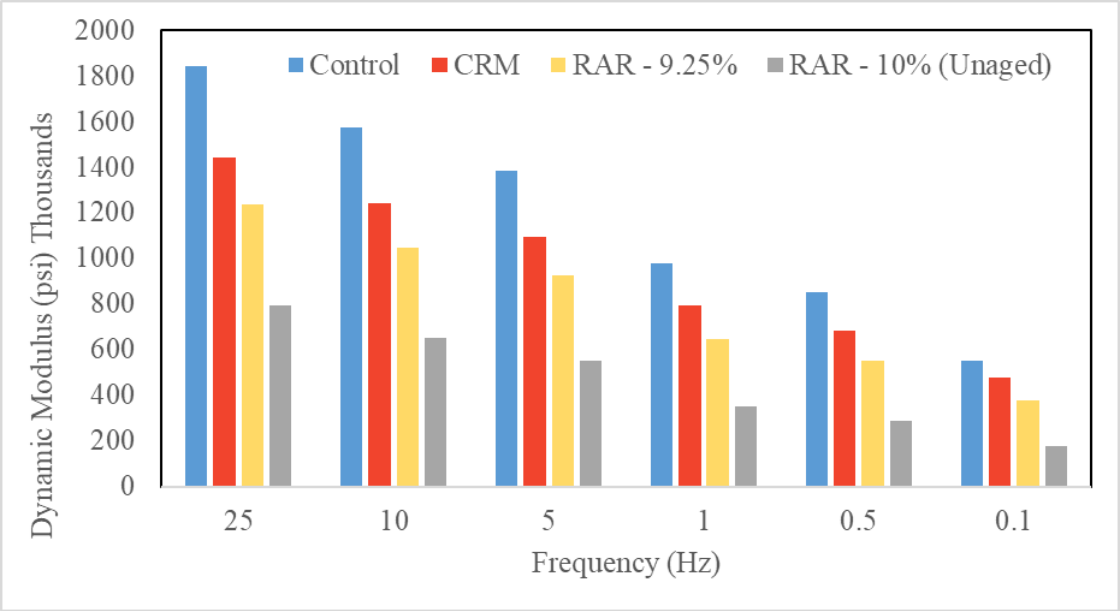

Figure 44. Modulus Comparison of All Mixtures at All Frequencies for 21.1°C

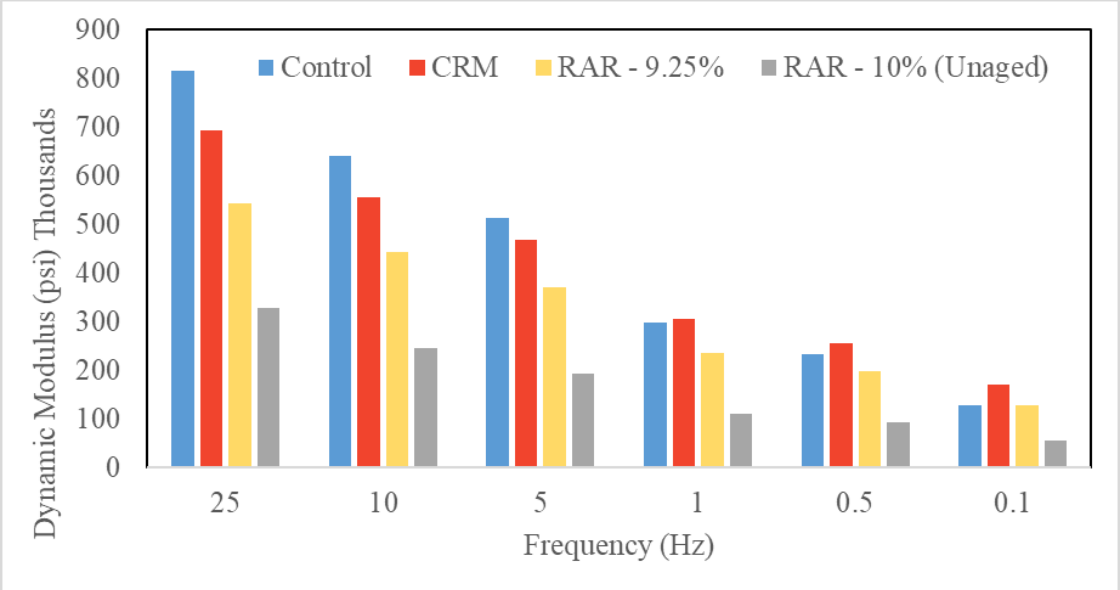

Figure 45. Modulus Comparison of All Mixtures at All Frequencies for 37.8°C

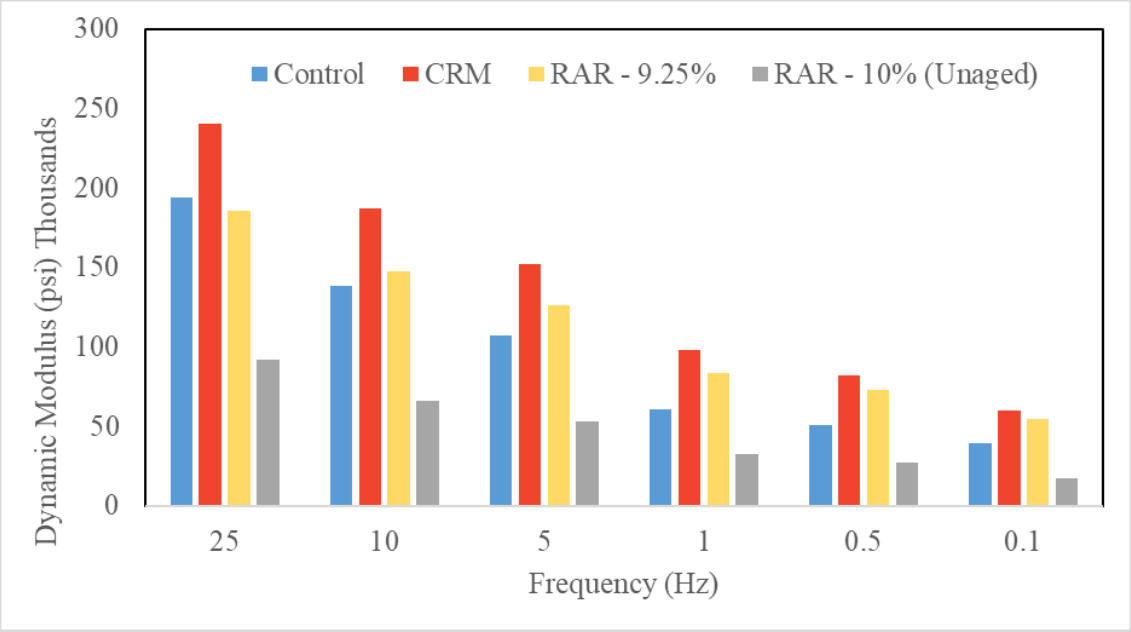

Figure 46. Modulus Comparison of All Mixtures at All Frequencies for 54.4°C

7.2. Flow Number Test

Test samples for all the mixes were tested unconfined at a deviator loading stress of 400KPa and a temperature of 50°C. The 10% Unaged RAR mix was added to the summary Flow Number test results as well. Keeping in mind that the new modified 10% RAR mix was unaged and had more binder, thus resulting in lower Flow Number values. However, these samples also showed much better resistance to deformation compared to other mixes. This is indicative by the higher strain at failure compared to the other mixtures. The results for the Flow Number test are summarized in Table 9. Appendix C Figure 68 to Figure 71 show plots for accumulated strain versus the number of cycles of all replicates for all the mixes.

Table 9. Summary of Flow Number Test Results

Mix	Flow Number Rep.1	Flow Number Rep.2	Average Flow Number	Resilient Modulus (psi) at FN Rep.1	Resilient Modulus (psi) at FN Rep.2	Axial Permanent strain at failure εp (%) Rep.1	Axial Permanent strain at failure εp (%) Rep.2
CRM	6879	5823	6351	111490	162496	1.19	1.27
RAR (9.25% Binder)	2639	2343	2491	108874	102098	1.76	1.84
RAR (10% Binder)	1919	1575	147	87582	92420	2.24	2.24
Control	1311	959	1135	107331	118489	1.56	1.20

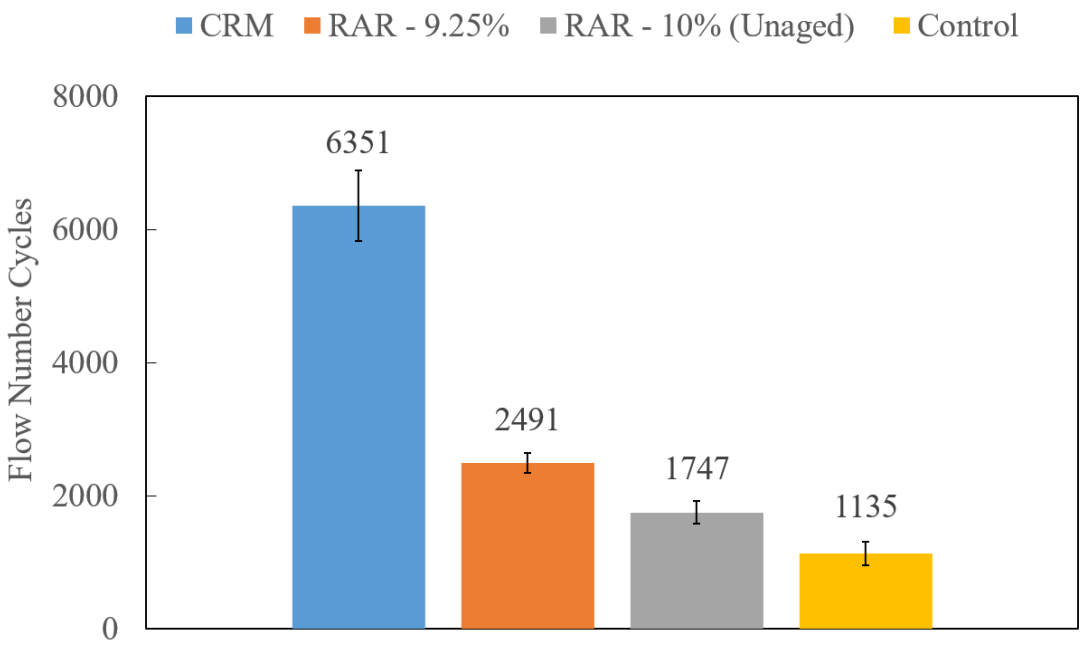

Figure 47. Flow Number Result for All Mixes

7.3. Tensile Strength Ratio

The TSR value of the modified 10% RAR mix is given below:

Table 10. Tensile Strength Ratio Results for 10% RAR Mix (Unaged)

10% RAR Mix	**Conditioned**			**Dry (Unconditioned)**		
Average Air Voids	6.481 %			6.396 %		
Tensile strength (kPa)	717.1	775.8	795.4	933.2	830.7	985.6
Average tensile strength (kPa)	762.7			916.5		
Tensile Strength Ratio (%)	83					

The 10% RAR mix achieved a TSR value of 83% indicating good resistance to moisture susceptibility.

7.4. C* Fracture Test

The Crack Growth Rate versus the C* are plotted for the mixes to compare the performance of each mix through the slope of this relationship where the higher the slope, lower the resistance of the mix to crack propagation. Figure 48 shows almost similar slope values for both 10% RAR mix and CRM mix indicating better resistance to cracking. The new RAR mix at the higher binder content was somewhat equivalent in performance to the CRM mix.

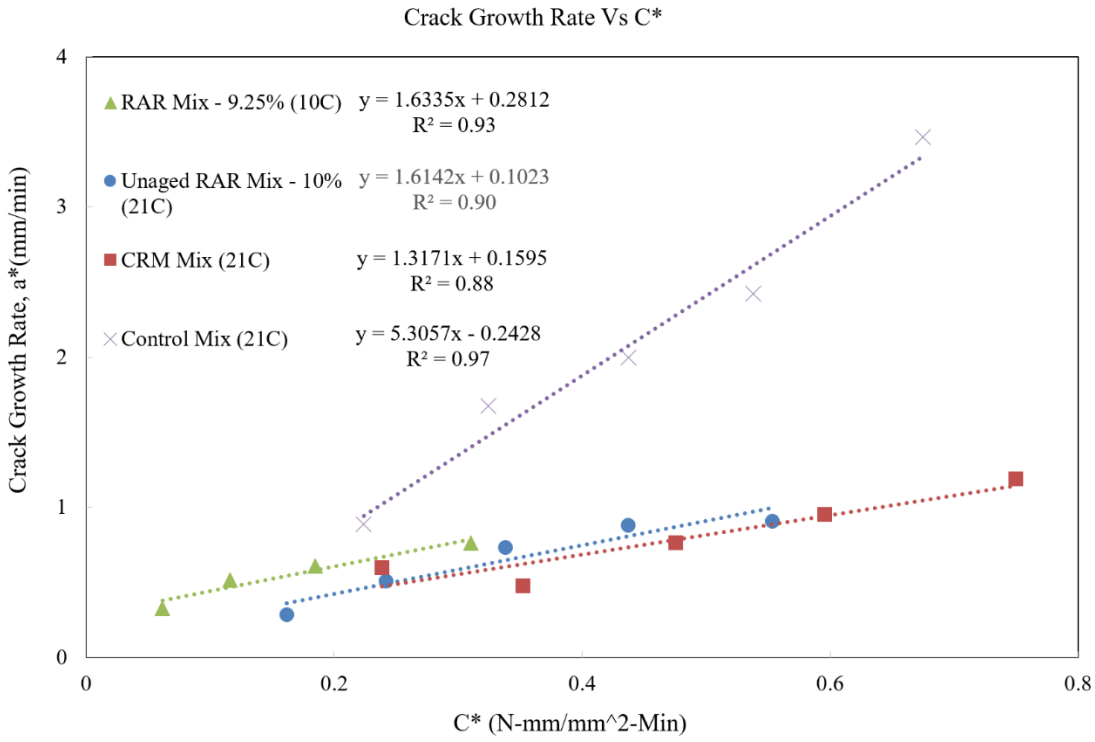

Figure 48. Crack Growth Rate vs C* Comparison

7.5. Axial Cyclic Fatigue Test

Figure 49 shows the Material Integrity (C) versus the Damage (S) curves for all the mixes, and Figure 50 shows the strain level (100th cycle) versus Nf at 300 µs. Material integrity at failure was also higher for Control mix and CRM mix than for 10% RAR mix. This means that the material in Control mix and CRM mix failed for less evolved damaged conditions (with less damage tolerance) compared to 10% RAR mix.

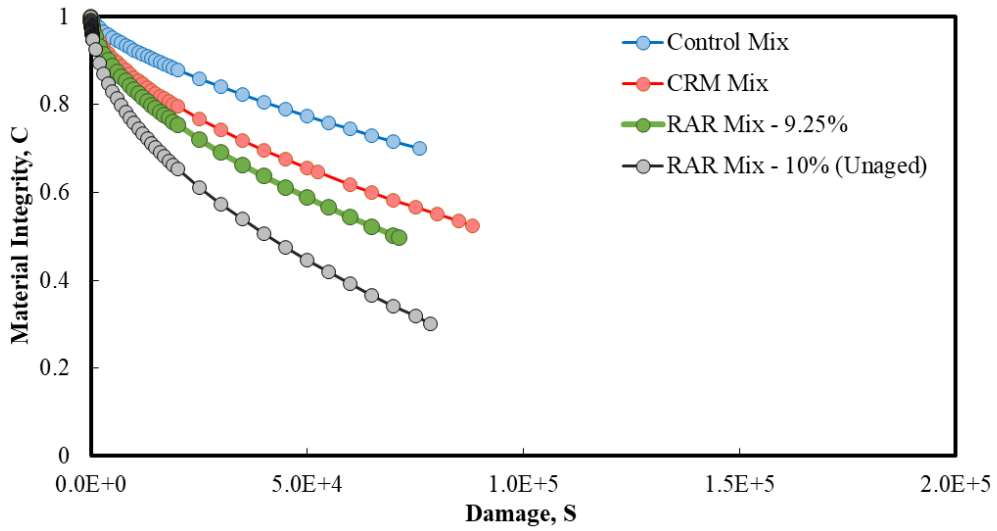

Figure 49. C vs S Curves for All Mixes

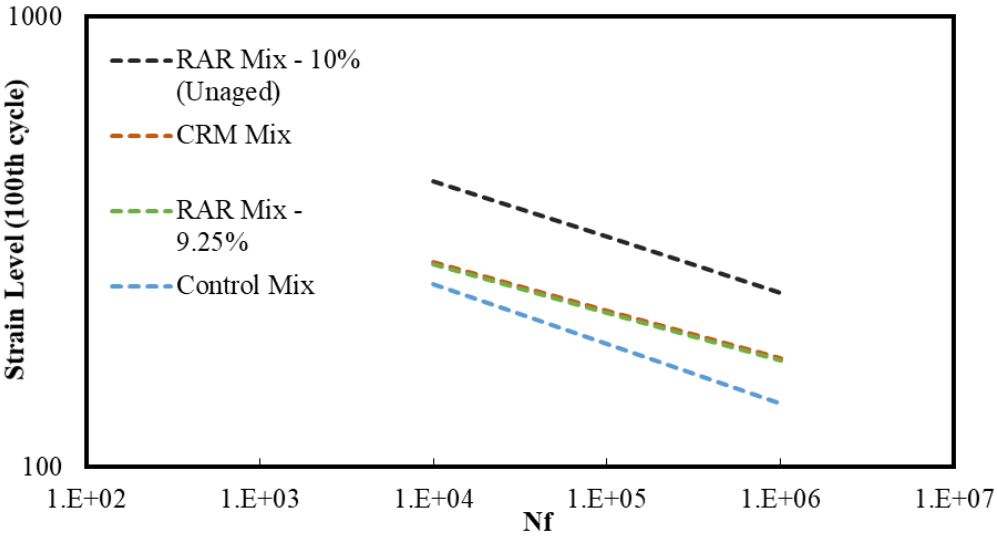

Figure 50. Nf vs Stain Level (100th cycle)

Based on the values of Nf at 300 μs, the unaged 10% RAR mix showed an improvement in fatigue life of 64 times over control samples and an improvement of 30 times over CRM samples indicating excellent fatigue life of new modified RAR mix.

8. FILM THICKNESS CONSIDERATION

The minimum voids in the mineral aggregate (VMA) requirement property has been proposed since the late 1950s for use in asphalt mix design specifications. The conventional definition of the average film thickness was given by F. Hveem as a ratio of asphalt volume (not absorbed into the aggregate particles) to the surface area of the aggregate.

Kandhal (et al, 1998) proposed that rather than specifying a minimum VMA requirement based on minimum asphalt content and adopted by Superpave, a more rational approach would be to directly specify a minimum average asphalt film thickness of 8 μm. They also pointed out that the term film thickness is difficult to define. To calculate an average film thickness, the surface area is determined by multiplying the surface area factors by the percentage passing the various sieve sizes. However, they could not find the background research data for the surface area factors in the literature. Therefore, Kandhal concluded that further research is needed to verify these surface factors and the concept of film thickness.

8.1. Conventional procedure to determine asphalt film thickness

Consideration of film thickness is a part of the Hveem method of designing paving mixtures. Hveem assumed that each aggregate particle needed to be covered with the same optimum film thickness. The surface area calculation is a starting point to select asphalt content in the test series. Hveem used a method of calculating surface area developed by a Canadian engineer, L. N. Edwards, but this method is not available in the literature. The asphalt film thickness is calculated as a ratio of the effective volume of asphalt to the

surface area of aggregate. Table 11 shows how the total surface area is calculated for a given aggregate gradations.

Table 11. The Surface Area Factors and Obtained Surface Area

Sieve Size (mm)	% Passing	Surface Area Factor	Surface Area = Surface factor x % Passing
26.5	100	0.41	0.41 x 1 = 0.41
19	96.85		
13.2	76.18		
9.5	69.019		
4.75	55.68	0.41	0.228288
2.36	41.51	0.82	0.340382
1.18	32.1	1.64	0.52644
0.6	24.18	2.87	0.693966
0.3	16.1	6.14	0.98854
0.15	6.016	12.29	0.739366
0.075	2.93	32.77	0.960161
DUST	2.016	32.77	0.660643
FILLER	2	32.77	0.6554
Total Surface Area (SA)			5.79

The current technique for calculating film thickness is based on the surface area factors considered previously. The asphalt film thickness is commonly calculated using the following formula:

$$TF = \frac{V_{asp}}{(SA \times W_{agg})} = \left(\frac{P_{be}}{SA \times G_b}\right) \times 10^{-5}$$

Where,

TF = conventional film thickness (m),

V_{asp} = effective volume of asphalt (m^3),

W_{agg} = weight of the aggregate (kg),

P_{be} = effective binder content by weight of mixture (%), and

G_b = specific gravity of asphalt.

The inaccuracies of the film thickness determination are widely recognized, however, historical data can be analyzed to determine a best fit criterion based on the surface area coefficients commonly used, so the question of the accuracy of those coefficients is less important. In other words, it makes little difference if the result of the equation is correct as long as that result can be correlated with some measure of performance. There is a substantial amount of evidence on file to support the use of the film thickness equation as an empirical measure of the proper volume of asphalt (Badovskiy et.al, 2003). Therefore, the only assumption made in the calculation of minimum VMA is what minimum film thickness value should be used in the equations. Close examination of aggregates reveals that all aggregates are composed of a variety of different shapes, particularly the combined aggregates usually used in HMA. Evidence that surface area does not vary greatly between aggregates can be seen in the fine aggregate angularity test used in the Superpave mix design system. The relatively narrow range of test results indicates that volumes and, therefore, surface areas of a standard gradation are similar for most aggregates.

8.2. Film thickness calculation for all mixes

An Excel™ sheet was setup with all the surface area factors that was shown in Table 11, and was be used to calculate the film thickness of the all the mixes based on their gradation and modifier added. Figure 51 shows an example calculation of film thickness for the 9.25% Gap graded RAR mix. The Film Thickness calculated for all mixes are presented in Table 12 below.

		Bitumen 64-22	%	9.25							
			% to mixture	6.0125							
			% to bitumen	65							
		Additive (RAR)	% to mixture	3.2375							
Mixture			% to bitumen	35							
RAR Gap Graded				90.75							
					Film Thickness - Grading Curve						
Sieve size (series "base +2) (mm)	Mix Design Criterion	Sieve size	Aggregate Grading Curve	% RARX (weight of mix)	Surface area Factor	Grading Curve (RARX)	Surface area Factor (RARX)		NO RARX consideration	Surface Area 'SA',m2/kg (Surface factor x Passing %) (with RARX)	
				3.2375							
	x.x - x.x				0.41					0,41 x 1 = 0,41	
31.5	x.x - x.x	26.5	100.0	100.0							
22.4	x.x - x.x	19.0	100.0	100.0							
20	x.x - x.x										
16	x.x - x.x										
14	x.x - x.x			100.0							
12.5	x.x - x.x	12.7	95.0								
10	x.x - x.x										
8	x.x - x.x										
6.3	x.x - x.x	9.5	65.0	62.9					0.41	0.41	
4	x.x - x.x	4.75	25.0	24.2	0.41				0.1025	0.1025	
2	x.x - x.x	2.36	20.0	19.4	0.82				0.1640	0.1640	
1	x.x - x.x	1.18	16.0	15.5	1.64	3.2375	16.4		0.2624	0.7849	
0.500	x.x - x.x	0.60	12.0	11.6	2.87	1.61875	28.7		0.3444	0.7978	
0.250	x.x - x.x	0.300	10.0	9.7	6.14	0.6313125	61.4		0.6140	0.9817	
0.125	x.x - x.x	0.150	6.0	5.8	12.29	0.3075625	122.9		0.7374	1.0915	
0.063	x.x - x.x	0.075	4.0	3.9	32.77	0.0809375	327.7		1.3108	1.5336	
		Total Surface area SA`m2/kg´							3.95	5.87	
		$TF = \frac{V_{ssp}}{SA \times W} \times 1000\ \mu m$							25.8	11.3	

Figure 51. Excel Setup to Compute Film Thickness

Table 12. Film Thickness Calculation for All Mixes

Mix	Film Thickness (in micron)	Film Thickness with no filler consideration (in micron)
RAR – 9.25%	11.3	25.8
RAR – 10%	12	28.2
CRM	13.6	20.8
Control	10	10

RAR acts as a very rough dry filler thus it becomes extremely important to verify the film thickness and incorporating it in the mix design for the specific project. The supplier, when contacted, recommended a minimum film thickness of 10 microns based on previous RAR paving projects and a surface factor of 10 for RAR. In previous projects, pavements laid with RAR and film thickness less than 10 microns developed early distresses such as cracking and raveling.

In this study, it was observed that the 9.25% RAR mix satisfied the 10 microns minimum film thickness level; however, insufficient binder coating was observed after the axial fatigue tests which lead to the preparation of another RAR mix with 10% asphalt content. The film thickness for the 10% RAR mix was verified to be 12 microns. Based on the performance test results, and specifically the axial fatigue, it is realistic to state that a difference of 0.5-0.7 microns in film thickness could have a big impact on the performance of the mix. Based on this study's limited testing and findings, a minimum film thickness level of 12 microns is recommended to specify when using RAR in future mixtures and paving projects.

9. SUMMARY, CONCLUSIONS AND RECOMMENDATIONS

9.1. Summary

A testing program was initiated and completed to evaluate the laboratory testing of Reacted and Activated Rubber (RAR) modified asphalt mix prepared through a dry mixing process. It was compared with a traditional Crumb Rubber Mixture (CRM) mix prepared through the wet process and a reference Control mix. A modified RAR mix was created and later added into the testing program to re-address some issues encountered with the

original RAR mix. All the RAR mixes were modified with 35% RAR by weight of binder and the CRM mixes were modified with 20% of Crumb Rubber (CR) by weight of binder. A Superpave mix design performed to arrive at the optimum binder content for all the mixes. This RAR Superpave mix design is believed to be the first ever completed as part of a research study or field production.

The asphalt mixtures characterization tests included: Dynamic Modulus Test for stiffness evaluation, Flow Number Test for rutting evaluation, Tensile Strength Ratio to evaluate moisture susceptibility, C* Fracture Test to evaluate crack propagation and Axial Cyclic Fatigue Test for fatigue cracking evaluation. A short study on the asphalt film thickness was done and a recommendation was made for minimum asphalt film thickness when using RAR.

9.2. Conclusion

9.2.1. Dynamic Modulus Test

Low E* values at lower temperatures are desirable for resistance to thermal cracking, whereas high E* values at higher temperatures indicate resistance to permanent deformation. The Unaged 10% RAR mix had the lowest moduli at lower temperatures followed by the CRM mix, then the 9.25% RAR mix and finally Control mix whereas the CRM mix had the highest moduli values at higher temperatures followed by 9.25% RAR mix, then the Unaged 10% RAR mix and finally the Control mix. The Unaged 10% RAR mix had low moduli values throughout the temperature range, but that was attributed to skipping the short-term aging. In general, both the RAR mixes showed better resistance to

low temperature cracking whereas the conventional CRM mix showed high resistance to permanent deformation compared to all the mixes.

9.2.2. Flow Number Test

The results showed that the CRM mix had highest average FN value indicating a stiffer mix and high resistance to rutting followed by the 9.25% RAR, then the Unaged 10% RAR mix and finally the Control mix. This was consistent with the Dynamic Modulus test results obtained for high temperatures. On visual inspection, both of the RAR mixes showed very little deformation with a slight bulge on top and no visible signs of cracks whereas the CRM and Control mixes had large bulges and lots of cracks after the test was performed. To understand this phenomenon, the post-tertiary flow was investigated and it was found that both of the RAR mixes reached Flow Number at a higher % of accumulated strain, and showed a gradual rise in % accumulated strain post-tertiary flow; whereas the CRM and Control mixes showed a sharp rise for the same. A more comprehensive study needs to be undertaken to explore and understand this phenomenon.

9.2.3. Tensile Strength Ratio

As discussed in the results section, a TSR value of 65% is acceptable for Gap graded rubber mixes and 80% for dense graded mixes to suggest good resistance to moisture susceptibility. The Unaged 10% RAR mix had the highest TSR value of 83%, followed by CRM mix and Control mix both with TSR value of 81%. The E* Stiffness Ratio (ESR) (substitute for TSR) for the 9.25% RAR mix also had a value of 80%.

9.2.4. C* Fracture Test

Relationships between C* fracture values and crack growth rates for all mixtures were presented. The CRM mix had the highest power release rate immediately followed by the Unaged 10% RAR mix; however, the crack growth rate was slight higher for the CRM mix. The 9.25% RAR mix has least power release rate and crack growth rate. The slope of Control mix was roughly 3 times higher than the CRM mix and both of the RAR mix indicating least resistance to crack propagation. Both the Unaged 10% RAR mix and the CRM showed excellent resistance to crack propagation.

9.2.5. Axial Cyclic Fatigue Test

The Number of cycles to failure were computed for a strain level at 100^{th} cycle and compared for each mix. The Unaged 10% RAR mix showed excellent fatigue life with an improvement in fatigue life of 64 times over Control mix, an improvement of 33 times over 9.25% RAR mix and an improvement of 30 times over CRM mix.

9.2.6. Asphalt Film Thickness

A minimum film thickness of 10 microns was recommended by the manufacturer of RAR based on already completed projects and the distresses observed in the field. However, not all information such as the climatic conditions and traffic level were provided to justify the recommended minimum film thickness. Based on the asphalt film thickness analysis conducted in this study, the 9.25% RAR mix yielded a film thickness of 11.3 microns and showed binder deficiency. The Unaged 10% RAR mix yielded a film thickness of 12 microns and showed satisfactory results. Thus, based on the few mixtures evaluated in this study, a minimum film thickness level of 12 microns was recommended

to be used or specified when using RAR in future mixtures and paving projects. This is an increase of 2 microns currently used by the RAR manufacturer.

9.3. Recommendations for Future work

The following are some recommendations for future follow up work related to work in this research study:

- Conduct additional RAR Superpave mix designs and consider incorporating aggregate absorption and RAR film thickness as part of the specifications.
- Conduct a study to evaluate the effect of aging duration and temperatures on the stiffness of RAR mixtures.
- Conduct confined Flow Number and Dynamic Modulus testing for the Gap graded mixes to accurately simulate the state of stress under field conditions.
- For the Flow Number test, further investigation into the post-tertiary flow would be of interest to quantify and analyze.
- A more comprehensive study on Axial Cyclic Fatigue Test for Gap graded mixtures since none is reported in the literature.
- Perform studies to evaluate the impact of different RAR percentages and different gradations.
- Conduct a detailed study on factors affecting the asphalt film thickness calculations such as climatic conditions and traffic level along with latest methods to calculate the asphalt film thickness.

REFERENCES

AASHTO T 283. (2014). Standard Method of Test for Resistance of Compacted Asphalt Mixtures to Moisture-Induced Damage. Washington, D.C: American Association of State Highway and Transportation Officials.

AASHTO TP 107-14 (2016). Standard Method of Test for Determining the Damage Characteristic Curve of Asphalt Mixtures from Direct Tension Cyclic Fatigue Tests. Washington, D.C: American Association of State Highway and Transportation Officials.

AASHTO-T166. (2016). Standard Method of Test for Bulk Specific Gravity (Gmb) of Compacted Hot Mix Asphalt (HMA) Using Saturated Surface-Dry Specimens. Washington, D.C: American Association of State Highway and Transportation Officials.

AASHTO-T209. (2016). Standard Method of Test for Theoretical Maximum Specific Gravity (Gmm) and Density of Hot Mix Asphalt (HMA). Washington, D.C: American Association of State Highway and Transportation Officials.

AASHTO-T342. (2011). Standard Method of Test for Determining Dynamic Modulus of Hot Mix Asphalt (HMA). Washington, D.C: American Association of State Highway and Transportation Officials.

AASHTO MP 2 (2001), Standard Specification for Superpave Volumetric Mix Design. Washington, D.C: American Association of State Highway and Transportation Officials.

AASHTO-TP79-15. (2016). Standard Method of Test for Determining the Dynamic Modulus and Flow Number for Asphalt Mixtures Using the Asphalt Mixture Performance Tester (AMPT). Washington, D.C: American Association of State Highway and Transportation Officials.

Abdulshafi, O. "Effect of Aggregate on Asphalt Mixture Cracking Using TimeDependent Fracture Mechanics Approach". Effects of aggregate and Mineral Fillers on Asphalt Mixture Performance, ASTM STP1147-EB, American Society for Testing and Materials, Philadelphia, 1992

Adhikari, D. De, and S. Maiti, "Reclamation and recycling of waste rubber," Progress in Polymer Science, vol. 25, no. 7, pp. 909–948, 2000.

Atish A. Nadkarni, Kamil E. Kaloush, Waleed A. Zeiada, Krishna P. Biligiri. "Using the Dynamic Modulus Test for Moisture Susceptibility Evaluation of Asphalt Mixtures". Journal of the Transportation Research Board, TRR 2127, pp. 29-35, Washington, D. C., 2009.

Bahia H, Davis R, Effect of Crumb Rubber Modifiers (CRMs) on performance related properties of asphalt binders. AAPT 1994; 1994.

Boris Radovskiy (2003), "Analytical Formulas for Film Thickness in Compacted Asphalt Mixture", Transportation Research Record Journal of the Transportation Research Board, January 2003.

Caltrans. (2003). Asphalt rubber usage guide. Office of Flexible Pavement Materials, Sacramento (2003). State of California, Department of Transportation, Materials Engineering and Testing Services.

Caltrans. (2006). Asphalt Rubber Usage Guide. State of California, Department of Transportation, Materials Engineering and Testing Services.

Charania, J. O. Cano, and R. H. Schnormeier, "Twenty-year study of asphalt rubber pavement in Phoenix, Arizona," Transportation Research Record, no. 1307, pp. 29–38, 1991.

Christensen, D. and Bonaquist, R. (2005). "Practical Application of Continuum Damage Theory to Fatigue Phenomena in Asphalt Concrete Mixtures," Asphalt Paving Technology, Journal of the Association of Asphalt Paving Technologists, Vol. 74, pp. 963–1,002.

Christensen, D. and Bonaquist, R. (2008). "Analysis of HMA Fatigue Data Using the Concepts of Reduced Loading Cycles and Endurance Limit," Asphalt Paving Technology, Journal of the Association of Asphalt Paving Technologists, Vol. 78, pp. 377–416.

D. R. Brown, D. Jared, C. Jones, and D. Watson, "Georgia's experience with crumb rubber in hot-mix asphalt," Transportation Research Record, no. 1583, pp. 45–51, 1997.

Davide Lo Presti, "Recycled Tyre Rubber Modified Bitumens for road asphalt mixtures", Construction and Building Materials, 2013.

G. D. Airey, M. M. Rahman, and A. C. Collop, "Absorption of bitumen into crumb rubber using the basket drainage method," International Journal of Pavement Engineering, vol. 4, no. 2, pp. 105–119, 2003.

G. W. Maupin Jr., "Hot mix asphalt rubber applications in Virginia," Transportation Research Record, no. 1530, pp. 18–24, 1996.

H. Zhu and D. D. Carlson, "A spray based crumb rubber technology in highway noise reduction application," Journal of Solid Waste Technology and Management, vol. 27, no. 1, pp. 27–32, 2001.

Hou, T., Underwood, B.S., Kim, Y.R. (2010). “Fatigue Performance Prediction of North Carolina Mixtures Using the Simplified Viscoelastic Continuum Damage Model,” Asphalt Paving Technology, Journal of the Association of Asphalt Paving Technologists, Vol.

HUANG, S.C., and Pauli, A.T. 2008. Particle Size Effect of Crumb Rubber on Rheology and Morphology of Asphalt Binders with Long-Term Aging. Road Materials and Pavement Design, 9(1), (pp 73-95).

Ilan Ishail, Miki Amit, Tsafrir Kesler and Ronen Peled, New Advancements in Rubberized Asphalt Using an Elastomeric Asphalt Extender – Three Case Studies, Dept. of Civil & Environmental Engineering Technion IIT, Haifa, Israel, 2013.

Ishai, I., Sousa J.B. and Svechinsky, G. "Activated Minerals as Binder Stabilizers in SMA Paving Mixtures" Compendium, 90th Annual Meeting of the Transportation Research Board – TRB, Washington DC, January 2011

J. R. Lundy, R. G. Hicks, and H. Zhou, “Ground rubber tires in asphalt-concrete mixtures—three case histories,” ASTM Special Technical Publication, STP1193, pp. 262–275, 1993.

J. Shen and S. Amirkhanian, “The influence of crumb rubber modifier (CRM) microstructures on the high temperature properties of CRM binders,” International Journal of Pavement Engineering, vol. 6, no. 4, pp. 265–271, 2005.

J. Shen, S. Amirkhanian, F. Xiao, and B. Tang, “Influence of surface area and size of crumb rubber on high temperature properties of crumb rubber modified binders,” Construction and Building Materials, vol. 23, no. 1, pp. 304–310, 2009.

Jorge B. Sousa, “The Future of Rubberized Pavement: Reacted and Activated Rubber”, SHRP Corporation, 2016.

K. SAMPAT, “Performance characterization of Reacted and Activated Rubber dense graded asphalt mixtures”, M.S. Dissertation, Indian Institute Of Technology, Kharagpur, INDIA, 2016.

Kamil E. Kaloush, “Asphalt rubber: Performance tests and pavement design issues”, ARIZONA STATE UNIVERSITY, 2013.

Kutay, M.E., Gibson, N.H., and Youtcheff, J. (2008). “Conventional and Viscoelastic Continuum Damage (VECD) Based Fatigue Analysis of Polymer Modified Asphalt Pavements,” Asphalt Paving Technology, Journal of the Association of Asphalt Paving Technologists, Vol. 77, pp. 395–434.

Kutay, M.E., Gibson, N.H., Dongre, R., and Youtcheff, J (2009). "Use of Small Samples to Predict Fatigue Lives of Field Cores-Newly Developed Formulation Based on Viscoelastic Continuum Damage Theory," Transportation Research Record 2127, pp. 90–97.

Landes, J.D. & Begley, J., "A Fracture Mechanics Approach to Creep Crack Growth." Mechanics of Crack Growth; Proceedings of the Eighth National Symposium on Fracture Mechanics, 590, 1976: 128-148.

Lee, H.J. and Kim, Y.R. (1998). "Viscoelastic Constitutive Model for Asphalt Concrete Under Cyclic Loading," Journal of Engineering Mechanics, ASCE, Vol. 124, No. 1, pp. 32–40.

M. A. Abdelrahman and S. H. Carpenter, "Mechanism of interaction of asphalt cement with crumb rubber modifier," Transportation Research Record, no. 1661, pp. 106–113, 1999.

Majidzadeh, K., E.M. Kauffmann, D.V. Ramsamooj, and Chan, A.T. (1970). Analysis of Fatigue and Fracture of Bituminous Paving Mixtures, Report No. 2546. U.S. Bureau of Public Roads. Research and Development, 1970.

NCAT Report 12-09, (2014). Effect of Ground Tire Rubber Particle Size and Grinding Method on Asphalt Binder Properties.

Prithvi S. Kandhal, Kee Y Foo and Rajib B Mallick. (1998). A Critical Review Of Vma Requirements In Superpave. NCAT Report No. 98-1.

Reese, R. Properties of Aged Asphalt Binder Related to Asphalt Concrete Fatigue Life. Electronic Journal of the Association of Asphalt Paving Technologists, Vol. 66, 1997, pp. 604–632.

Sampat Kedarisetty, Krishna Prapoorna Biligiri, Jorge B. Sousa, "Advanced rheological characterization of Reacted and Activated Rubber (RAR) modified asphalt binders", CONSULPAV International, Milharado Mafra 2665-305, Portugal, 2016.

Stempihar, Jeffrey. Development of the C* Fracture Test for Asphalt Concrete Mixtures. Ph.D. Dissertation, Civil and Environmental Engineering, Arizona State University, 2013

Stempihar J, Kaloush KE (2017) A Notched Disk Crack Propagation Test for Asphalt Concrete. MOJ Civil Eng 3(5): 00084. DOI: 10.15406/mojce.2017.03.00084

Way, George B. "Asphalt-Rubber 45 Years of Progress." Asphalt Rubber. 2012.

WANG, H., You, Z., Mills-Beale, J. and Hao, P. 2012. Laboratory Evaluation on High Temperature Viscosity and Low Temperature Stiffness of Asphalt Binder with High Percent Scrap Tire Rubber. Construction and Building Materials, 26(1), (pp 583-590).

Willis, J. Richards, Clayton Plemons, Pamela Turner, Carolina Rodezno, and Tyler Mitchell. "Effect of Ground Tire Rubber Particle Size and Grinding Method on Asphalt Binder Properties." National Center for Asphalt Technology, Auburn, 2012.

Witczak, M.W. (2005). NCHRP Report 547: Simple Performance Tests: Summary of Recommended Methods and Database, Transportation Research Board, National Research Council, Washington, DC.

XIAO, F., Amirkhanian, S.N., Shen, J. and Putman, B. 2009. Influences of Crumb Rubber Size and Type on Reclaimed Asphalt Pavement (RAP) Mixtures. Construction and Building Materials, 23(2), (pp 1028-1034).

Y. Huang, R. N. Bird, and O. Heidrich, “A review of the use of recycled solid waste materials in asphalt pavements,” Resources, Conservation and Recycling, vol. 52, no. 1, pp. 58–73, 2007.

APPENDIX A

MATERIAL PROPERTIES

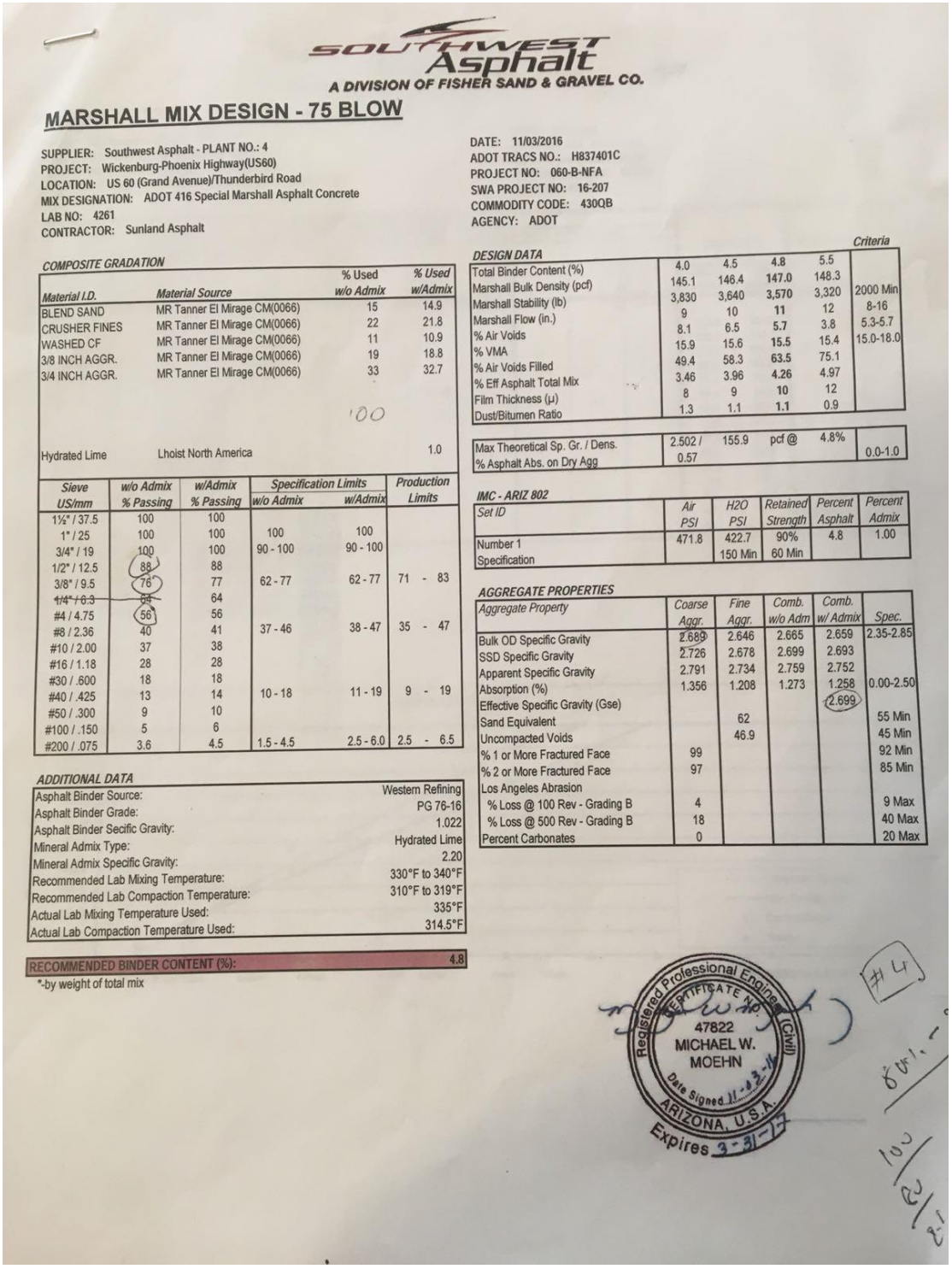

SOUTHWEST Asphalt
A DIVISION OF FISHER SAND & GRAVEL CO.

MARSHALL MIX DESIGN - 75 BLOW

SUPPLIER: Southwest Asphalt - PLANT NO.: 4
PROJECT: Wickenburg-Phoenix Highway(US60)
LOCATION: US 60 (Grand Avenue)/Thunderbird Road
MIX DESIGNATION: ADOT 416 Special Marshall Asphalt Concrete
LAB NO: 4261
CONTRACTOR: Sunland Asphalt

DATE: 11/03/2016
ADOT TRACS NO.: H837401C
PROJECT NO: 060-B-NFA
SWA PROJECT NO: 16-207
COMMODITY CODE: 430QB
AGENCY: ADOT

COMPOSITE GRADATION

Material I.D.	Material Source	% Used w/o Admix	% Used w/Admix
BLEND SAND	MR Tanner El Mirage CM(0066)	15	14.9
CRUSHER FINES	MR Tanner El Mirage CM(0066)	22	21.8
WASHED CF	MR Tanner El Mirage CM(0066)	11	10.9
3/8 INCH AGGR.	MR Tanner El Mirage CM(0066)	19	18.8
3/4 INCH AGGR.	MR Tanner El Mirage CM(0066)	33	32.7
		100	
Hydrated Lime	Lhoist North America		1.0

Sieve US/mm	w/o Admix % Passing	w/Admix % Passing	Specification Limits w/o Admix	Specification Limits w/Admix	Production Limits
1½" / 37.5	100	100			
1" / 25	100	100	100	100	
3/4" / 19	100	100	90 - 100	90 - 100	
1/2" / 12.5	88	88			
3/8" / 9.5	76	77	62 - 77	62 - 77	71 - 83
~~1/4" / 6.3~~	~~63~~	64			
#4 / 4.75	56	56			
#8 / 2.36	40	41	37 - 46	38 - 47	35 - 47
#10 / 2.00	37	38			
#16 / 1.18	28	28			
#30 / .600	18	18			
#40 / .425	13	14	10 - 18	11 - 19	9 - 19
#50 / .300	9	10			
#100 / .150	5	6			
#200 / .075	3.6	4.5	1.5 - 4.5	2.5 - 6.0	2.5 - 6.5

ADDITIONAL DATA

Asphalt Binder Source:	Western Refining
Asphalt Binder Grade:	PG 76-16
Asphalt Binder Secific Gravity:	1.022
Mineral Admix Type:	Hydrated Lime
Mineral Admix Specific Gravity:	2.20
Recommended Lab Mixing Temperature:	330°F to 340°F
Recommended Lab Compaction Temperature:	310°F to 319°F
Actual Lab Mixing Temperature Used:	335°F
Actual Lab Compaction Temperature Used:	314.5°F

RECOMMENDED BINDER CONTENT (%): 4.8

*-by weight of total mix

DESIGN DATA

					Criteria
Total Binder Content (%)	4.0	4.5	4.8	5.5	
Marshall Bulk Density (pcf)	145.1	146.4	147.0	148.3	
Marshall Stability (lb)	3,830	3,640	3,570	3,320	2000 Min
Marshall Flow (in.)	9	10	11	12	8-16
% Air Voids	8.1	6.5	5.7	3.8	5.3-5.7
% VMA	15.9	15.6	15.5	15.4	15.0-18.0
% Air Voids Filled	49.4	58.3	63.5	75.1	
% Eff Asphalt Total Mix	3.46	3.96	4.26	4.97	
Film Thickness (µ)	8	9	10	12	
Dust/Bitumen Ratio	1.3	1.1	1.1	0.9	

Max Theoretical Sp. Gr. / Dens.	2.502 /	155.9	pcf @	4.8%	
% Asphalt Abs. on Dry Agg	0.57				0.0-1.0

IMC - ARIZ 802

Set ID	Air PSI	H2O PSI	Retained Strength	Percent Asphalt	Percent Admix
Number 1	471.8	422.7	90%	4.8	1.00
Specification		150 Min	60 Min		

AGGREGATE PROPERTIES

Aggregate Property	Coarse Aggr.	Fine Aggr.	Comb. w/o Adm	Comb. w/ Admix	Spec.
Bulk OD Specific Gravity	2.689	2.646	2.665	2.659	2.35-2.85
SSD Specific Gravity	2.726	2.678	2.699	2.693	
Apparent Specific Gravity	2.791	2.734	2.759	2.752	
Absorption (%)	1.356	1.208	1.273	1.258	0.00-2.50
Effective Specific Gravity (Gse)				2.699	
Sand Equivalent		62			55 Min
Uncompacted Voids		46.9			45 Min
% 1 or More Fractured Face	99				92 Min
% 2 or More Fractured Face	97				85 Min
Los Angeles Abrasion					
% Loss @ 100 Rev - Grading B	4				9 Max
% Loss @ 500 Rev - Grading B	18				40 Max
Percent Carbonates	0				20 Max

Registered Professional Engineer (Civil)
CERTIFICATE NO.
47822
MICHAEL W. MOEHN
Date Signed 11-03-16
ARIZONA, U.S.A.
Expires 3-31-17

#4

Figure 52. Aggregate Properties

Table 13. RAR Properties

Physical State	Solid, Black/Grey Powder
Odor and Appearance	Mild Rubber, Black/Grey Powder with Brownish color granules
Bulk Density	0.6 ($\pm$ 0.03) g/cm^3
Specific Gravity	1.031 g/cm^3 ($\pm$ 0.03)
Flash Point (℃)	>300 (℃)
Solubility	Insoluble in water
Chemical Stability	Incompatible with strong oxidizing

Weight of Sample	7175				Air Voids	
Total Binder %	10	Total Binder	717.50		4%	
		PG 64-22(65%)	466.38			
		RARX (35%)	251.13			
		TOTAL	717.50			
Total Aggregate	6457.50					
Gradation of Aggregates						
sieve size in mm	sieve size in inch	Gradation Control Points	Cumulative % Passing	Cumulative % Retained	% Retained	Weigth
25.00	1.00	100 min	100.00	0.00	0.00	0.00
19.00	3/4	100 min	100.00	0.00	0.00	0.00
12.50	1/2	95-100	95.00	5.00	5.00	322.88
9.50	3/8	50-80	65.00	35.00	30.00	1937.25
4.75	#4	20-35	25.00	75.00	40.00	2583.00
2.36	#8	16-24	20.00	80.00	5.00	322.88
1.18	#16	-	16.00	84.00	4.00	258.30
0.60	#30	-	12.00	88.00	4.00	258.30
0.30	#50	-	10.00	90.00	2.00	129.15
0.15	#100	-	6.00	94.00	4.00	258.30
0.08	#200	4-10	4.00	96.00	2.00	129.15
	pan			100.00	4.00	258.30

Figure 53. Gap Gradation for RAR Mix

Weight of Sample	7175				Air Voids	
Total Binder %	7.6	Total Binder	545.30		4%	
		PG 64-22(65%)	436.24			
		CRM (35%)	109.06			
		TOTAL	545.30			
Total Aggregate	6629.70					
Gradation of Aggregates						
sieve size in mm	sieve size in inch	Gradation Control Points	Cumulative % Passing	Cumulative % Retained	% Retained	Weigth
25.00	1.00	100 min	100.00	0.00	0.00	0.00
19.00	3/4	100 min	100.00	0.00	0.00	0.00
12.50	1/2	95-100	95.00	5.00	5.00	331.49
9.50	3/8	50-80	65.00	35.00	30.00	1988.91
4.75	#4	20-35	25.00	75.00	40.00	2651.88
2.36	#8	16-24	20.00	80.00	5.00	331.49
1.18	#16	-	16.00	84.00	4.00	265.19
0.60	#30	-	12.00	88.00	4.00	265.19
0.30	#50	-	10.00	90.00	2.00	132.59
0.15	#100	-	6.00	94.00	4.00	265.19
0.08	#200	4-10	4.00	96.00	2.00	132.59
	pan			100.00	4.00	265.19

Figure 54. Gap Gradation for CRM Mix

Control Mix				Total mix weight	7175
Binder percentage	5.1			Binder weight	365.9
Aggregate %	94.9			Aggregate weight	6809.1
	Cum % Pas	Cum % Ret	% retained	weight	
1"	100	0	0	0.0	
3/4"	100	0	0	0.0	
1/2"	86	14	14	953.3	
3/8"	72	28	14	953.3	
1/4"	59	41	13	885.2	
#4	56	44	3	204.3	
#8	43	57	13	885.2	
#16	32	68	11	749.0	
#30	21	79	11	749.0	
50	11	89	10	680.9	
100	6	94	5	340.5	
#200	4.8	95.2	1.2	81.7	
Pan			3.7	251.9	
Lime			1.1	74.9	
			100	6809.1	

Figure 55. Dense Gradation for Control Mix

APPENDIX B

SUPERPAVE MIX DESIGN CALCULATIONS

9.25% RAR Mix

Table 14. Gmb Calculations – RAR Mix

Binder Percent (%)	Gmm	Mass in air (A) Gm	Mass SSD (C) gm	Mass in water (B) gm	Gmb $\frac{A}{B-C}$	% Air Voids $(1 - \frac{Gmb}{Gmm})*100$
8.5	2.40	4700	2672.9	4715.6	2.30	4.2
8.5	2.40	4700	2641.2	4760.0	2.22	7.6
9.0	2.38	4700	2658.6	4719.1	2.28	4.1
9.0	2.38	4700	2659.7	4719.6	2.28	4.0
9.5	2.37	4700	2653.7	4714.0	2.28	3.8
9.5	2.37	4706	2660.3	4718.0	2.29	3.5

Table 15. Correction Factor Calculation – RAR Mix

Pb (%)	Volume at different heights (cm^3)			Gmb (estimated)			Gmb (measured)	Correction factor
	$N_{initial}$	N_{design}	N_{max}	$N_{initial}$	N_{design}	N_{max}		
8.5	2330.3	2118.5	2089.1	2.02	2.22	2.25	2.26	1.004
9.0	2355.3	2116.5	2086.1	2.00	2.22	2.25	2.28	1.013
9.5	2332.5	2102.6	2073.6	2.02	2.24	2.27	2.28	1.008

Table 16. Design Air Voids Calculation – RAR Mix

Pb (%)	Gmb corrected			Gmm	%Gmm			%Air Voids
	$N_{initial}$	N_{design}	N_{max}		$N_{initial}$	N_{design}	N_{max}	N_{design}
8.5	2.03	2.23	2.26	2.40	84.33	92.77	94.07	7.23
9.0	2.02	2.25	2.28	2.38	84.67	94.22	95.59	5.78
9.5	2.03	2.25	2.28	2.37	85.64	95.00	96.33	5.00

Table 17. Final Volumetric Properties – RAR Mix

Pb (%)	% Air Voids	% VMA	% VFA	%Gmm $N_{initial}$	%Gmm N_{max}	D.P.
8.5	5.9	22.2	75.8	87.6	97.3	0.6
9.0	4.4	21.9	79.8	86.4	97.4	0.7
9.5	3.7	22.3	83.6	86.6	97.3	0.7

CRM Mix

Table 18. Gmb Calculations – CRM Mix

Binder Percent (%)	Gmm	Mass in air (A) gm	Mass SSD (C) gm	Mass in water (B) gm	Gmb $\frac{A}{B-C}$	% Air Voids $(1 - \frac{Gmb}{Gmm})*100$
7.0	2.46	4699.5	2726.4	4718.3	2.36	4.1
7.0	2.46	4700.3	2716.7	4724.8	2.34	4.9
7.5	2.45	4698.5	2709.8	4711.9	2.35	4.1
7.5	2.45	4699.3	2713.5	4714.4	2.35	4.1
8.0	2.44	4701.5	2688.1	4725.0	2.35	3.7
8.0	2.44	4698.7	2693.7	4716.9	2.34	4.1

Table 19. Correction Factor Calculation – CRM Mix

Pb (%)	Volume at different heights (cm^3)			Gmb (estimated)			Gmb (measured)	Correction factor
	$N_{initial}$	N_{design}	N_{max}	$N_{initial}$	N_{design}	N_{max}		
7.0	2303.4	2092.7	2065.6	2.04	2.25	2.28	2.35	1.033
7.5	2295.4	2088.2	2061.3	2.05	2.25	2.28	2.35	1.031
8.0	2308.2	2107.3	2082.8	2.04	2.23	2.26	2.35	1.041

Table 20. Design Air Voids Calculation – CRM Mix

Pb (%)	Gmb corrected			Gmm	%Gmm			%Air Voids
	$N_{initial}$	N_{design}	N_{max}		$N_{initial}$	N_{design}	N_{max}	N_{design}
7.0	2.11	2.32	2.35	2.46	85.67	94.29	95.53	5.71
7.5	2.11	2.32	2.35	2.45	86.13	94.68	95.92	5.32
8.0	2.12	2.32	2.35	2.44	86.9	95.19	96.31	4.81

Table 21. Final Volumetric Properties – CRM Mix

Pb (%)	% Air Voids	% VMA	% VFA	%Gmm	%Gmm	D.P.
				$N_{initial}$	N_{max}	
7.0	4.5	17.8	74.7	87.4	97.2	0.6
7.5	4.1	18.2	77.5	87.5	97.2	0.6
8.0	3.7	18.7	80.2	87.7	97.1	0.6

Control Mix

Table 22. Gmb Calculations – Control Mix

Binder Percent (%)	Gmm	Mass in air (A) gm	Mass SSD (C) gm	Mass in water (B) gm	Gmb $\frac{A}{B-C}$	% Air Voids $(1 - \frac{Gmb}{Gmm})*100$
4.5	2.52	4702.8	2732.8	4723.7	2.36	6.3
4.5	2.52	4704.5	2740.7	4722.8	2.37	6.0
5.0	2.50	4704.2	2752.3	4714.6	2.40	4.0
5.0	2.50	4702.2	2742.2	4712.3	2.39	4.4
5.5	2.48	4701.1	2753.5	4706.9	2.41	2.8

Table 23. Correction Factor Calculation – Control Mix

Pb (%)	Volume at different heights (cm^3)			Gmb (estimated)			Gmb (measured)	Correction factor
	$N_{initial}$	N_{design}	N_{max}	$N_{initial}$	N_{design}	N_{max}		
4.5	2211.9	2042.7	2021.6	2.12	2.30	2.32	2.37	1.019
5.0	2192.7	2025.9	2004.1	2.14	2.32	2.35	2.39	1.019
5.5	2175.2	2010.2	1988.0	2.16	2.34	2.36	2.41	1.019

Table 24. Design Air Voids Calculation – Control Mix

Pb (%)	Gmb corrected			Gmm	%Gmm			%Air Voids
	$N_{initial}$	N_{design}	N_{max}		$N_{initial}$	N_{design}	N_{max}	N_{design}
4.5	2.17	2.35	2.37	2.52	85.96	93.04	94.05	6.9
5.0	2.18	2.36	2.39	2.50	87.38	94.57	95.60	5.4
5.5	2.20	2.38	2.41	2.48	88.82	96.11	97.18	3.9

Table 25. Final Volumetric Properties – Control Mix

Pb (%)	% Air Voids	% VMA	% VFA	%Gmm	%Gmm	D.P.
				$N_{initial}$	N_{max}	
4.5	5.6	14.9	62.4	88.9	97.0	0.9
5.0	4.2	14.6	71.3	88.8	97.0	1.0
5.5	3.0	14.3	79.1	88.7	97.1	1.0

Volumetric Property Curves for 9.25% RAR Mix from Superpave Mix Design:

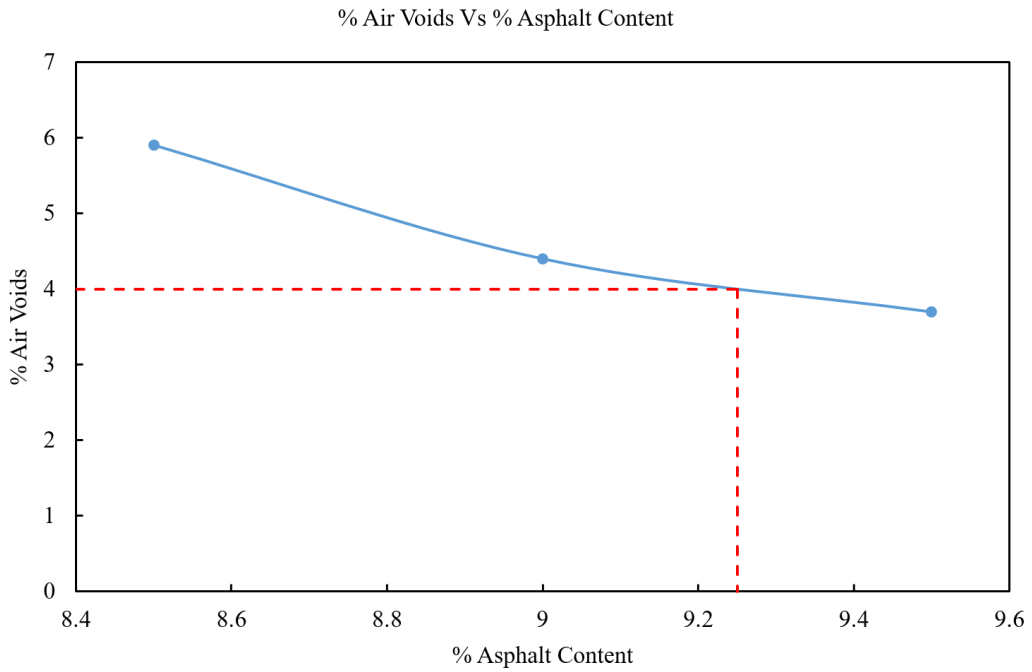

Figure 56. Air Voids % Vs Asphalt Content %

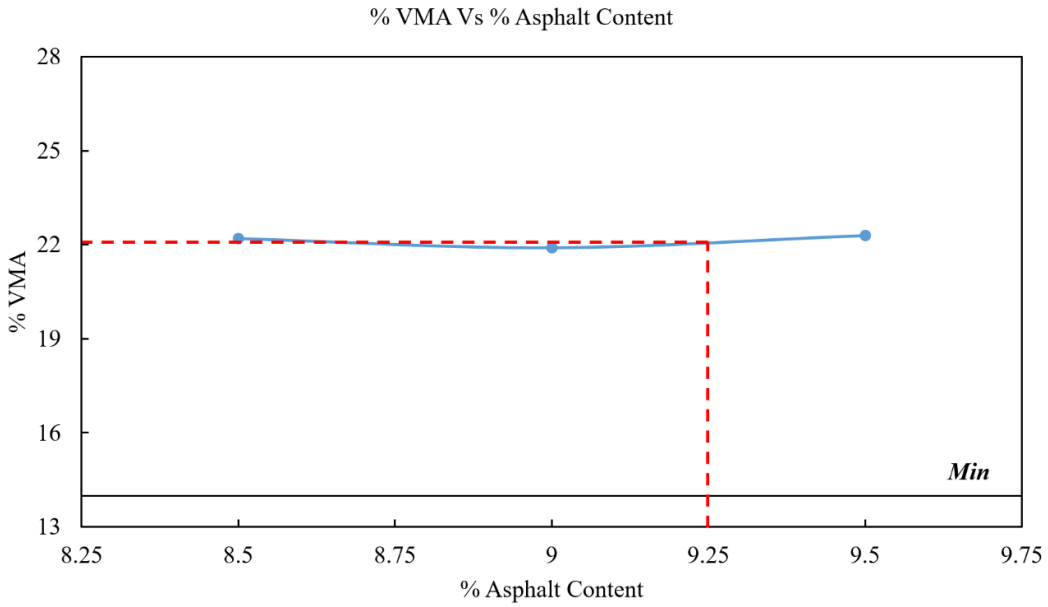

Figure 57. VMA Vs Asphalt Content %

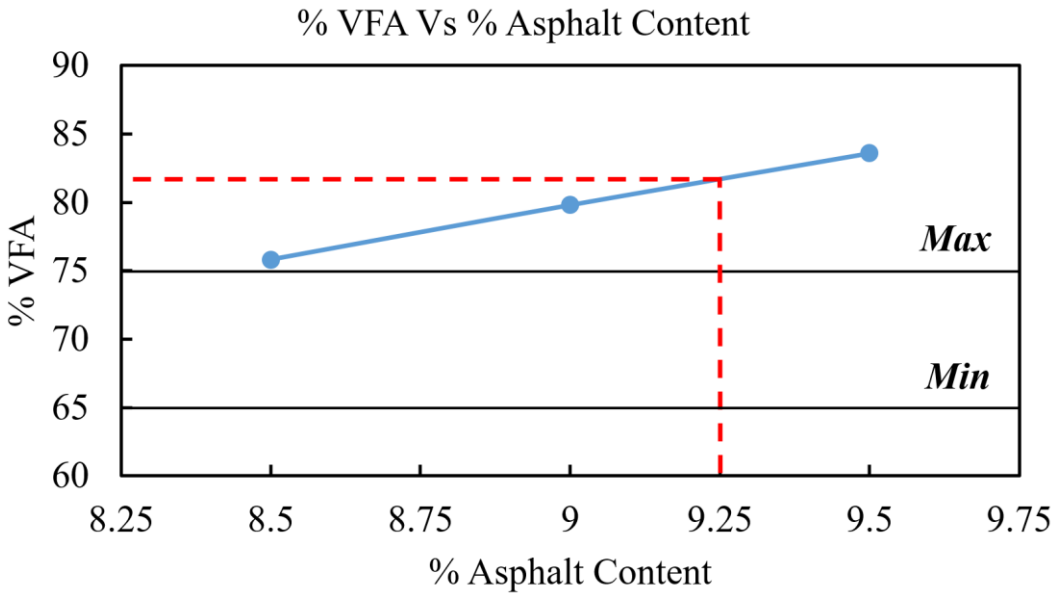

Figure 58. % VFA % Vs Asphalt Content %

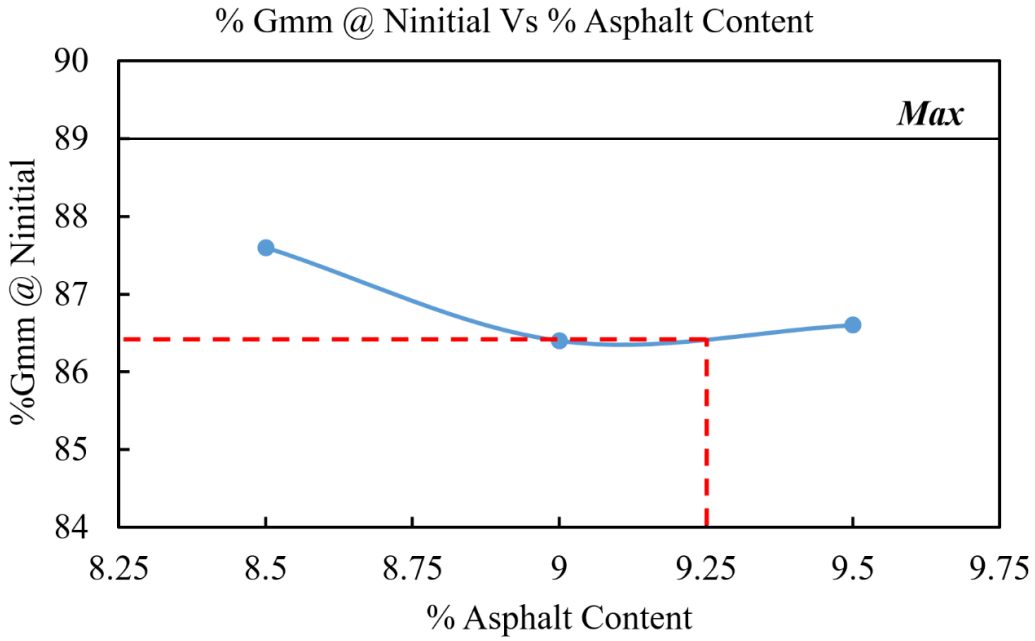

Figure 59. % Gmm @ Ninitial Vs % Asphalt Content

Volumetric Property Curves for 7.6% CRM Mix from Superpave Mix Design:

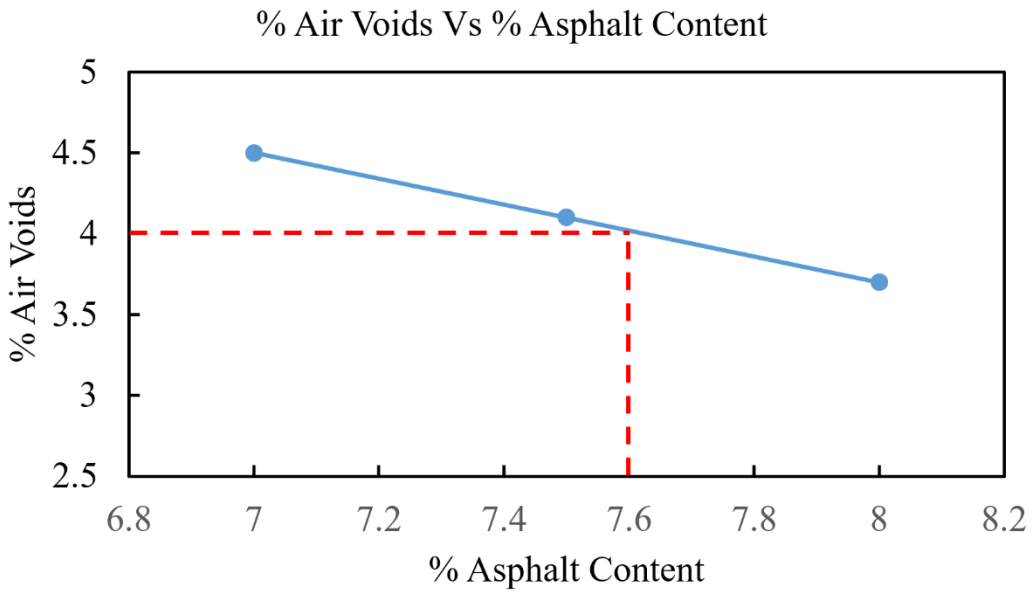

Figure 60. Air Voids % Vs Asphalt Content %

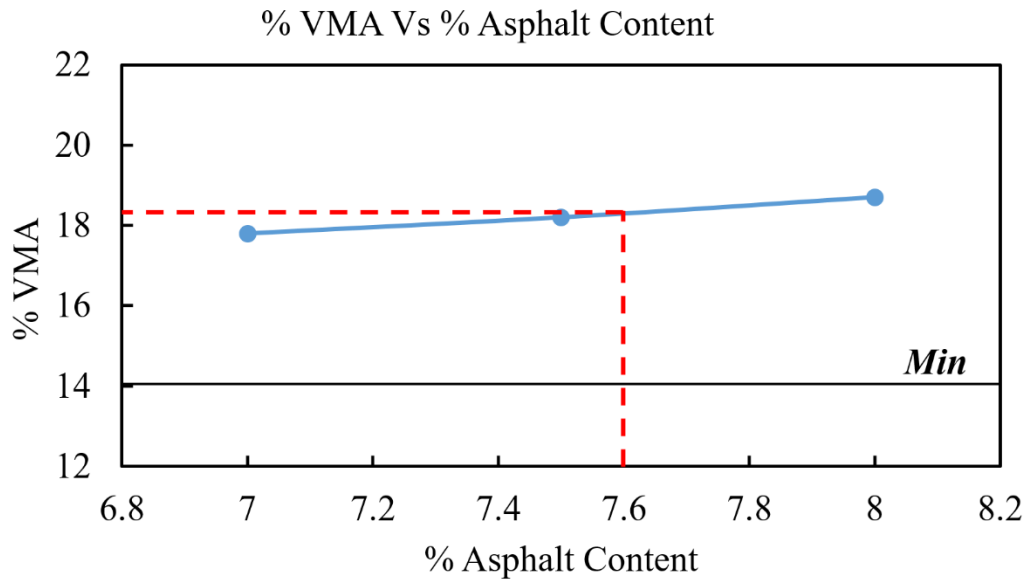

Figure 61. % VMA Vs Asphalt Content %

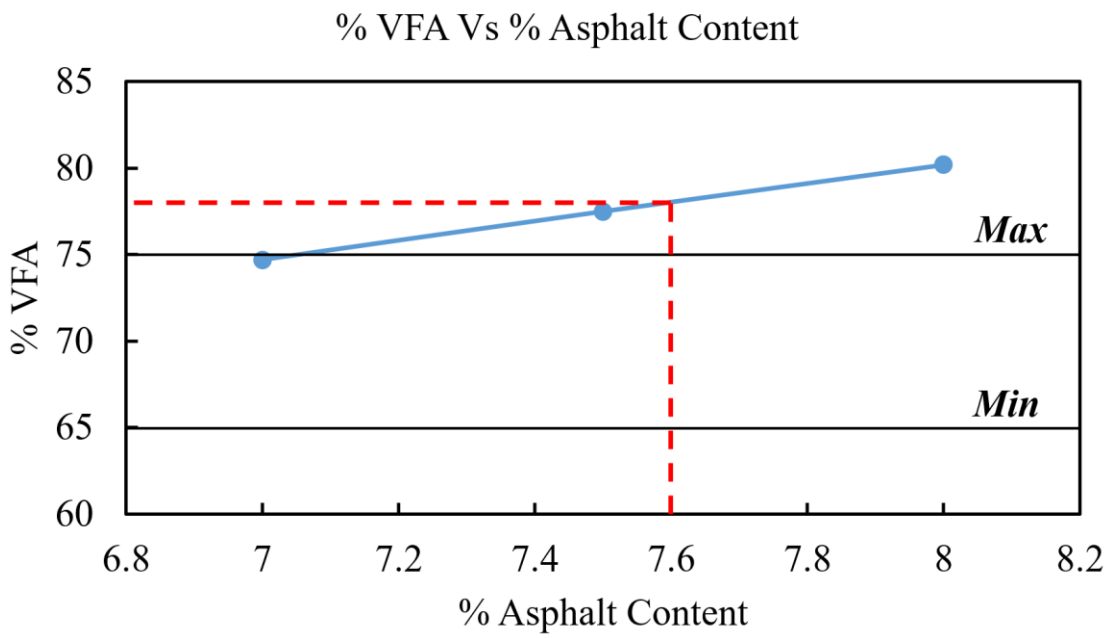

Figure 62. % VFA % Vs Asphalt Content %

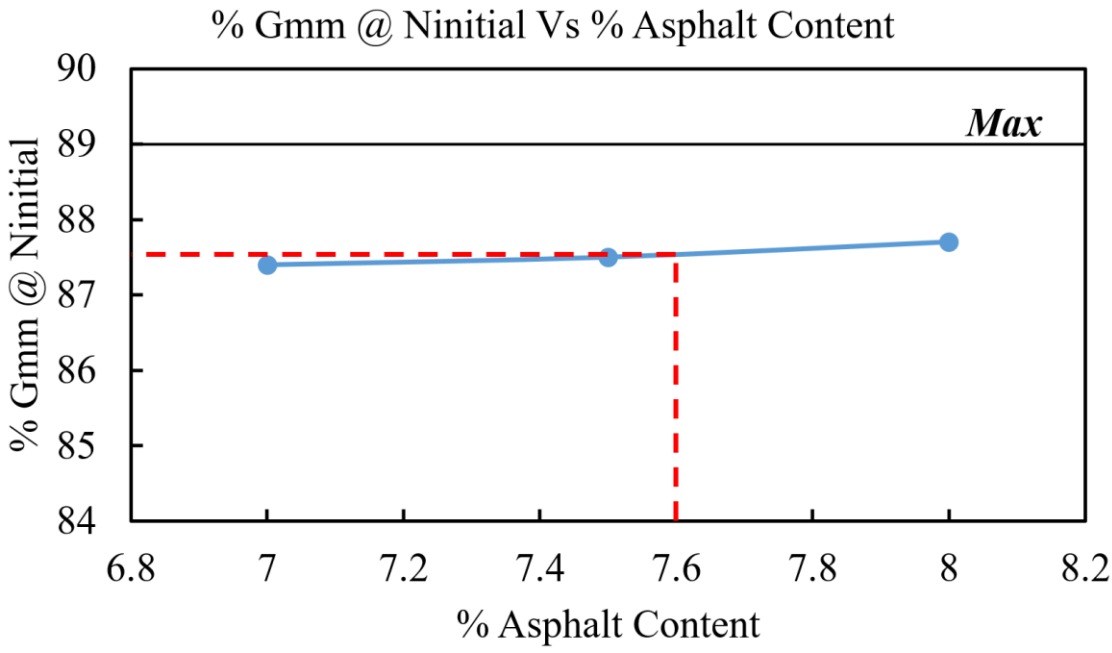

Figure 63. % Gmm @ Ninitial Vs % Asphalt Content

Volumetric Property Curves for 5.1% Control Mix from Superpave Mix Design:

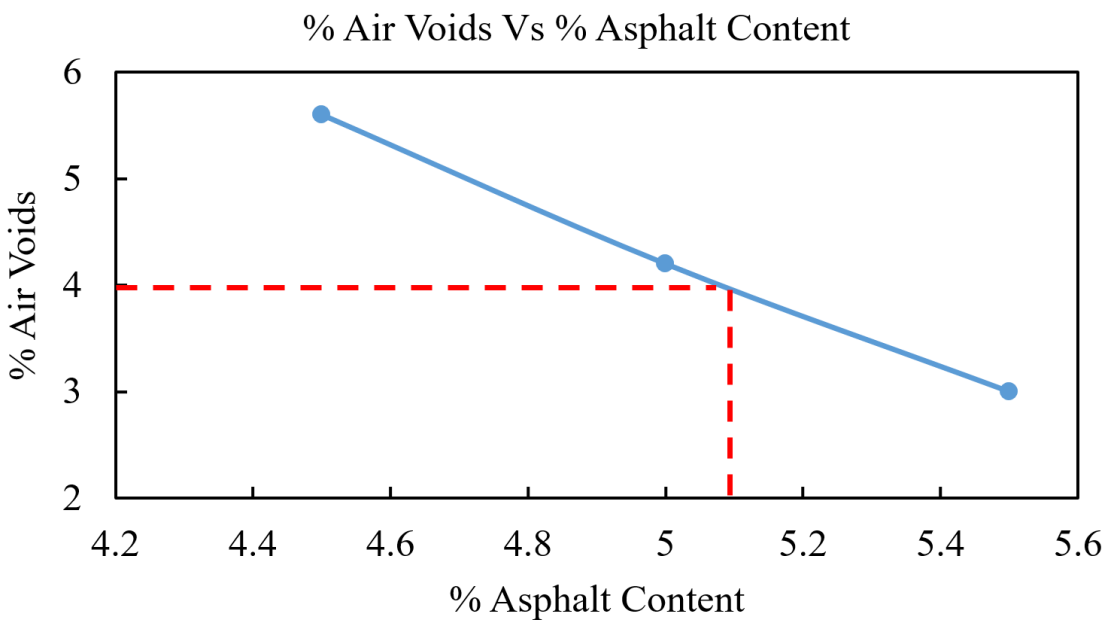

Figure 64. % Air Voids Vs % Asphalt Content

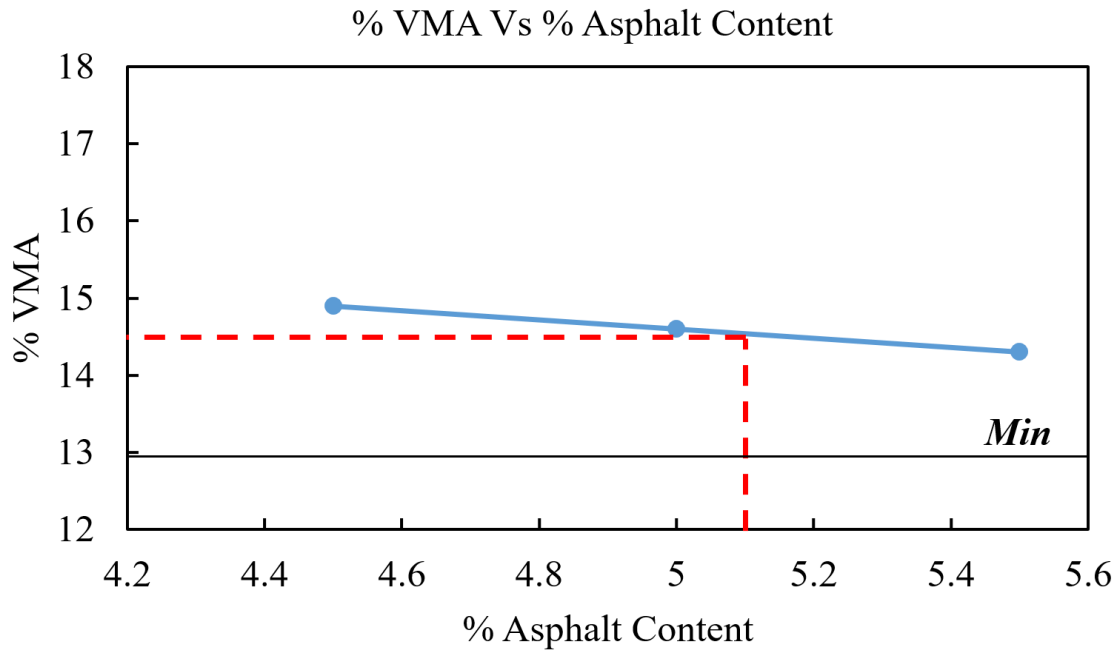

Figure 65. % VMA Vs Asphalt Content %

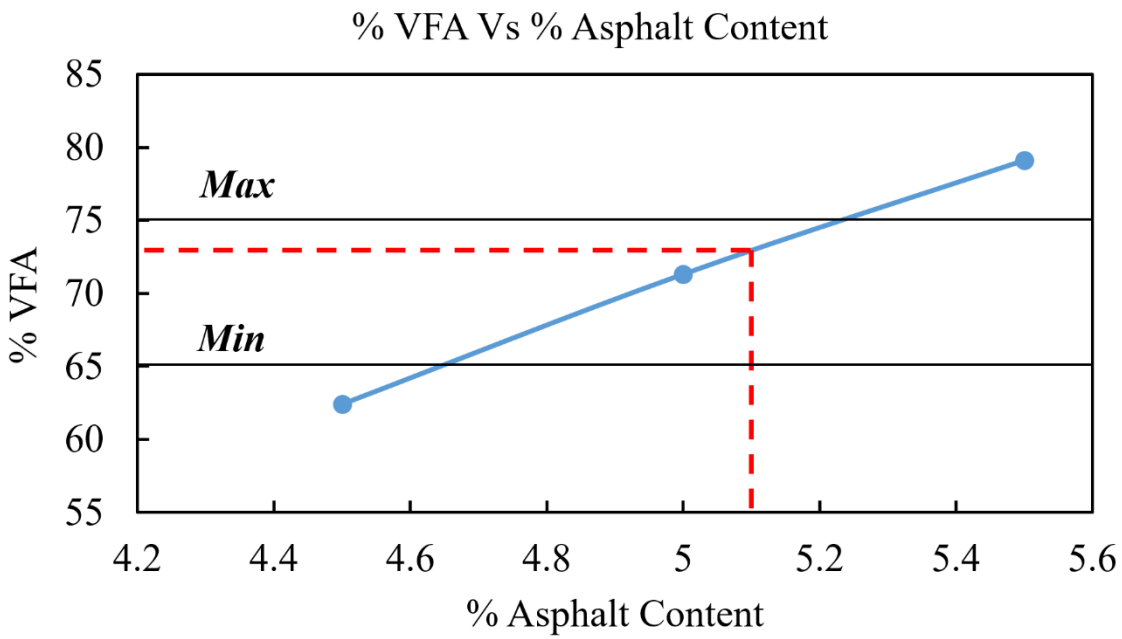

Figure 67. % VFA % Vs Asphalt Content %

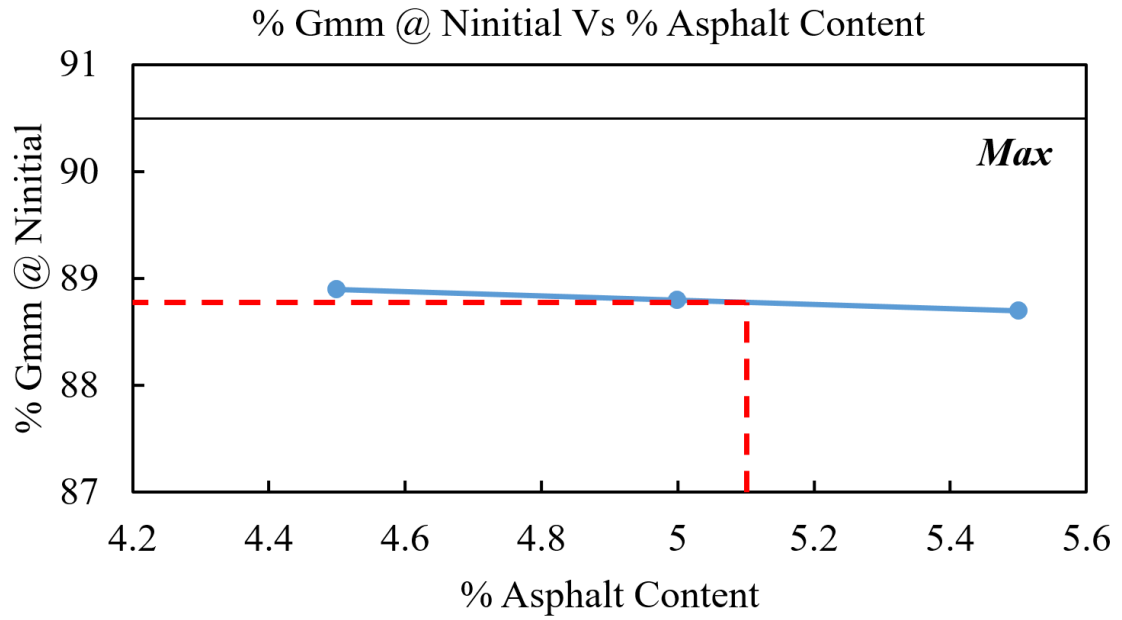

Figure 66. % Gmm @ Ninitial Vs % Asphalt Content

APPENDIX C

RESULTS OF LABORATOTRY TESTING

Table 26. Dynamic Modulus |E*| for 9.25% RAR Mix

Temperature (℃)	Frequency (Hz)	Dynamic Modulus, |E*| ksi				
		Replicate 1	Replicate 2	Replicate 3	Average	Std. Dev.
-10	25	3821.60	4013.48	3675.40	3836.83	138.44
-10	10	3648.42	3828.27	3583.16	3686.62	103.65
-10	5	3503.39	3615.21	3426.52	3515.04	77.47
-10	1	3183.87	3285.68	3042.02	3170.52	99.92
-10	0.5	3040.86	3132.09	2875.52	3016.16	106.19
-10	0.1	2718.30	2821.71	2551.94	2697.31	111.13
4.4	25	2873.34	2893.50	2409.66	2725.50	223.49
4.4	10	2614.16	2652.88	2195.73	2487.59	206.98
4.4	5	2419.37	2464.48	2028.93	2304.26	195.56
4.4	1	1977.44	2079.26	1645.16	1900.62	185.36
4.4	0.5	1819.21	1949.89	1508.54	1759.21	185.11
4.4	0.1	1489.54	1613.69	1231.23	1444.82	159.31
21,1	25	1232.68	1335.65	1140.58	1236.30	79.68
21,2	10	1052.10	1102.72	979.58	1044.80	50.53
21,3	5	924.33	966.97	890.24	927.18	31.39
21,4	1	626.71	708.07	605.82	646.87	44.11
21,5	0.5	536.20	604.66	515.90	552.26	37.97
21,6	0.1	357.52	416.84	357.95	377.44	27.86
37.8	25	505.89	605.68	520.11	543.89	44.07
37.8	10	408.72	487.47	436.13	444.11	32.64
37.8	5	344.32	404.08	363.75	370.72	24.89
37.8	1	213.50	256.14	235.54	235.06	17.41
37.8	0.5	176.37	219.01	197.83	197.73	17.41
37.8	0.1	109.65	143.73	131.40	128.26	14.09
54.4	25	166.07	213.50	178.25	185.94	20.11
54.4	10	131.69	172.59	137.79	147.36	18.02
54.4	5	110.66	146.63	120.96	126.09	15.12
54.4	1	70.34	100.22	80.50	83.69	12.40
54.4	0.5	58.74	91.08	68.89	72.91	13.51
54.4	0.1	41.05	71.94	51.49	54.82	12.83

Table 27. Dynamic Modulus |E*| for 10% RAR Mix

Temperature (℃)	Frequency (Hz)	Dynamic Modulus, |E*| ksi				
		Replicate 1	Replicate 2	Replicate 3	Average	Std. Dev.
-10	25	3746.03	4719.67	3054.93	3840.21	682.88
-10	10	3541.10	4505.02	2870.73	3638.95	670.77
-10	5	3364.87	4267.88	2745.71	3459.49	625.01
-10	1	2996.04	3697.88	2445.92	3046.61	512.36
-10	0.5	2847.96	3535.00	2331.77	2904.91	492.87
-10	0.1	2495.37	3093.36	2041.70	2543.48	430.69
4.4	25	2282.02	2817.21	1799.19	2299.48	415.79
4.4	10	2057.94	2484.50	1605.71	2049.38	358.81
4.4	5	1868.81	2221.69	1440.95	1843.82	319.22
4.4	1	1460.24	1721.74	1104.75	1428.91	252.86
4.4	0.5	1318.97	1531.45	984.81	1278.41	225.00
4.4	0.1	988.87	1176.55	712.72	959.38	190.50
21,1	25	803.36	926.94	643.68	791.33	115.95
21,2	10	662.82	776.53	519.96	653.10	104.97
21,3	5	561.88	655.14	434.68	550.56	90.36
21,4	1	346.93	425.54	273.25	348.57	62.18
21,5	0.5	280.94	354.47	223.79	286.40	53.49
21,6	0.1	172.01	226.98	139.24	179.41	36.20
37.8	25	318.65	384.64	283.26	328.85	42.01
37.8	10	238.15	285.58	212.34	245.36	30.33
37.8	5	185.94	227.85	166.50	193.43	25.60
37.8	1	102.83	133.72	95.29	110.62	16.63
37.8	0.5	82.82	111.68	81.95	92.15	13.82
37.8	0.1	49.60	66.43	51.05	55.69	7.61
54.4	25	85.72	108.78	80.50	91.66	12.29
54.4	10	64.83	75.27	58.02	66.04	7.10
54.4	5	50.76	60.05	47.57	52.79	5.29
54.4	1	30.89	37.71	28.72	32.44	3.83
54.4	0.5	26.40	30.60	24.66	27.22	2.50
54.4	0.1	20.02	22.34	10.44	17.60	5.15

Table 28. Dynamic Modulus |E*| for CRM Mix

Temperature (℃)	Frequency (Hz)	Dynamic Modulus, |E*| ksi				
		Replicate 1	Replicate 2	Replicate 3	Average	Std. Dev.
-10	25	5362.48	4388.41	4477.60	4742.83	439.67
-10	10	5157.54	4158.81	4343.15	4553.17	433.93
-10	5	5016.13	4013.92	4204.35	4411.47	434.57
-10	1	4622.35	3661.48	3818.84	4034.22	420.80
-10	0.5	4420.46	3529.78	3670.76	3873.67	390.90
-10	0.1	3966.35	3232.46	3296.85	3498.55	331.82
4.4	25	3473.94	2829.25	2982.85	3095.35	274.95
4.4	10	3261.03	2611.55	2810.40	2894.32	271.71
4.4	5	3015.33	2425.76	2642.01	2694.37	243.53
4.4	1	2558.03	2045.61	2235.03	2279.56	211.55
4.4	0.5	2368.90	1917.40	2060.84	2115.71	188.36
4.4	0.1	1954.09	1614.85	1697.81	1755.58	144.39
21,1	25	1561.33	1358.57	1408.32	1442.74	86.28
21,2	10	1336.81	1164.65	1218.75	1240.07	71.88
21,3	5	1175.53	1045.43	1065.74	1095.57	57.15
21,4	1	854.71	757.24	763.19	791.71	44.61
21,5	0.5	734.91	658.91	654.85	682.89	36.82
21,6	0.1	513.29	464.27	457.01	478.19	24.99
37.8	25	754.05	650.20	678.49	694.25	43.84
37.8	10	600.31	518.51	549.26	556.03	33.74
37.8	5	504.15	437.29	462.09	467.84	27.60
37.8	1	334.75	284.13	298.49	305.79	21.30
37.8	0.5	275.57	238.73	249.17	254.49	15.50
37.8	0.1	184.49	161.86	166.07	170.81	9.83
54.4	25	231.63	249.75	239.17	240.18	7.44
54.4	10	187.53	190.58	183.04	187.05	3.10
54.4	5	149.82	157.08	150.26	152.39	3.32
54.4	1	95.87	99.93	98.34	98.05	1.67
54.4	0.5	80.64	82.96	82.09	81.90	0.96
54.4	0.1	57.58	62.08	60.92	60.19	1.91

Table 29. Dynamic Modulus |E*| for Control Mix

Temperature (℃)	Frequency (Hz)	Dynamic Modulus |E*|, ksi				
		Replicate 1	Replicate 2	Replicate 3	Average	Std. Dev.
-10	25	5238.04	4584.50	5165.08	4995.87	292.41
-10	10	5172.91	4892.41	5094.30	5053.21	118.14
-10	5	5056.01	4771.60	4926.06	4917.89	116.26
-10	1	4706.47	4462.81	4557.95	4575.75	100.27
-10	0.5	4608.86	4315.16	4383.47	4435.83	125.49
-10	0.1	4306.31	3983.17	4021.46	4103.65	144.16
4.4	25	3657.42	3619.56	3694.55	3657.17	30.61
4.4	10	3493.67	3453.06	3454.65	3467.13	18.78
4.4	5	3318.46	3265.38	3232.02	3271.95	35.59
4.4	1	2881.75	2824.61	2697.56	2801.31	76.98
4.4	0.5	2686.68	2641.28	2480.00	2602.65	88.69
4.4	0.1	2238.66	2191.37	1995.72	2141.92	105.16
21,1	25	1774.83	1973.38	1787.59	1845.27	90.74
21,2	10	1552.92	1638.20	1531.02	1574.05	46.24
21,3	5	1371.91	1445.88	1342.32	1386.71	43.55
21,4	1	959.57	1037.89	934.33	977.26	44.09
21,5	0.5	845.42	897.64	805.39	849.49	37.77
21,6	0.1	556.80	580.01	520.54	552.45	24.47
37.8	25	717.94	865.29	866.60	816.61	69.78
37.8	10	560.14	658.47	707.35	641.99	61.22
37.8	5	446.28	524.89	570.29	513.82	51.23
37.8	1	257.73	301.68	331.56	296.99	30.32
37.8	0.5	199.86	233.80	264.84	232.83	26.54
37.8	0.1	108.63	126.04	152.72	129.13	18.13
54.4	25	159.83	199.72	223.21	194.25	26.16
54.4	10	109.65	141.56	164.76	138.66	22.59
54.4	5	83.54	106.17	131.69	107.13	19.67
54.4	1	44.67	57.00	81.37	61.01	15.25
54.4	0.5	35.97	45.54	70.49	50.67	14.55
54.4	0.1	35.97	30.75	50.47	39.06	8.34

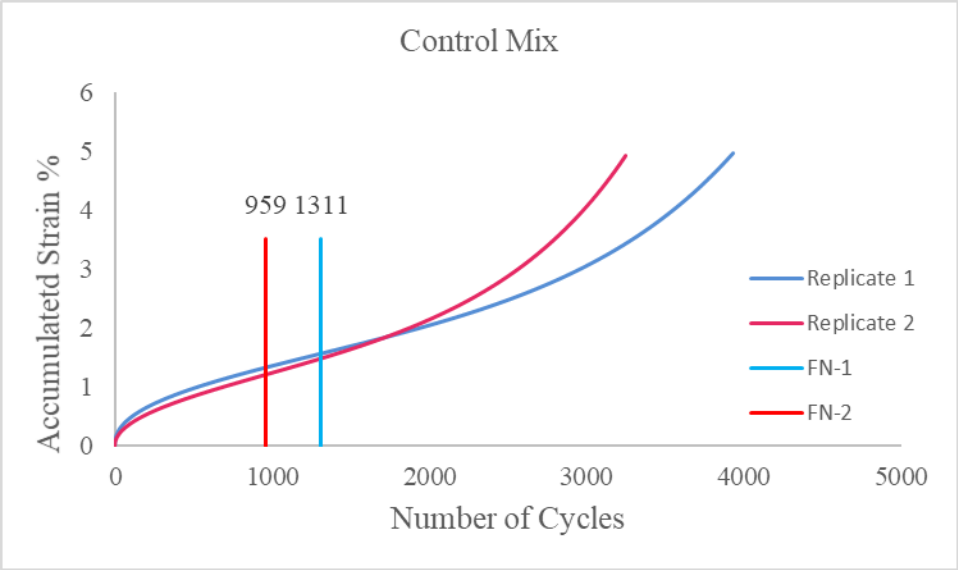

Figure 68. Accumulated Strain Vs Number of Cycles for All Replicates of Control Mix

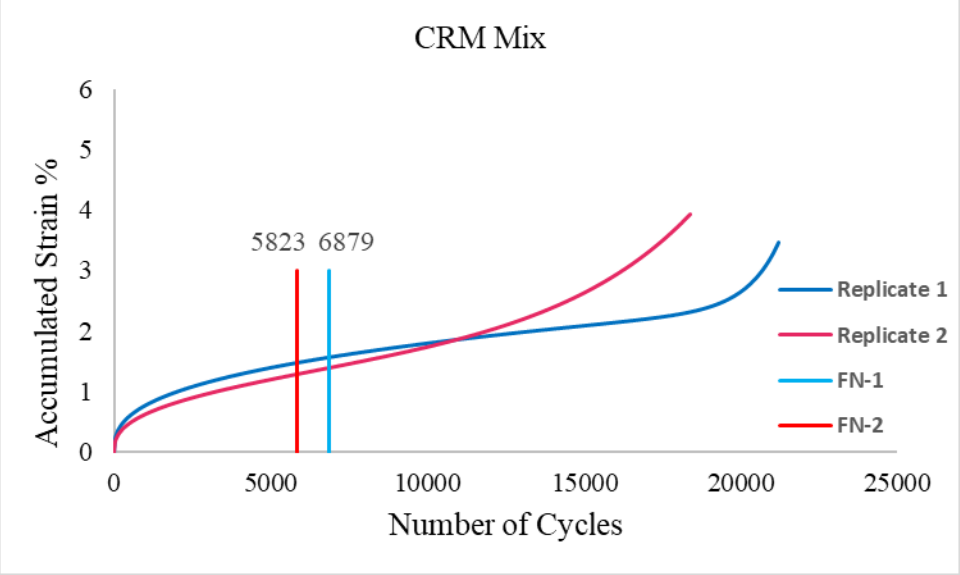

Figure 69. Accumulated Strain Vs Number of Cycles for All Replicates of CRM Mix

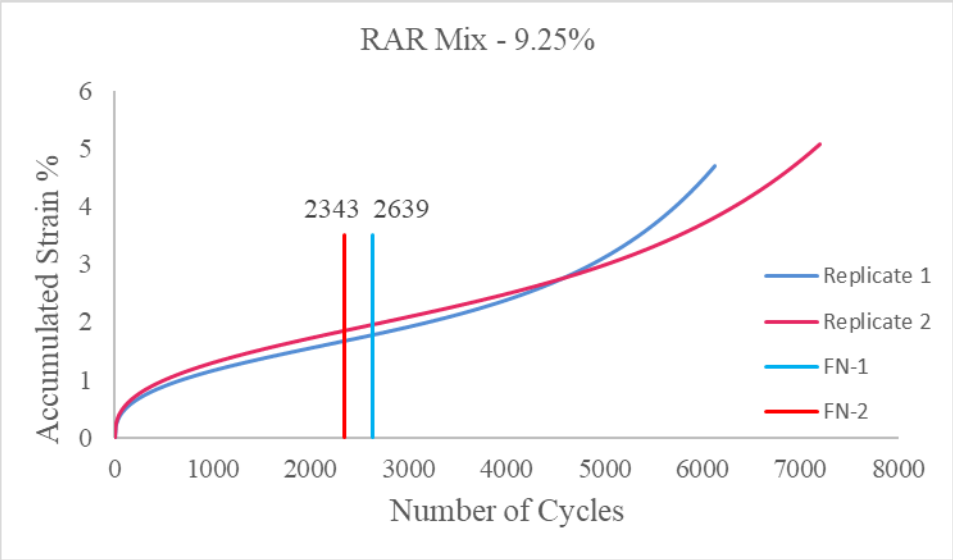

Figure 70. Accumulated Strain Vs Number of Cycles for All Replicates of RAR Mix - 9.25%

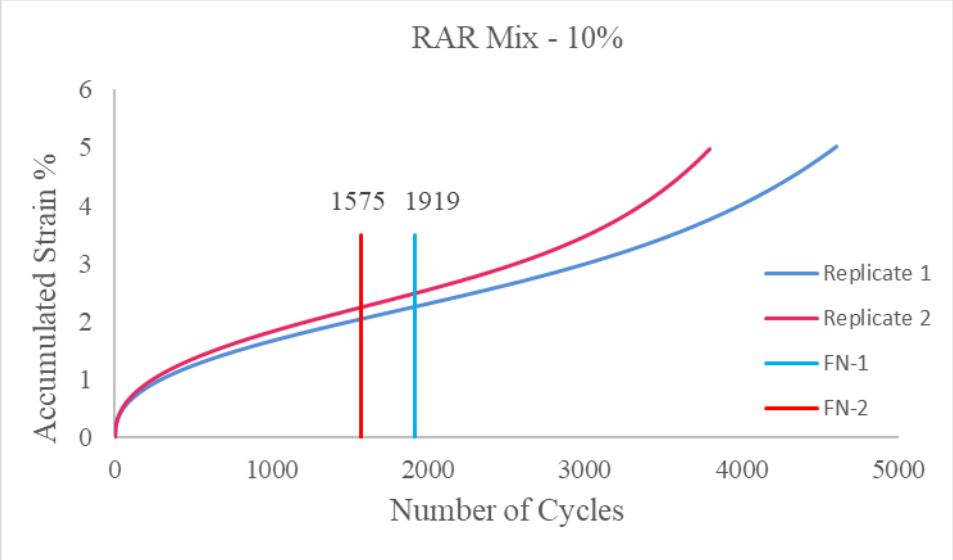

Figure 71. Accumulated Strain Vs Number of Cycles for All Replicates of Unaged RAR Mix – 10%

Table 30. Tensile Strength Ratio Calculation Steps for Control Mix

Mix		Control					
Condition		Wet Subset			Dry Subset		
Sample No.		1	2	3	1	2	3
Diameter, mm	D	102.5	102.2	102.2	102.0	102.2	102.3
Thickness, mm	t	66.5	62.4	65.0	63.9	64.4	64.9
Dry mass in air (gm)	A	1223.0	1161.8	1216.3	1192.1	1215.0	1216.2
SSD mass (gm)	B	1225.0	1163.3	1222.8	1194.3	1220.4	1220.8
Mass in water (gm)	C	692.6	658.8	695.7	674.4	693.3	693.8
Volume (B – C), cu.cm	E	532.4	504.5	527.1	519.9	527.1	527.0
Bulk specific gravity (A/E)	Gmb	2.297	2.303	2.308	2.293	2.305	2.308
Maximum specific gravity	Gmm	2.458	2.458	2.458	2.458	2.458	2.458
% Air voids [100(Gmm – Gmb)/Gmm]	Pa	6.54	6.31	6.12	6.72	6.22	6.11
Average % air voids	%		6.33			6.35	
Volume of air voids (Pa*E/100), cu.cm	Va	34.841	31.839	32.267	34.912	32.796	32.207
After Saturation							
Load, N (lbf)	P				15985.0	15662.0	14990.0
SSD mass (gm)	B'	1248.400	1183.200	1237.800			
Volume of absorbed water (B′ – A), cu.cm	J'	25.400	21.400	21.500			
% saturation (100J′/Va)	S'	72.903	67.213	66.632			
Load, N (lbf)	P'	13065.0	12839.0	13315.0			
Dry strength [2000P/πtD (2P/πtD)], kPa	S1				1561.1	1516.0	1518.8
Wet strength [2000P′/πt′D (2P/πt′D)], kPa	S2	1219.7	1245.8	1274.4			
Average tensile strenght Dry subset, kPa	S1 avg					1532.0	
Average tensile strenght Wet subset, kPa	S2 avg		1246.6				
TSR (S2/S1)			81				

Table 31. Tensile Strength Ratio Calculation Steps for CRM Mix

Mix		CRM					
Condition		Wet Subset			Dry Subset		
Sample No.		1	2	3	1	2	3
Diameter, mm	D	99.0	99.0	99.0	99.0	99.0	99.0
Thickness, mm	t	65.0	63.0	63.8	62.7	64.2	63.8
Dry mass in air (gm)	A	1156.7	1129.1	1143.2	1095.8	1144.9	1139.0
SSD mass (gm)	B	1159.8	1133.3	1144.8	1103.3	1149.4	1141.2
Mass in water (gm)	C	655.9	636.4	647.0	621.4	651.0	644.5
Volume (B – C), cu.cm	E	503.9	496.9	497.8	481.9	498.4	496.7
Bulk specific gravity (A/E)	Gmb	2.295	2.272	2.297	2.274	2.297	2.293
Maximum specific gravity	Gmm	2.450	2.450	2.450	2.450	2.450	2.450
% Air voids [100(Gmm – Gmb)/Gmm]	Pa	6.31	7.25	6.27	7.19	6.24	6.40
Average % air voids	%		6.61			6.61	
Volume of air voids (Pa*E/100), cu.cm	Va	31.78	36.04	31.19	34.65	31.09	31.80
After Saturation							
Load, N (lbf)	P				7947.0	8704.0	10028.0
SSD mass (gm)	B'	1179.100	1154.400	1165.100			
Volume of absorbed water (B′ – A), cu.cm	J'	22.400	25.300	21.900			
% saturation (100J′/Va)	S'	70.490	70.194	70.220			
Load, N (lbf)	P'	6901.0	7257.0	7470.0			
Dry strength [2000P/πtD (2P/πtD)], kPa	S1				815.4	872.4	1010.3
Wet strength [2000P′/πt′D (2P/πt′D)], kPa	S2	682.7	740.7	752.6			
Average tensile strenght Dry subset, kPa	S1 avg					899.4	
Average tensile strenght Wet subset, kPa	S2 avg		725.3				
TSR (S2/S1)			81				

Table 32. Tensile Strength Ratio Calculation Steps for RAR Mix – 10%

Mix		RAR - 10%					
Condition		Wet Subset			Dry Subset		
Sample No.		1	2	3	1	2	3
Diameter, mm	D	99.0	99.0	99.0	99.0	99.0	99.0
Thickness, mm	t	63.0	62.0	63.8	63.9	64.4	64.9
Dry mass in air (gm)	A	1127.8	1091.8	1131.9	1129.0	1112.2	1120.5
SSD mass (gm)	B	1129.6	1093.6	1133.2	1131.1	1114.8	1121.7
Mass in water (gm)	C	638.4	610.3	635.8	634.2	625.0	630.0
Volume (B – C), cu.cm	E	491.2	483.3	497.4	496.9	489.8	491.7
Bulk specific gravity (A/E)	Gmb	2.190	2.180	2.195	2.186	2.190	2.195
Maximum specific gravity	Gmm	2.340	2.340	2.340	2.340	2.340	2.340
% Air voids [100(Gmm – Gmb)/Gmm]	Pa	6.41	6.84	6.20	6.58	6.41	6.20
Average % air voids	%		6.48			6.40	
Volume of air voids (Pa*E/100), cu.cm	Va	31.49	33.05	30.82	32.70	31.40	30.47
After Saturation							
Load, N (lbf)	P				9271.0	8313.0	9943.0
SSD mass (gm)	B'	1149.900	1117.500	1154.500			
Volume of absorbed water (B′ – A), cu.cm	J'	22.100	25.700	22.600			
% saturation (100J′/Va)	S'	70.187	77.770	73.325			
Load, N (lbf)	P'	7025.0	7480.0	7895.0			
Dry strength [2000P/πtD (2P/πtD)], kPa	S1				933.2	830.7	985.6
Wet strength [2000P′/πt′D (2P/πt′D)], kPa	S2	717.1	775.8	795.4			
Average tensile strenght Dry subset, kPa	S1 avg					916.5	
Average tensile strenght Wet subset, kPa	S2 avg		762.7				
TSR (S2/S1)			83				

Table 33. Summary of C* Fracture Test Results for Unaged 10% RAR Samples

Sample ID:		**Avg. Thickness b (mm):**	**Displacement Rate Δ* (mm/min):**	
sample 1		**52.50**	**0.380**	
Crack Length, a (mm)	**Time T, (Min)**	**Force (KN)**	**Force per Unit Thickness P* (N/mm)**	**Crack Growth Rate, a* (mm/min)**
10.00	3.00	2.545	48.48	0.284
20.00	3.23	2.337	44.51	
30.00	4.23	2.060	39.24	
40.00	4.85	1.694	32.27	
50.00	5.17	1.448	27.58	
60.00	5.73	1.253	23.87	
70.00	6.67	0.930	17.52	
80.00	7.20	0.623	11.87	
90.00	8.36	0.311	5.92	
Sample ID:		**b (mm):**	**Displacement Rate, Δ* (mm/min):**	
Sample 2		**49.00**	**0.510**	
10.00	2.63	3.352	68.41	0.510
20.00	2.73	2.920	59.59	
30.00	2.83	2.670	54.49	
40.00	3.00	2.260	46.12	
50.00	3.47	1.930	39.39	
60.00	3.83	1.663	33.94	
70.00	4.33	1.320	26.94	
80.00	4.67	0.956	19.51	
90.00	5.83	0.517	10.55	
Sample ID:		**b (mm):**	**Displacement Rate, Δ* (mm/min):**	
Sample 3		**49.00**	**0.640**	
10.00	2.35	3.465	70.71	0.568
20.00	2.48	3.210	65.51	
30.00	2.55	2.967	60.55	
40.00	2.70	2.501	51.04	
50.00	2.85	1.950	39.80	
60.00	2.97	1.559	31.82	
70.00	3.10	1.309	26.71	
80.00	3.93	0.799	16.31	
90.00	4.58	0.555	11.33	

Sample ID:		b (mm):	Displacement Rate, Δ* (mm/min) :	
Sample 4		**53.00**	**0.760**	
10.00	2.47	4.642	87.58	0.881
20.00	2.80	4.175	78.77	
30.00	3.03	3.673	69.30	
40.00	3.33	3.276	61.81	
50.00	3.48	2.600	49.06	
60.00	3.90	2.244	42.34	
70.00	4.00	1.873	35.34	
80.00	4.10	1.320	24.91	
90.00	4.18	1.110	20.94	
Sample ID:		**b (mm):**	**Displacement Rate, Δ* (mm/min) :**	
Sample 6		**47.50**	**0.890**	
10.00	1.50	4.300	90.53	0.905
20.00	1.87	3.660	77.05	
30.00	2.07	3.224	67.87	
40.00	2.18	2.634	55.45	
50.00	2.47	2.239	47.14	
60.00	2.58	1.759	37.03	
70.00	2.77	1.451	30.55	
80.00	3.07	0.989	20.82	
90.00	3.36	0.772	16.25	

Table 34. Summary of C* Fracture Test Results for 9.25% RAR Samples

Sample ID:		**Avg. Thickness b (mm):**	**Displacement Rate Δ* (mm/min):**	
sample 1		**49.50**	**0.150**	
Crack Length, a (mm)	**Time T, (Min)**	**Force (KN)**	**Force per Unit Thickness P* (N/mm)**	**Crack Growth Rate, a* (mm/min)**
10.00	9.73	3.590	72.53	0.330
20.00	9.80	3.170	64.04	
30.00	10.07	2.840	57.37	
40.00	10.40	2.540	51.31	
50.00	10.80	2.350	47.47	
60.00	11.23	2.180	44.04	
70.00	12.58	1.940	39.19	
80.00	14.03	1.690	34.14	
90.00	14.63	1.430	28.89	
Sample ID:		**b (mm):**	**Displacement Rate, Δ* (mm/min):**	
Sample 2		**51.50**	**0.228**	
10.00	6.53	5.360	104.08	0.518
20.00	6.63	4.920	95.53	
30.00	6.75	4.680	90.87	
40.00	7.10	4.240	82.33	
50.00	7.43	3.780	73.40	
60.00	7.80	3.100	60.19	
70.00	8.10	2.830	54.95	
80.00	8.43	2.240	43.50	
90.00	9.53	1.750	33.98	
Sample ID:		**b (mm):**	**Displacement Rate, Δ* (mm/min):**	
Sample 3		**51.50**	**0.300**	
10.00	5.20	6.310	122.52	0.613
20.00	5.37	5.780	112.23	
30.00	5.50	5.380	104.47	
40.00	5.63	4.940	95.92	
50.00	5.75	4.340	84.27	
60.00	5.92	3.880	75.34	
70.00	6.13	3.410	66.21	
80.00	6.82	2.610	50.68	
90.00	7.73	1.990	38.64	

Sample ID:		b (mm):	Displacement Rate, Δ* (mm/min) :	
Sample 4		49.00	0.420	
10.00	4.70	6.510	132.86	0.763
20.00	4.87	6.020	122.86	
30.00	5.37	5.640	115.10	
40.00	5.72	5.080	103.67	
50.00	5.90	4.860	99.18	
60.00	6.05	4.350	88.78	
70.00	6.47	3.660	74.69	
80.00	6.75	2.780	56.73	
90.00	6.84	2.320	47.35	

Table 35. Summary of C* Fracture Test Results for CRM samples

Sample ID:		**Avg. Thickness b (mm):**	**Displacement Rate Δ* (mm/min) :**	
sample 1		**52.00**	**0.380**	
Crack Length, a (mm)	**Time T, (Min)**	**Force (KN)**	**Force per Unit Thickness P* (N/mm)**	**Crack Growth Rate, a* (mm/min)**
10.00	3.37	3.812	73.31	
20.00	4.08	3.469	66.71	
30.00	4.33	3.024	58.15	
40.00	4.60	2.534	48.73	
50.00	4.77	2.239	43.06	0.476
60.00	4.93	1.659	31.90	
70.00	5.10	1.351	25.98	
80.00	5.33	0.889	17.10	
90.00	6.60	0.672	12.92	
Sample ID:		**b (mm):**	**Displacement Rate, Δ* (mm/min) :**	
Sample 2		**49.50**	**0.510**	
10.00	3.27	4.311	87.09	
20.00	4.07	3.896	78.71	
30.00	4.23	3.413	68.95	
40.00	4.37	2.937	59.33	
50.00	4.50	2.450	49.49	0.599
60.00	4.65	1.961	39.62	
70.00	4.93	1.503	30.36	
80.00	5.33	0.957	19.33	
90.00	5.97	0.590	11.92	
Sample ID:		**b (mm):**	**Displacement Rate, Δ* (mm/min) :**	
Sample 3		**49.50**	**0.640**	
10.00	2.60	4.642	93.78	
20.00	2.63	4.275	86.36	
30.00	2.75	3.773	76.22	
40.00	2.90	3.376	68.20	
50.00	3.03	2.700	54.55	0.764
60.00	3.18	2.344	47.35	
70.00	3.93	1.973	39.86	
80.00	4.17	1.420	28.69	
90.00	4.72	0.940	18.99	

Sample ID:		b (mm):	Displacement Rate, Δ* (mm/min) :	
Sample 4		**49.00**	**0.760**	
10.00	1.87	5.120	104.49	0.951
20.00	1.97	4.610	94.08	
30.00	2.08	4.274	87.22	
40.00	2.23	3.519	71.82	
50.00	2.53	2.820	57.55	
60.00	2.75	2.436	49.71	
70.00	2.88	1.981	40.43	
80.00	3.17	1.486	30.33	
90.00	3.58	1.146	23.39	
Sample ID:		**b (mm):**	**Displacement Rate, Δ* (mm/min) :**	
Sample 5		**47.50**	**0.890**	
10.00	1.40	5.511	116.02	1.186
20.00	1.57	5.310	111.79	
30.00	1.67	4.220	88.84	
40.00	1.93	3.533	74.38	
50.00	2.02	2.850	60.00	
60.00	2.08	2.410	50.74	
70.00	2.35	1.674	35.24	
80.00	2.52	1.207	25.41	
90.00	2.82	0.713	15.01	

Table 36. Summary of C* Fracture Test Results for Control Samples

Sample ID:		**Avg. Thickness b (mm):**	**Displacement Rate Δ* (mm/min) :**	
sample 1		**50.50**	**0.380**	
Crack Length, a (mm)	**Time T, (Min)**	**Force (KN)**	**Force per Unit Thickness P* (N/mm)**	**Crack Growth Rate, a* (mm/min)**
10.00	3.88	3.713	73.52	0.888
20.00	3.93	2.869	58.55	
30.00	3.97	2.465	50.31	
40.00	4.03	2.279	46.51	
50.00	4.13	1.895	38.67	
60.00	4.20	1.482	30.24	
70.00	4.33	1.193	24.35	
80.00	4.72	0.946	19.31	
90.00	5.67	0.467	9.53	
Sample ID:		**b (mm):**	**Displacement Rate, Δ* (mm/min) :**	
Sample 2		**47.70**	**0.510**	
10.00	3.47	3.940	82.60	1.677
20.00	3.70	2.937	59.33	
30.00	3.75	2.496	50.42	
40.00	3.78	1.972	39.84	
50.00	3.82	1.574	31.80	
60.00	3.88	1.324	26.75	
70.00	3.95	1.129	22.81	
80.00	4.05	0.806	16.28	
90.00	4.47	0.531	10.73	
Sample ID:		**b (mm):**	**Displacement Rate, Δ* (mm/min) :**	
Sample 3		**49.00**	**0.640**	
10.00	2.33	4.114	83.96	1.999
20.00	2.38	3.619	73.86	
30.00	2.42	3.189	65.08	
40.00	2.45	2.389	48.76	
50.00	2.50	1.763	35.98	
60.00	2.58	1.417	28.92	
70.00	2.63	1.201	24.51	
80.00	2.75	0.895	18.27	
90.00	3.15	0.573	11.69	

Sample ID:		b (mm):	Displacement Rate, Δ* (mm/min) :	
Sample 6		**49.50**	**0.760**	
10.00	1.70	4.390	88.69	
20.00	1.80	3.466	70.02	
30.00	1.83	2.847	57.52	
40.00	1.87	2.443	49.35	
50.00	1.88	2.293	46.32	2.424
60.00	1.92	1.882	38.02	
70.00	1.97	1.678	33.90	
80.00	2.02	1.416	28.61	
90.00	2.37	1.044	21.09	
Sample ID:		**b (mm):**	**Displacement Rate, Δ* (mm/min) :**	
Sample 5		**49.50**	**0.890**	
10.00	2.07	6.243	126.12	
20.00	2.08	5.652	114.18	
30.00	2.10	5.033	101.68	
40.00	2.13	4.496	90.83	
50.00	2.28	3.752	75.80	3.463
60.00	2.47	2.998	60.57	
70.00	2.48	2.105	42.53	
80.00	2.50	1.495	30.20	
90.00	2.53	1.149	23.21	

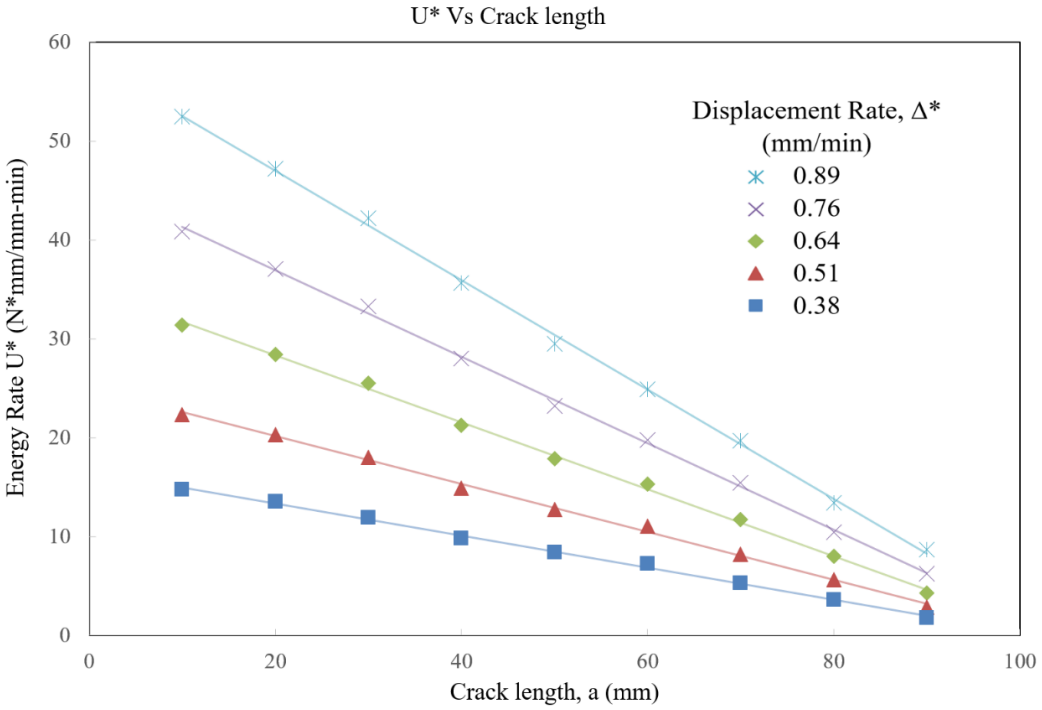

Figure 73. Energy Rate Vs Crack Length for 10% RAR samples

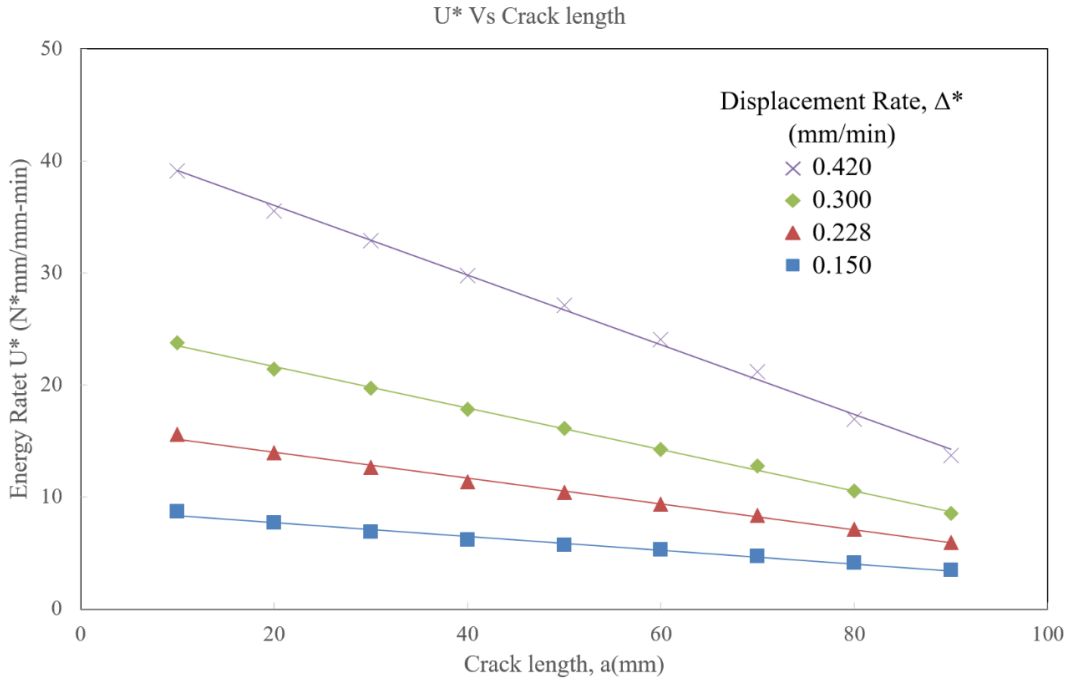

Figure 72. Energy Rate Vs Crack Length for 9.25% RAR samples

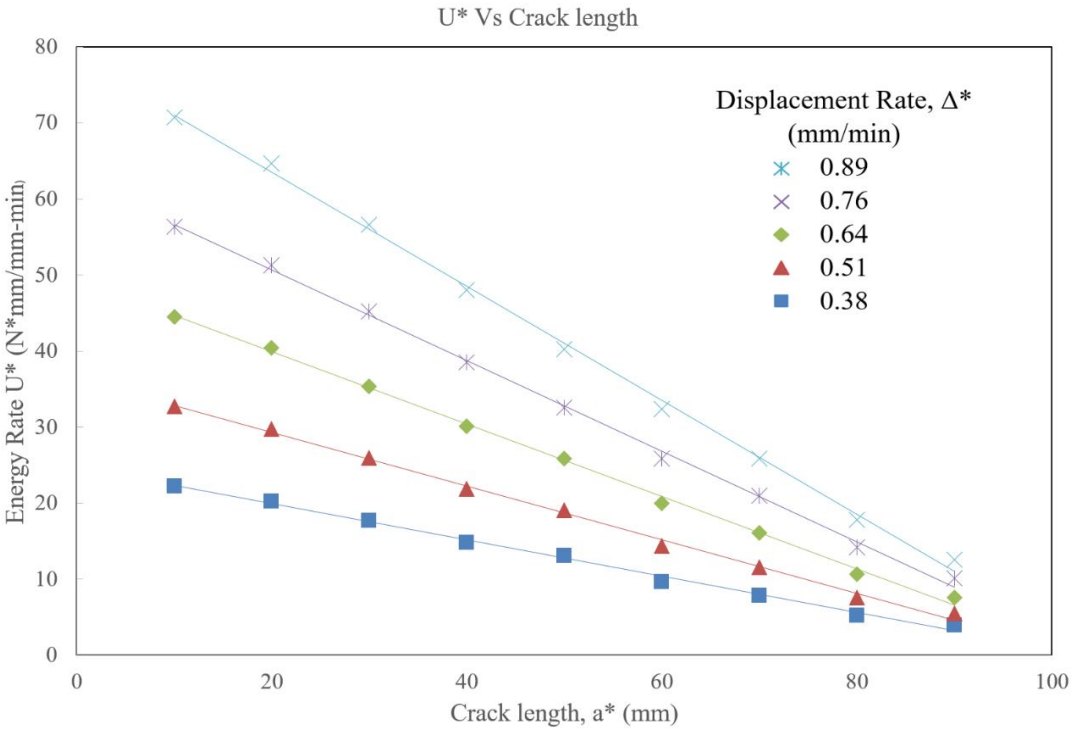

Figure 75. Energy Rate Vs Crack Length for 10% CRM samples

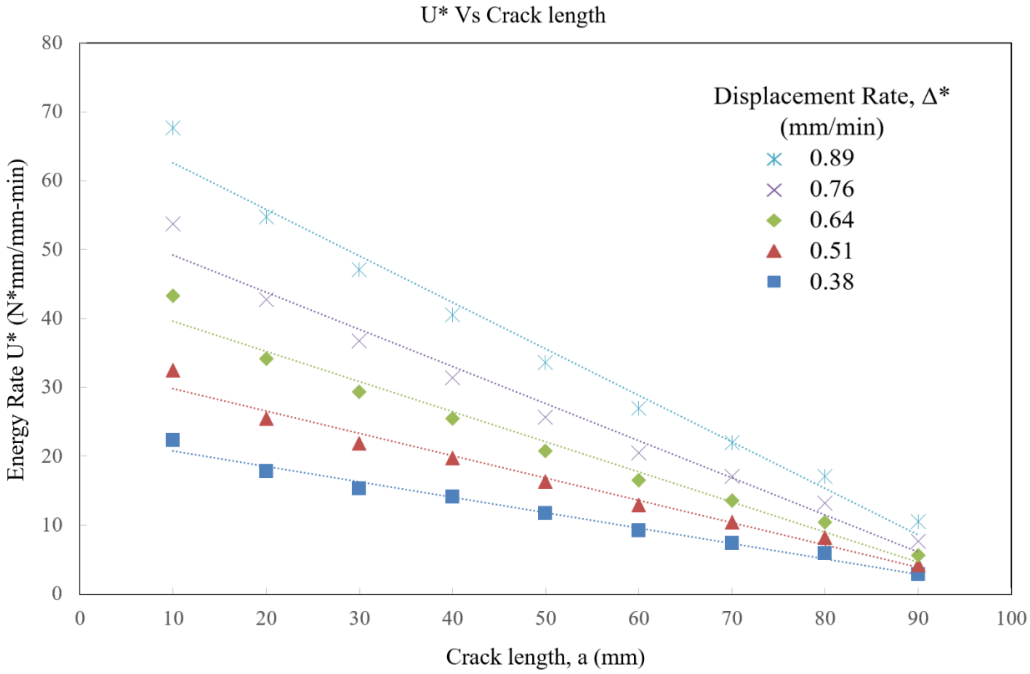

Figure 74. Energy Rate Vs Crack Length for Control samples

Figure 76. Tested C* Fracture Test sample

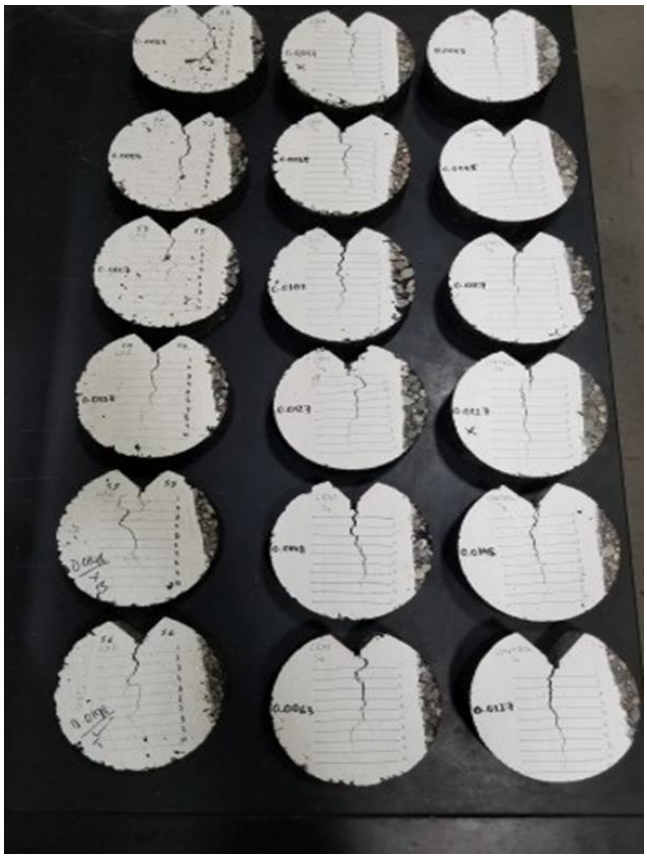

Figure 77. Tested C* Fracture Test samples for all mixes

APPENDIX D

ASPHALT FILM THICKNESS CALCULATIONS

		Bitumen 60/70	%	9.25					
			% to mixture	6.0125					
			% to bitumen	65					
		Additive (RAR)	% to mixture	3.2375					
Mixture			% to bitumen	35					
RAR Gap Graded				**90.75**					
Sieve size (series "base +2) (mm)	**Mix Design Criterion**	**Film Thickness - Grading Curve**							
		Sieve size	**Aggregate Grading Curve**	**% RARX (weight of mix)**	**Surface area Factor**	**Grading Curve (RARX)**	**Surface area Factor (RARX)**	**NO RARX consideration**	**Surface Area ´SA`,m2/kg (Surface factor x Passing %) (with RARX)**
				3.2375					
					0.41				0,41 x 1 = 0,41
31.5	x.x - x.x	26.5	100.0	100.0					
22.4	x.x - x.x	19.0	100.0	100.0					
20	x.x - x.x								
16	x.x - x.x								
14	x.x - x.x			100.0					
12.5	x.x - x.x	12.7	95.0						
10	x.x - x.x								
8	x.x - x.x								
6.3	x.x - x.x	9.5	65.0	62.9				0.41	0.41
4	x.x - x.x	4.75	25.0	24.2	0.41			0.1025	0.1025
2	x.x - x.x	2.36	20.0	19.4	0.82			0.1640	0.1640
1	x.x - x.x	1.18	16.0	15.5	1.64	3.2375	16.4	0.2624	0.7849
0.500	x.x - x.x	0.60	12.0	11.6	2.87	1.61875	28.7	0.3444	0.7978
0.250	x.x - x.x	0.300	10.0	9.7	6.14	0.631313	61.4	0.6140	0.9817
0.125	x.x - x.x	0.150	6.0	5.8	12.29	0.307563	122.9	0.7374	1.0915
0.063	x.x - x.x	0.075	4.0	3.9	32.77	0.080938	327.7	1.3108	1.5336
		Total Surface area SA´m2/kg´						3.95	5.87
		$TF = \frac{V_{asp}}{SA \times W} \times 1000\ \mu m$						**25.8**	**11.3**

Figure 78. Film Thickness Calculation for RAR Mix - 9.25%

		Bitumen 60/70	%	10.00					
			% to mixture	6.50					
			% to bitumen	65					
		Additive (RAR)	% to mixture	3.50					
Mixture			% to bitumen	35					
RAR Gap Graded				**90.00**					
Sieve size (series "base +2) (mm)	**Mix Design Criterion**	**Film Thickness - Grading Curve**							
		Sieve size	**Aggregate Grading Curve**	**% RARX (weight of mix)**	**Surface area Factor**	**Grading Curve (RARX)**	**Surface area Factor (RARX)**	**NO RARX consideration**	**Surface Area ´SA`,m2/kg (Surface factor x Passing %) (with RARX)**
				3.50					
					0.41				0,41 x 1 = 0,41
31.5	x.x - x.x	26.5	100.0	100.0					
22.4	x.x - x.x	19.0	100.0	100.0					
20	x.x - x.x								
16	x.x - x.x								
14	x.x - x.x			100.0					
12.5	x.x - x.x	12.7	95.0						
10	x.x - x.x								
8	x.x - x.x								
6.3	x.x - x.x	9.5	65.0	62.7				0.41	0.41
4	x.x - x.x	4.75	25.0	24.1	0.41			0.1025	0.1025
2	x.x - x.x	2.36	20.0	19.3	0.82			0.1640	0.1640
1	x.x - x.x	1.18	16.0	15.4	1.64	3.5	16.4	0.2624	0.8272
0.500	x.x - x.x	0.60	12.0	11.6	2.87	1.75	28.7	0.3444	0.8346
0.250	x.x - x.x	0.300	10.0	9.7	6.14	0.6825	61.4	0.6140	1.0116
0.125	x.x - x.x	0.150	6.0	5.8	12.29	0.3325	122.9	0.7374	1.1202
0.063	x.x - x.x	0.075	4.0	3.9	32.77	0.0875	327.7	1.3108	1.5517
		Total Surface area SA´m2/kg´						3.95	6.02
		$TF = \frac{V_{asp}}{SA \times W} \times 1000\ \mu m$						**28.2**	**12.0**

Figure 79. Film Thickness Calculation for Unaged RAR Mix - 10%

	Bitumen 60/70	%	7.60
		% to mixture	6.08
		% to bitumen	80
	Additive (CRM)	% to mixture	1.52
		% to bitumen	20
Mix			92.40
CRM Gap Graded			

Sieve size (series "base +2) (mm)	Mix Design Criterion	Film Thickness - Grading Curve							
		Sieve size	Aggregate Grading Curve	% RARX (weight of mix)	Surface area Factor	Grading Curve (CRM)	Surface area Factor (CRM)	NO CRM consideration	Surface Area ´SA`,m2/kg (Surface factor x Passing %) (with CRM)
				1.52					
					0.41				0,41 x 1 = 0,41
31.5	x.x - x.x	26.5	100.0	100.0					
22.4	x.x - x.x	19.0	100.0	100.0					
20	x.x - x.x								
16	x.x - x.x								
14	x.x - x.x			100.0					
12.5	x.x - x.x	12.7	95.0						
10	x.x - x.x								
8	x.x - x.x								
6.3	x.x - x.x	9.5	65.0	64.0				0.41	0.41
4	x.x - x.x	4.75	25.0	24.6	0.41			0.1025	0.1025
2	x.x - x.x	2.36	20.0	19.7	0.82			0.1640	0.1640
1	x.x - x.x	1.18	16.0	15.8	1.64	1.52	16.4	0.2624	0.5077
0.500	x.x - x.x	0.60	12.0	11.8	2.87	0.76	28.7	0.3444	0.5573
0.250	x.x - x.x	0.300	10.0	9.8	6.14	0.2964	61.4	0.6140	0.7867
0.125	x.x - x.x	0.150	6.0	5.9	12.29	0.1444	122.9	0.7374	0.9037
0.063	x.x - x.x	0.075	4.0	3.9	32.77	0.038	327.7	1.3108	1.4154
		Total Surface area SA´m2/kg´						3.95	4.85
		$TF = \frac{V_{asp}}{SA \times W} \times 1000\ \mu m$						**20.8**	**13.6**

Figure 80. Film Thickness Calculation for CRM Mix

		Bitumen 60/70	%	5.10					
			% to mixture	5.10					
			% to bitumen	100					
		No Additive	% to mixture	0.00					
Mixture			% to bitumen	0					
Control Dense Graded				**94.90**					
		Film Thickness - Grading Curve							
Sieve size (series "base +2) (mm)	Mix Design Criterion	Sieve size	Aggregate Grading Curve	% Filler (weight of mix)	Surface area Factor	Grading Curve (RARX)	Surface area Factor (RARX)	NO RARX consideration	Surface Area ´SA`,m2/kg (Surface factor x Passing %) (with RARX)
				0.00					
					0.41				0,41 x 1 = 0,41
31.5	x.x - x.x	26.5	100.0	100.0					
22.4	x.x - x.x	19.0	100.0	100.0					
20	x.x - x.x								
16	x.x - x.x								
14	x.x - x.x			100.0					
12.5	x.x - x.x	12.7	86.0						
10	x.x - x.x								
8	x.x - x.x								
6.3	x.x - x.x	9.5	72.0	72.0				0.41	0.41
		6.4	59.0	59.0	0.41			0.24	0.2419
4	x.x - x.x	4.75	56.0	56.0	0.41			0.2296	0.2296
2	x.x - x.x	2.36	43.0	43.0	0.82			0.3526	0.3526
1	x.x - x.x	1.18	32.0	32.0	1.64	0	16.4	0.5248	0.5248
0.500	x.x - x.x	0.60	21.0	21.0	2.87	0	28.7	0.6027	0.6027
0.250	x.x - x.x	0.300	11.0	11.0	6.14	0	61.4	0.6754	0.6754
0.125	x.x - x.x	0.150	6.0	6.0	12.29	0	122.9	0.7374	0.7374
0.063	x.x - x.x	0.075	4.8	4.8	32.77	0	327.7	1.5730	1.5730
		Total Surface area SA´m2/kg´						5.35	5.35
		$TF = \frac{V_{asp}}{SA \times W} \times 1000\ \mu m$						**10.0**	**10.0**

Figure 81. Film Thickness Calculation for Control Mix

MIX TYPE	LOCATION	FILM THICKNESS (micron)	PERFORMANCE
SMA11	MALAGA	6.5	ravelled
TF-SMA 08	MADRID	6.5	not built YET expected to ravel/crack
TF-SMA11	MADRID	7.5	not built YET expected to ravel/crack
SMA16	OVIED	8.2	ravelled
THINGAP	MADRID	8.4	cracks
THINGAP	A8 PORTUGAL	9.2	great
THINGAP	MALAGA	9.8	not built
		10	**minimum recommended level**
SMA11	MADRID	11.5	not built
GAP	indonesia	11.8	great
GAP	indonesia	15.3	great
THINGAP	LNEC	17.0	great

Figure 82. Film Thickness for Actual Projects Provided by Consulpav, Portugal